UNIVERSITY OF SOUTHAMPTON

FACULTY OF ENGINEERING, SCIENCE AND MATHEMATICS

School of Chemistry

Investigating the Chemistry of Lipoyl Synthase

By

Paul Douglas

Thesis for Degree of Doctor of Philosophy

September 2008

UNIVERSITY OF SOUTHAMPTON

ABSTRACT

FACULTY OF ENGINEERING, SCIENCE AND MATHEMATICS

SCHOOL OF CHEMISTRY

Doctor of Philosophy

INVESTIGATING THE CHEMISTRY OF LIPOYL SYNTHASE

by Paul Douglas

Abstract

The radical SAM protein lipoyl synthase (LipA) is essential for lipoic acid biosynthesis via sulfur insertions into the unactivated C6 and C8 centres of a protein-bound octanoyl group. Using an *in vitro* assay which makes use of a small peptide mimic of the protein substrate, it has now been shown at which carbon centre sulfur insertion first occurs. LCMS analysis of reactions using labeled substrates and proton NMR characterization of an isolated monothiolated adduct have been used to show that sulfur insertion proceeds in a stepwise manner, with sulfur insertion occurring preferentially at the C6 centre. The associated kinetic isotope effects (KIE's) for hydrogen atom abstraction from the C6 and C8 centres have been calculated and found to equal 2 and 15 respectively.

The inhibition of LipA by methionine and AdoH, which are products from reactions involving radical SAM proteins, was investigated. Methionine offered no clear inhibition whilst AdoH had a slight inhibitionary effect (IC_{50} = 990 ± 83 μM). When both methionine and AdoH were used together, a strong synergistic inhibition was present (IC_{50} = 327 ± 22 μM). However, when an enzyme (Pfs) which cleaves the glycosidic bond in AdoH was added to the reaction, this inhibition was removed and a 1.4 fold increase in activity was observed.

The ability of LipA to accept larger substrates was also tested using a nonanoyl peptide analogue. LCMS analysis of these reactions identified that as well as the expected single and double sulfur inserted products there were two further unexpected products formed in the reaction mixture. Proton NMR characterized these as a trans-alkene and a thietane. Mechanisms for their formations have been proposed.

Table of Contents

DECLARATION OF AUTHORSHIP

I, Paul Douglas, declare that the thesis entitled 'Investigating the Chemistry of Lipoyl Synthase' and the work presented in the thesis are both my own, and have been generated by me as the result of my own original research. I confirm that:

- this work was done wholly or mainly while in candidature for a research degree at this University;
- where any part of this thesis has previously been submitted for a degree or any other qualification at this University or any other institution, this has been clearly stated;
- where I have consulted the published work of others, this is always clearly attributed;
- where I have quoted from the work of others, the source is always given. With the exception of such quotations, this thesis is entirely my own work;
- I have acknowledged all main sources of help;
- where the thesis is based on work done by myself jointly with others, I have made clear exactly what was done by others and what I have contributed myself;
- parts of this work have been published as:

  Douglas, P., M. Kriek, P. Bryant, and P.L. Roach, Lipoyl synthase inserts sulfur atoms into an octanoyl substrate in a stepwise manner. *Angewandte Chemie International Edition* 2006. **45**(31): p. 5197-9.

Signed:

Date: September 2008

Aknowledgements

I thank those here mentioned for their contributions toward this work; David Skinner, a project student in my second year for the synthesis of the nonanoyl substrate analogue, Martin Challand, a second project student who later joined our research group for investigating the heptanoyl substrate analogue, John Langley and Julie Herniman (Mass spectrometry), Joan Street, Neil Wells and Stuart Findlow (NMR) for their expert help

.

I would like to warmly thank Peter Roach for his supervision throughout this work and his great help in the process of writing this thesis. I am grateful for his interesting thoughts and ideas throughout the duration of the project which has allowed me learn a broad range of skills. His overwhelming enthusiasm for this and his other projects was a great encouragement during my time in the lab and kept me going when things were not working. I would also like to thank Bruno Linclau for his encouragement and advice throughout the project.

I would like to particularly thank Marco Kriek and Penny Bryant for the work they did on LipA before and after my arrival. I was fortunate to join the project at such a good time. Conditions for the expression of the protein were known and the development of the *in vitro* assay complete which allowed me to focus on understanding the protein. Thanks also for passing on your knowledge, teaching me how everything works in the lab and helping me to fix equipment when it went wrong.

Many thanks to Rob Wood, as well as a being a good friend throughout the project he gave up his free time to proof read this thesis and offered a lot of advice throughout my time here.

I can not thank my parents enough for their continued encouragement and support during my time in Southampton and more importantly, for putting a roof over my head whilst I wrote this thesis. Thanks especially to my girlfriend Penny for her support and encouragement in a tough year. You knew how to keep me motivated through a tough year and kept me happy.

Finally thanks to all the members of the Roach, Neylon and Brown groups who made life at Southampton during my Ph.D very enjoyable.

Abbreviations

ACP	Acyl carrier protein
Ado$^{\bullet}$	5'-Deoxyadenosine radical
AdoD	5'-D-5'-deoxyadenosine
AdoH	5'-Deoxyadenosine
AMP	Adenosine monophosphate
A. thaliana	*Arabidopsis thaliana*
ARR	Anaerobic ribonucleotide reductase
ARR-AE	Anaerobic ribonucleotide reductase activating enzyme
ATP	Adenosine triphosphate
A. thaliana	*Arabidopsis thaliana*
B. anthracis	*Bacillus anthracis*
B. sphaericus	*Bacillus sphaericus*
B. subtilis	*Bacillus subtilis*
B. suis	*Brucella suis*
CAS	Clavaminic acid synthase
CoA	Coenzyme A
COSY	Correlation spectroscopy
d	Doublet
DCC	Dicyclohexylcarbodiimide
DCM	Dichloromethane
DHL	Dihydrolipoyl
DIC	Diisopropylcarbodiimide
DIPEA	N,N'-diisopropylethylamine
DMF	*N*,*N*-Dimethylformamide
DO	Dissolved Oxygen
DTT	Dithiothreitol
E1	Pyruvate decarboxylase
E2	Dihydrolipoate transacetylase
E3	Dihydrolipoyl dehydrogenase

EI	Electron impact ionisation
ENDOR	Electron nuclear double resonance spectroscopy
EPR	Electron paramagnetic resonance
E. Coli	*Escherichia coli*
FAD	Flavin adenine dinucleotide
$FADH_2$	Flavin adenine dinucleotide (reduced)
Fldx	Flavodoxin
Fmoc	9-Fluorenylmethyloxycarbonyl
FPLC	Fast protein liquid chromatography
GC-MS	Gas chromatography mass spectrometry
h	Hour
HemN	Oxygen independent coproporphyrinogen III oxidase
HEPES	4-(2-hydroxyethyl)-1-piperazineethanesulphonic acid
His tag	Hexahistidine tag
HOBt	Hydroxybenzotriazole
HPLC	High performance liquid chromatography
HRES-MS	High resolution mass spectrometry
Hz	Hertz
H. sapiens	*Homo sapiens*
IC_{50}	Half maximal inhibitory concentration
ICP	Inductively coupled plasma atomic emission spectroscopy
isc	iron sulphur cluster (genes)
Isc	Iron sulphur cluster
KAM	Lysine 2,3-aminomutase
KIE	Kinetic isotope effect
lipA	Lipoyl synthase (gene)
LipA	Lipoyl synthase (protein)
LipB	lipoyl-[acyl-carrier-protein]-protein-*N*-lipoyltransferase
M	Molar
MALDI	Matrix assisted laser desorption ionisation
MAT	Methionine adenosyltransferase
min	Minute
MS	Mass spectrometry
MTA	5'-methylthioadenosine

M/W	Molecular weight
MWCO	Molecular weight cut off
m/z	Mass charge ration
NAD+	Nicotinamide adenine dinucleotide
NADH	Nicotinamide adenine dinucleotide (reduced)
NADPH	Nicotinamide adenine dinucleotide phosphate (reduced)
NifS	Cysteine desulphurase
NMP	*N*-methylpyrrolidone
PDH	Pyruvate dehydrogenase
PFL	Pyruvate formate lyase
PFL-AE	Pyruvate formate lyase activating enzyme
Pfs	5'-methylthioadenosine/ S-adenosylhomocysteine nucleosidase
PLP	Pyridoxal 5'-phosphate
ppm	Parts per million
PyBOP	Benzotriazole-1-yl-oxy-tris-pyrrolidino-phosphonium hexafluorophosphate
P. torridus.	*Picrophilus torridus*
q	*quartet*
qi	*quintet*
R. bellii	*Rickettsia bellii*
RPM	Revolutions per minute
Rt	Retention time
RT	Room temperature
s	Second
s	Singlet
SAH	*S*-adenosylhomocysteine
SAM	S-adenosyl methionine
SDS-PAGE	Sodium dodecyl sulphate polyacrylamide gel electrophoresis
S. cerevisiae	*Saccharomyces cerevisiae*
S. solfataricus	*Solfolubus solfataricus*
t	Triplet
TCEP	Tris(2-carboxyethyl)phosphine hydrochloride
TFA	Trifluoroacetic acid
THF	Tetrahydrofuran

TIC	Total ion chromatogram
TIM	Triosephosphate isomerase
TEMED	N,N,N',N'-Tetramethylethylenediamine
TOCSY	Total Correlation Spectroscopy
TPP	Thiamine pyrophosphate
Tris	trishydroxymethylaminomethane
UV/vis	Ultraviolet-visable spectroscopy
V	Volt
wrt	With respect to
Y. pestis.	*Yersinia pestis*

Notations

In this report, gene names are quoted in italics with no capitalization of the first letter, eg. *lipA*.

Gene products are named in normal type, with first letter capitalized, eg. LipA.

Chapter 1. Introduction

The protein lipoyl synthase (LipA) which is encoded by the *lipA* gene (1-3), has been identified as the protein responsible for the conversion of protein bound octanoyl groups into lipoyl groups (1-5) (fig. 1.1).

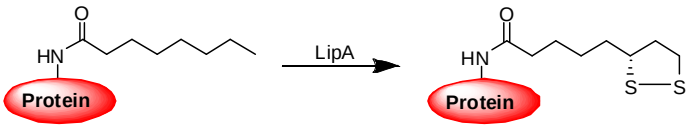

Figure 1.1 The conversion of protein bound octanoyl groups into lipoyl groups by the protein LipA.

1.1 α-Lipoic acid

First isolated in 1951 as pale yellow platelets, (6) α-lipoic acid (1,2-dithiolane-3-pentanoic acid, thioctic acid) **1** (fig. 1.2) is a naturally occurring biomolecule, which is found in a wide range of prokaryotic and eukaryotic micro-organisms (7). Characterisation of isolated lipoic acid **1** determined that the molecule contained an octanoyl backbone, with two sulfur atoms, one bonded to the C6 position and the other attached to the terminal C8 position. The two sulfur atoms form a disulfide bond to generate the 1,2-dithiolane ring, with stereochemistry at the C6 carbon defined as the R-enantiomer (6, 8). α-Lipoic acid and its reduced metabolite, dihydrolipoic acid **2** (fig. 1.2) form a redox couple which can effectively scavenge a wide range of reactive oxygen species, acting as an antioxidant that has been identified as a potential treatment for numerous conditions including diabetes insipidus and Alzheimer's disease (9-11).

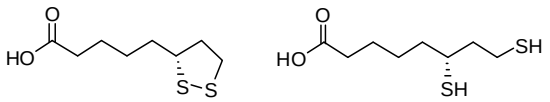

1 **2**

Figure 1.2 The structure of α-lipoic acid **1** and dihydrolipoic acid **2**.

Within the cell, lipoic acid is primarily found covalently attached to proteins by an amide linkage (fig. 1.3) between the acid group of lipoic acid and the ε-amino groups of specific

lysine residues within certain proteins forming a 14 Å "swinging arm" (12, 13). In this form it serves as an essential co-factor for these enzymes.

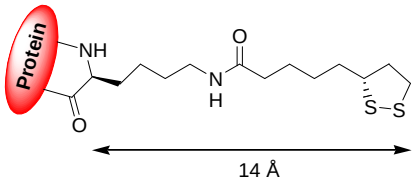

Figure 1.3 The structure of protein bound lipoic acid **1** showing the 14 Å "swinging arm".

1.2 The role of α-lipoic acid

Lipoic acid is essential as a cofactor in a number of multienzyme complexes that are required for cellular function (12). These include the E2 subunit of oxo-acid dehydrogenases pyruvate dehydrogenase (PDH) (fig. 1.4, a) and α-ketoglutarate dehydrogenase (fig. 1.4, b) (14) and the H-protein of the glycine cleavage system (15) (fig.1.4, c). These proteins are large multidomain complexes, with the lipoyl cofactor acting as a "swinging arm" for substrate transfer between subunits.

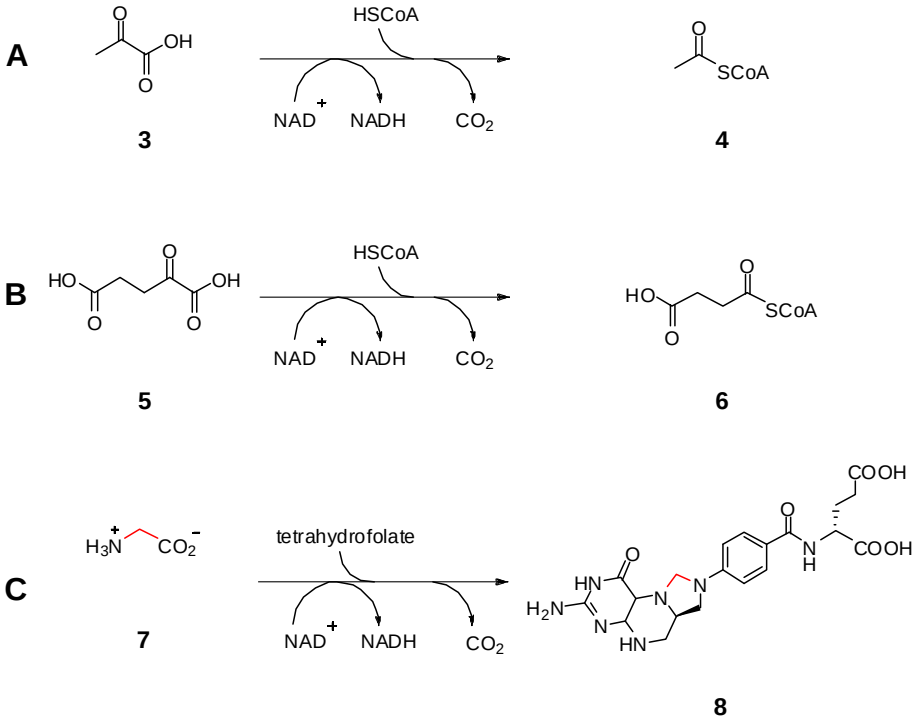

Figure 1.4 Reactions catalysed by enzymes using lipoic acid as a cofactor: (**A)** conversion of pyruvate **3** to acetyl CoA **4** by pyruvate dehydrogenase; (**B)** conversion of α-ketoglutarate **5** to succinoyl CoA **6** by α-ketoglutarate dehydrogenase; (**C)** reaction of glycine **7** with tetrahydrofolate to form N^5,N^{10} methylene THF **8** catalysed by the glycine cleavage system.

1.2.1 Oxo-acid dehydrogenases

Pyruvate dehydrogenase

Oxo-acid dehydrogenases are responsible for the oxidative decarboxylation of α-keto acids. PDH is an example of these complexes and is responsible for the catalytic conversion of pyruvate **3** (fig. 1.4) to acetyl coenzyme A (acetyl CoA) **4** (fig 1.4), which is used in many critical biological reactions that include the Krebs cycle and fatty acid biosynthesis. PDH is comprised of multiple copies of three subunits; pyruvate decarboxylase (E1), dihydrolipoate transacetylase (E2) and dihydrolipoyl dehydrogenase (E3) (14). The core of the *Escherichia coli* (*E. coli*) PDH complex is made up of twenty four E2 subunits arranged around the eight vertices of a cube (14, 16). Twelve E1 dimers occupy each of the edges of the E2 core with each face binding an E3 dimer. The E1 subunit utilises thiamine pyrophosphate (TPP) as a cofactor and the E3 subunit binds flavin adenine dinucleotide (FAD). The E2 domain contains a lysine residue within a peptide loop that forms the lipoyl binding domain (fig. 1.5).

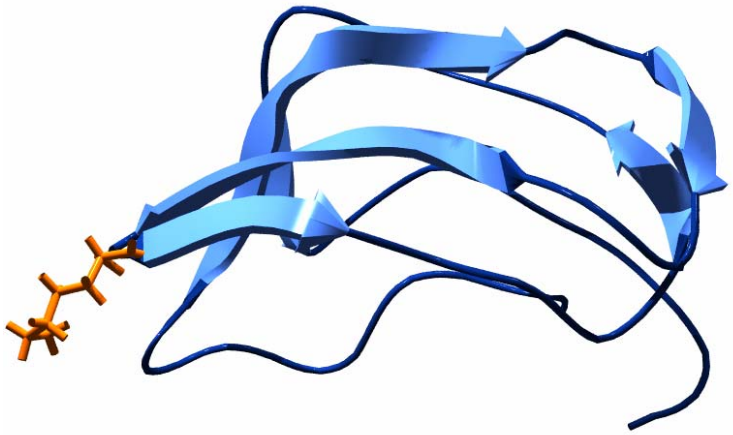

Figure 1.5 NMR structure of the E2 lipoyl domain (residues 1-79 of the E2 polypeptide chain) of *Bacillus stearothermophilus* pyruvate dehydrogenase prepared using Swiss PDB viewer taken from (17). The lysine residue involved in lipoyl binding is shown in orange.

The conversion of pyruvate to acetyl CoA is achieved by a sequence of reactions catalysed by PDH (fig. 1.6) which proceed as follows: (a) at the E1 subunit, nucleophilic attack of the TPP ylid (formed by intramolecular deprotonation of TPP) on the keto carbon of pyruvate is followed by decarboxylation to yield hydroxyethyl-TPP; (b) transfer of the

hydroxyethyl group to lipoic acid on E2 then occurs with reduction of the disulfide resulting in formation of acetyl-dihydrolipoamide; (c) the lipoyl-lysyl appendage moves back to E2 where the acyl group of acetyl-dihydrolipoamide transfers to CoA forming acetyl CoA and dihydrolipoamide; (d) the dihydrolipoamide moiety swings round to E3 where it is reoxidised to lipoamide by FAD generating an $FADH_2$ containing E3 domain; (e) oxidation of the reduced E3 domain by nicotinamide adenine dinucleotide (NAD+) completes the cycle and the complex is ready for further turnovers.

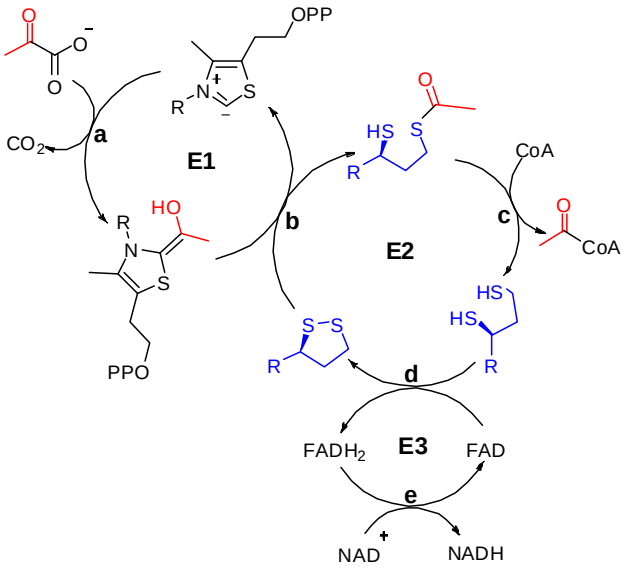

Figure 1.6 Conversion of pyruvate to acetyl CoA by PDH. The Lipoic acid moiety is shown in blue.

1.2.2 Glycine cleavage system

Lipoic acid also plays a crucial role is in the cleavage of glycine **7** by the glycine cleavage system to generate carbon dioxide, ammonia and N^5,N^{10}-methylene tetrahydrofolate **8**. The glycine cleavage sytem is a complex made up of four enzymes; glycine dehydrogenase (P protein), aminomethyltransferase (T protein), dihydrolipoyl dehydrogenase (L protein) and the H protein to which lipoic is covalently bound (15, 18-21). The lipoyl group again functions as a "swinging arm" moving between the four enzymes (fig. 1.7) to generate N^5,N^{10}-methylene tetrahydrofolate via the following reactions: (a) the lipoyl-methylamino H-protein (fig 1.8, A) is derived from glycine in a reaction catalysed by the P protein; (b) the methylamino group is delivered by the lipoyl-lysyl moiety to the T protein where it is attached to tetrahydrofolate generating N^5,N^{10}-methylene tetrahydrofolate and reduced

lipoamide H-protein (fig. 1.8, B); (c) the lipoyl group then swings to the L protein where it is oxidised to restore the lipoyl H protein (fig. 1.8, C) ready to repeat the cycle.

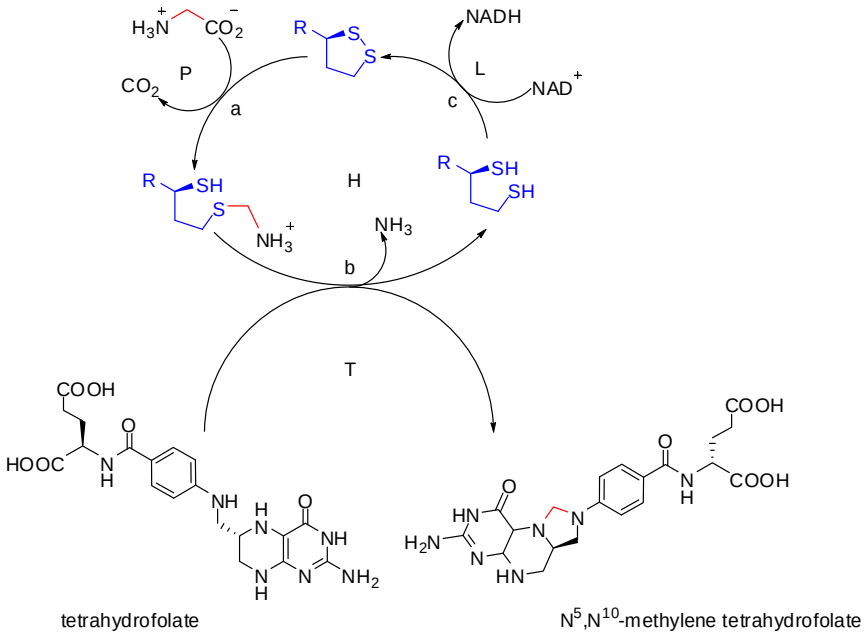

Figure 1.7 Reactions catalysed by the glycine cleavage system. The lipoic acid moiety is shown in blue.

1.3 α-Lipoic acid biosynthesis

Genetic and biochemical studies have identified that the insertion of both sulfur atoms into protein bound octanoyl groups in *E. coli* is dependant on the product of the *lipA* gene, LipA (1-3) and mutations in this gene prevent the production of lipoic acid (4). LipA is found in prokaryotes (22, 23), plants (24, 25) and mammals (26, 27).

In vivo feeding studies using ^{14}C labelled and specifically tritiated octanoic acids at the C5, C6, C7 and C8 positions confirmed that octanoic acid can act as a precursor for lipoic acid (28). The turnover of these tritium labelled acids indicated that lipoyl formation occurred with only the loss of hydrogen / tritium atoms from the C6 and C8 positions, suggesting that an unsaturated intermediate was unlikely. By the means of octanoic acids stereospecifically tritiated at the C6 position (29) and deuterium labelled acetate (30) in the feeding studies it was shown that the *Pro R* hydrogen atom is abstracted from the C6 position, showing sulfur insertion occurs at C6 with inversion.

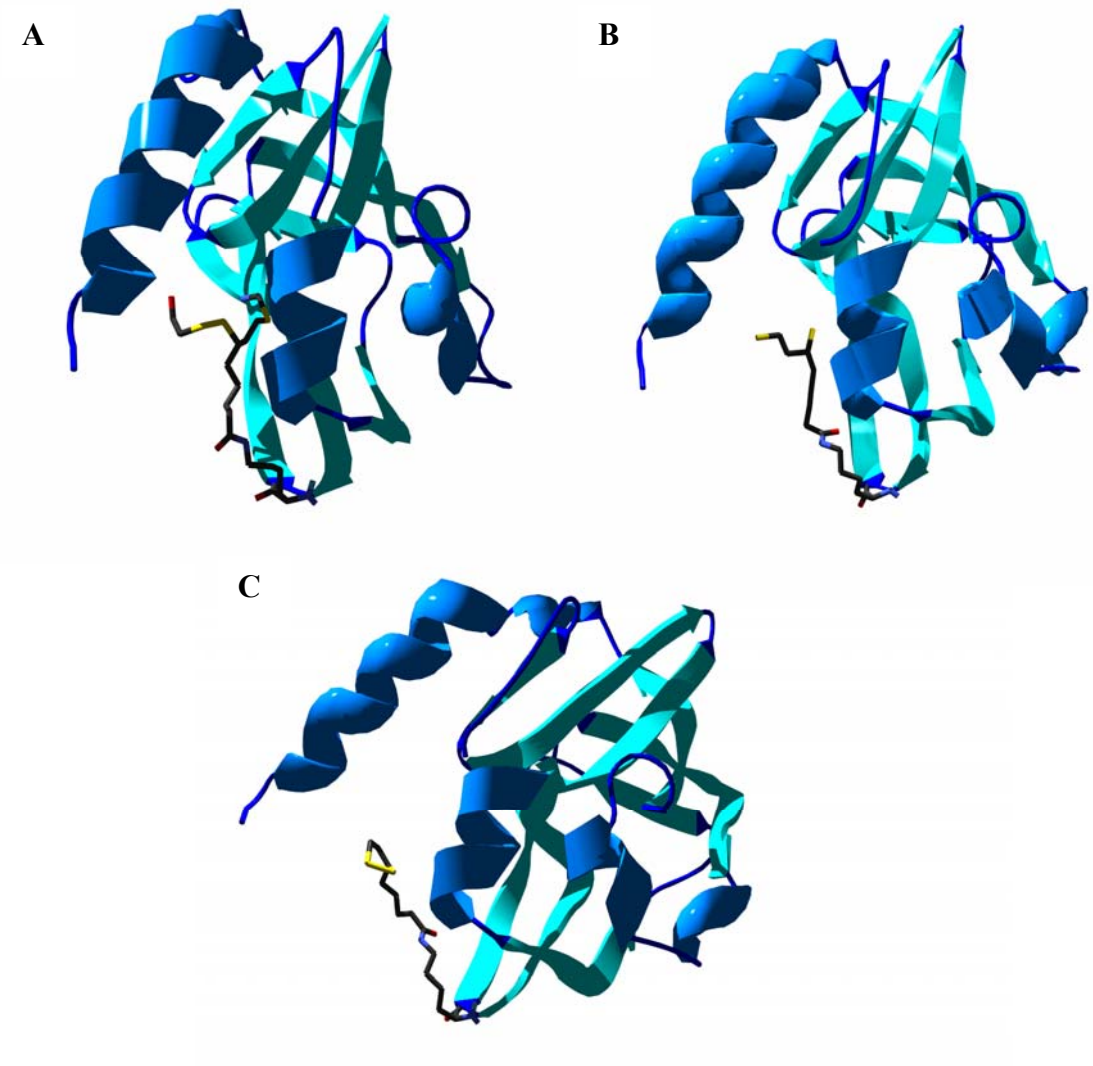

Figure 1.8 X-ray crystal structures of the *Pisum sativum* H-protein prepared using Swiss PDB viewer including lipoyl group from the glycine cleavage system: (**A**) The lipoyl group is reduced with the methylamino group bound to the C8 sulfur atom taken from (19). β-mercaptoethanol is attached at the C6 sulfur atom, however this was not present is a crystal sample prepared from protein which was purified in the absence of β-mercaptoethanol; (**B**) The lipoyl group is in the reduced form taken from (21); (**C**) the lipoyl group is in the oxidised form taken from (20).

LipA has been identified as a member of the emerging "radical S-adenosyl methionine (SAM) superfamily" (31) which uses SAM as a cofactor to generate highly reactive 5'-deoxadenosyl radical (Ado•) that can then be used in subsequent chemistry.

1.3.1 Radical SAM superfamily

The radical SAM superfamily of proteins consists of at least 600 members which are largely uncharacterised (31). The common characteristics of proteins within this family are the presence of a $[4Fe\text{-}4S]^{1+/2+}$ cluster coordinated by three cysteine residues of a conserved CX_3CX_2C motif (table. 1.1) (32-36) and the requirement of SAM **9** (fig. 1.9, a) for activity. The proposed CX_3CX_2C binding motif was first shown by mutagenesis of the CX_3CX_2C binding site in the *E. coli* proteins BioB (32, 33), HemN (34), ARR-AE (35) and LipA (36).

Members of this family are involved in a diverse range of reactions (fig. 1.9, b-e) but are believed to share a common mechanistic step that utilise their iron sulfur cluster to initiate the reductive cleavage of SAM **9** (fig. 1.9, a) by donation of an electron to the sulfonium centre of SAM **9** to generate a highly reactive 5'-deoxadenosyl radical (Ado•) **10** (fig. 1.9) to initiate radical chemistry on the substrate (37, 38).

Protein	**Residues**	**Sequence**											
LipA	92-103	A	I	**C**	T	R	R	**C**	P	F	**C**	D	V
BioB	51-62	G	A	**C**	P	E	D	**C**	X	Y	**C**	P	Q
MiaB	155-166	E	G	**C**	N	K	Y	**C**	T	Y	**C**	P	Q
ARR-AE	24-35	S	G	**C**	V	H	E	**C**	P	G	**C**	Y	N
PFL-AE	28-39	Q	G	**C**	L	M	R	**C**	L	Y	**C**	H	N
KAM	131-142	N	Q	**C**	S	M	Y	**C**	R	Y	**C**	T	R
HemN	60-71	P	F	**C**	H	K	L	**C**	Y	F	**C**	G	C

Table 1.1 Alignment of amino acid sequences of radical SAM enzymes from *E. coli*; lipoyl synthase (LipA), biotin synthase (BioB), 2-methylthio-N-6-isopentyl adenosine synthase (MiaB), anaerobic ribonucleotide reductase activating enzyme (ARR-AE), pyruvate formate lyase activating enzyme (PFL-AE), lysine 2,3-aminomutase (KAM) and oxygen independent coproporphyrinogen III oxidase HemN. The CX_3CX_2C motifs that are involved in iron sulfur cluster binding are highlighted.

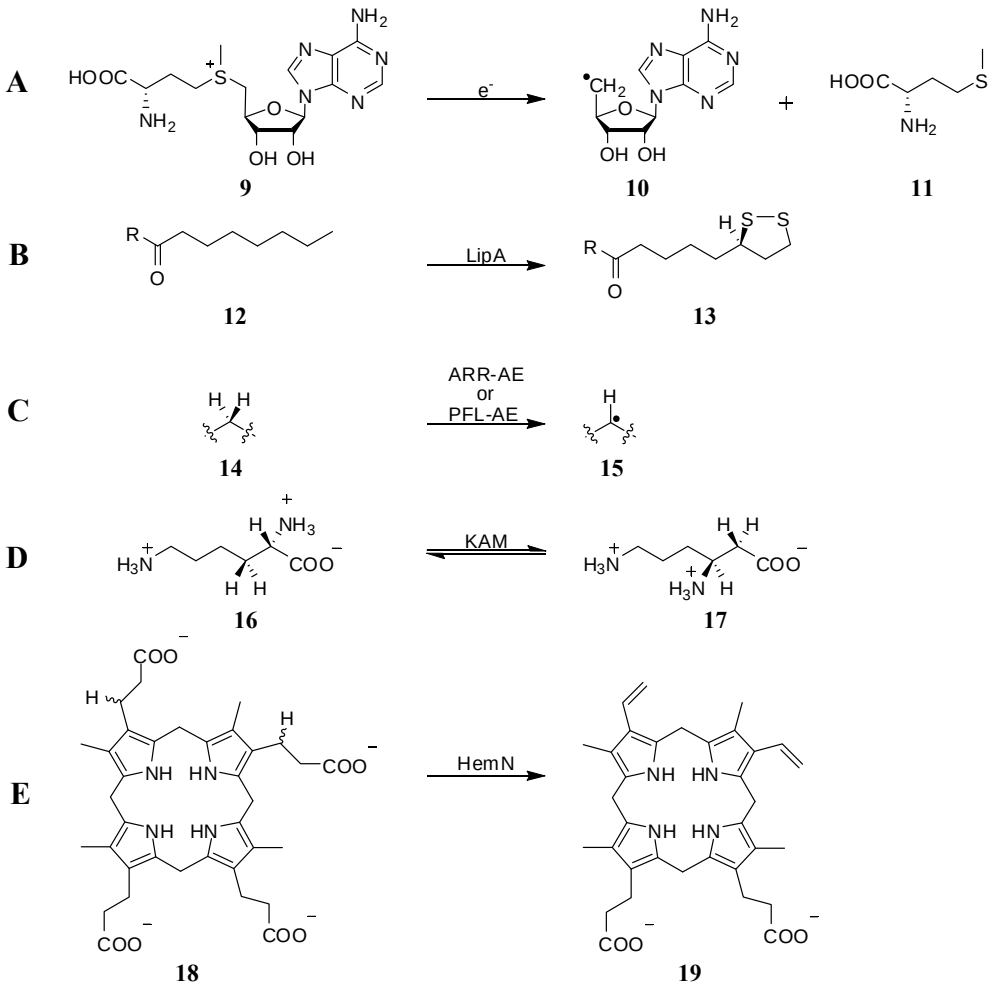

Figure 1.9 Example reactions which utilise radical SAM proteins: (**A**) reductive cleavage of SAM **9** to generate Ado• **10** and methionine **11**, a reaction common to all radical SAM proteins; (**B**) sulfur insertion into an octanoyl group **12** by LipA to generate a lipoyl group **13**; (**C**) hydrogen atom abstraction from a glycine residue **14** to generate a glycyl radical **15** at specific residues of anaerobic ribonucleotide reductase (ARR) and pyruvate formate lyase (PFL) by their respective activating enzymes (ARR-AE and PFL-AE); (**D**) conversion of the amino acid lysine **16** to β-lysine **17** by lysine 2,3-aminomutase (KAM); (**E**) oxidative decarboxylation of coproporphyrinogen III **18** to protoporphrinogen **19** by oxygen independent coproporphyrinogen III oxidase (HemN).

A close interaction between SAM and the $[4Fe\text{-}4S]^{1+}$ cluster cofactors exists as indicated by Mössbauer, electron paramagnetic resonance (EPR) and resonance Raman spectroscopy (39-42). The interaction of SAM and the $[4Fe\text{-}4S]^{1+/2+}$ cluster of PFL-AE and KAM has also been probed using electron nuclear double resonance spectroscopy (ENDOR) which shows that that SAM binds as a bidentate ligand coordinated through the amino nitrogen and a carboxylate oxygen of the methionine moiety (fig. 1.10)

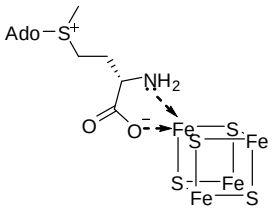

Figure 1.10 Binding of SAM to a unique Fe site of the $[4Fe\text{-}4S]^{1+}$ cluster of radical SAM superfamily.

Publication of the crystal structures of BioB (fig. 1.11, **A**) (43), KAM (fig. 1.11, **B**) (44), HemN (fig. 1.11, **D**) (45) and MoaA (fig. 1.11, **E**) (46) in the presence of SAM provided confirmation that three of the four iron centers in the cluster are coordinated by one of the cysteines in the CX_3CX_2C motif whilst the fourth iron center binds SAM.

General mechanism common to all radical SAM proteins

Although it has been shown that it is only the $[4Fe\text{-}4S]^{1+}$ cluster that is used to initiate the radical chemistry (47-49), both $[3Fe\text{-}4S]^{1+}$ and $[2Fe\text{-}2S]^{1+/2+}$ clusters have been observed in radical SAM proteins (50). These other cluster types can be formed as a result of oxidative degradation of the $[4Fe\text{-}4S]^{1+}$ cluster. A $[4Fe\text{-}4S]^{2+}$ cluster containing species can also be observed which is the inactive form. The active $[4Fe\text{-}4S]^{1+}$ cluster can be reformed upon reduction (50-54) or reconstitution with exogenous iron and sulfide.

The generation of Ado• by radical SAM proteins begins with the reduction of the inactive $[4Fe\text{-}4S]^{2+}$ cluster to the active $[4Fe\text{-}4S]^{1+}$ state (fig. 1.12, a). The reducing equivalents can be supplied by the natural reducing system *ie*. flavodoxin, flavodoxin reductase and NADPH (55-57), by a chemical reductant *ie*. sodium dithionite (5) or by photoreduced deazaflavin (58). It has been stereoscopically observed using PFL-AE and BioB that turnover is accompanied by oxidation of the $[4Fe\text{-}4S]^{1+}$ cluster to a $[4Fe\text{-}4S]^{2+}$ cluster (48, 59), which is consistent with the donation of a single electron to the to the sulfonium center of SAM. It has been proposed that this results in homolytic cleavage of the C-S bond between the adenosine and methionine moieties to generate the Ado• radical and methionine (fig. 1.12, b). The Ado• radical then abstracts a hydrogen atom from the substrate (fig. 1.12, c) leading to product formation.

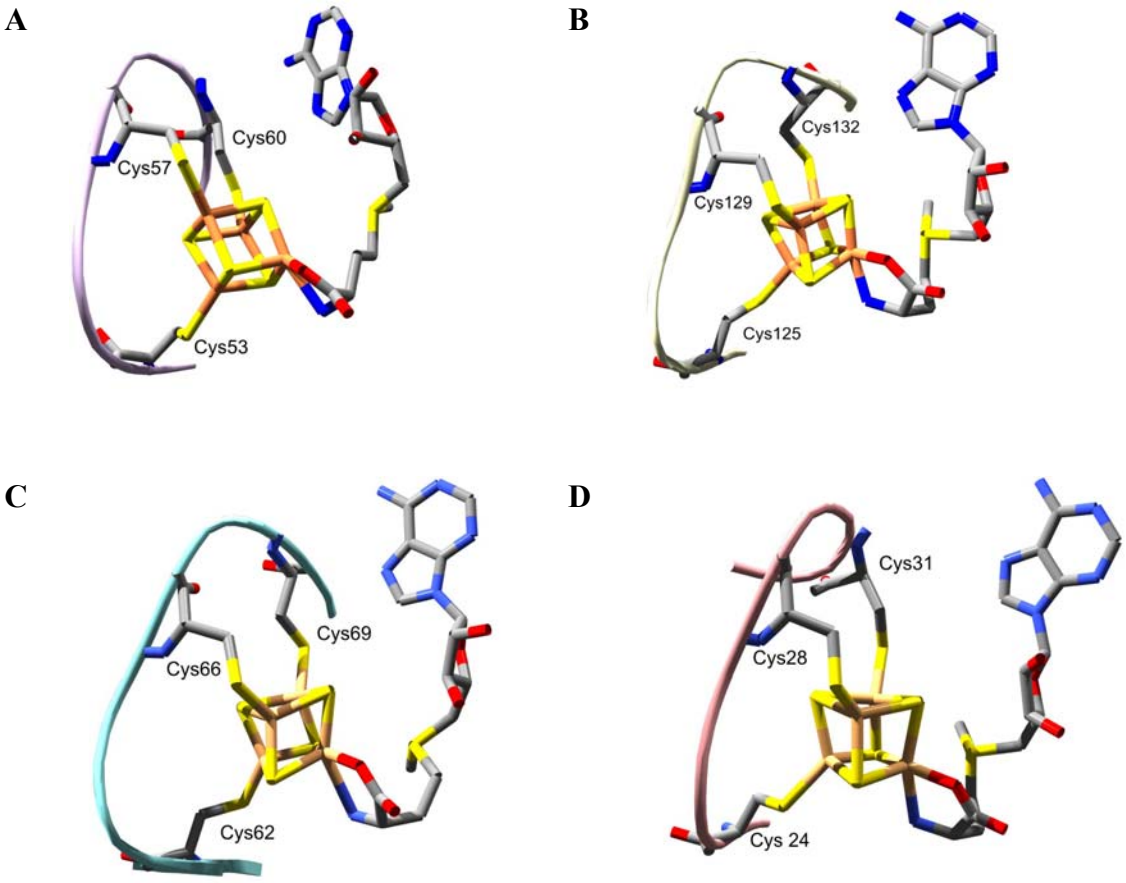

Figure 1.11 Binding of SAM to a unique Fe site of the $[4Fe\text{-}4S]^{1+}$ cluster of radical SAM proteins from *E. coli* unless otherwise stated: (**A**) BioB (*54*); (**B**) KAM (*Clostridium subterminale*) (*55*); (**C**) HemN (*56*); (**D**) MoaA (*57*).

The abstraction of a hydrogen atom from the substrate by Ado• has been demonstrated using deuterated substrates (5, 60-63) but a substrate radical has only been observed in the case of PFL-AE and ARR-AE where the hydrogen atom abstraction generates a stable glycyl radical which can be observed by EPR (48, 64). Although the formation of methionine and AdoH has been detected in reactions using radical SAM proteins (59, 60, 65, 66) the Ado• radical has not been directly observed. However, experiments using S-3',4'-anhydroadenosylmethionine **19** (fig. 1.13) (an unsaturated analogue of SAM) in a reaction with KAM produced a stabilised allylic radical **20** (fig. 1.13) which has been characterised by EPR spectroscopy (49, 51).

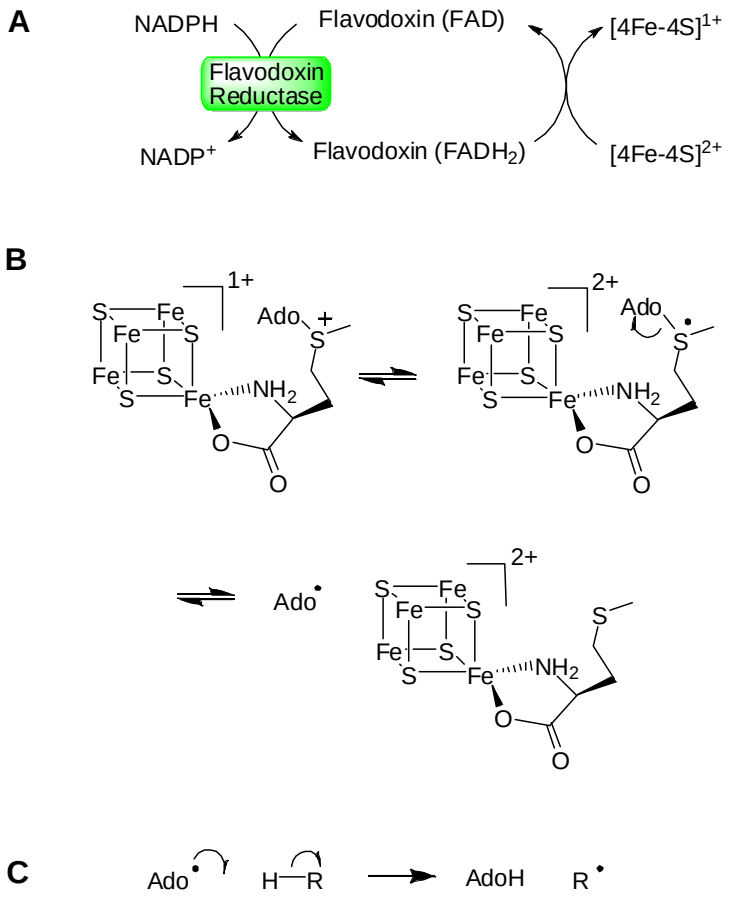

Figure 1.12 General mechanism common to all radical SAM proteins: (**A**) Reduction of the [4Fe-4S] cluster which is ligated by a CX_3CX_2C motif common to these proteins; (**B**) electron transfer from the reduced cluster to the sulfonium group of SAM and subsequent homolytic cleavage of the C-S bond to generate an Ado• radical; (**C**) hydrogen atom abstraction from the substrate by an Ado• radical.

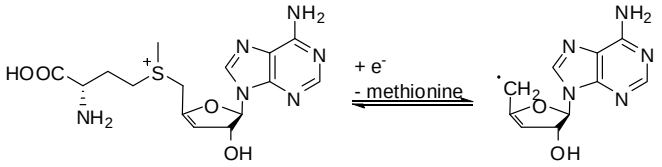

Figure 1.13 S-3',4'-anhydroadenosylmethionine **19**, a SAM analogue which when cleaved in a reaction using KAM generated the stabalised allylic radical **20**.

Sulfur insertion by radical SAM proteins

Radical SAM proteins are involved in a broad range of chemistry and one intriguing area is the ability of some members to mediate the insertion of sulfur into unactivated C-H bonds.

This leads to the biosynthesis of important metabolites such as lipoic acid by LipA and biotin by BioB.

The best characterised member of the radical SAM family involved in sulfur insertion reactions is BioB and a number of parallels can be drawn between this protein and LipA.

1.3.2 Lipoyl synthase (LipA)

The protein LipA is responsible for the final step in lipoate biosynthesis, the formation of lipoate **12** from octanoate **11** (fig. 1.14) (1-3).

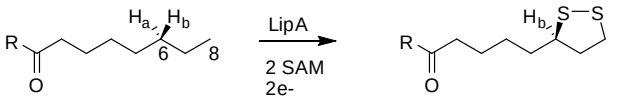

12 **13**

Figure 1.14 Conversion of an octanoyl moiety **12** to a lipoyl moiety by LipA **13** showing inversion of steroechemestry at C6. In octanoate **12**, H_a is *pro-R* and H_b is *pro-S*

Due to the sequence similarities with BioB and of the reactions catalyzed by LipA and BioB, it was postulated that LipA was an iron sulfur protein (2, 4). Inductively coupled plasma atomic emission spectroscopy (ICP) has confirmed that iron was the only metal detected in isolated homogenous LipA protein, which has a dark reddish-brown colour (67). Iron and sulfide were detected in equimolar quantities and further characterisation by UV/vis, resonance Raman and EPR spectroscopy was consistent with the presence of only a single $[4Fe\text{-}4S]^{1+/2+}$ cluster per dimer (67, 68). Exposure to air resulted in the quantitative conversion of the $[4Fe\text{-}4S]^{1+/2+}$ cluster to a $[2Fe\text{-}2S]^{2+}$ cluster, whist anaerobic treatment with sodium dithionite or photoreduced 5'-deazaflavin generated purely the $[4Fe\text{-}4S]^{1+}$ cluster containing form (69). Reconstitution of the protein under anaerobic conditions with iron and sulfide in the presence of DTT was reported to generate one $[4Fe\text{-}4S]^{1+/2+}$ cluster per LipA monomer (69).

Detailed spectroscopic studies have recently showed that *E. coli* LipA can accommodate a second iron sulfur cluster (36). Two potential binding sites were identified, the CX_3CX_2C motif characteristic to radical SAM proteins and a CX_4CX_5C motif found in the N-terminal

region. The second iron sulfur cluster binding motif is conserved among LipA sequences from a wide range of organisms (table. 1.2). Mössbauer spectroscopy of labelled mutants has shown that both binding sites are capable of binding a $[4Fe\text{-}4S]^{2+}$ cluster (36). EPR spectroscopy has been used to show that the protein can still bind an intact $[4Fe\text{-}4S]^{1+}$ cluster in samples containing triple variants in which the three cysteine residues from either of the sites were replaced with alanine. The spectroscopic data for each of these mutants varies slightly, consistent with clusters bound in slightly different local environments. The CX_3CX_2C motif most closely resembles the clusters typically observed in radical SAM proteins and is thought to be responsible for the reductive cleavage of SAM. The second cluster is postulated to function as the sulfur donor, but this has not been unequivocally demonstrated.

LipA substrate identification

Although octanoic acid is a precursor for the biosynthesis of lipoic acid, it can not directly serve as the substrate for LipA in *in vitro* assays (fig. 1.15) (5). *In vitro* activity was first achieved by incubating sodium dithionite reduced *E. coli* LipA with octanoylated acyl carrier protein (ACP), SAM, apo-PDH and lipoyl-[ACP]-protein-*N*-lipoyltransferase (LipB) (fig. 1.15). Confirmation of lipoyl formation was achieved in a coupled enzymatic assay by spectrophotometrically monitoring the reduction of a NAD+ analogue and by matrix assisted laser desorption ionisation (MALDI) mass spectroscopy of the lipoylated E2-PDH (5). The assay showed for the first time that SAM was required for activity of LipA as well as reduction to generate the $[4Fe\text{-}4S]^{1+}$ cluster.

However, lipoyl-ACP **24** was not isolated or detected and therefore the true product of LipA could not be conclusively determined since LipB can transfer either octanoyl or lipoyl groups (70), meaning octanylation of E2-PDH might precede lipoyl formation (fig. 1.16).

Organism	Binding sequence 1 (XCX_4CX_5CX)															Binding sequence 2 (XCX_3CX_2CX)										
	Residues	Sequence														Residues	Sequence									
E. coli	67-80	V	**C**	E	E	A	S	**C**	P	N	L	A	E	**C**	F	93-102	I	**C**	T	R	R	**C**	P	F	**C**	D
Anabaena sp	43-56	V	**C**	E	E	A	S	**C**	P	N	I	G	E	**C**	F	69-78	A	**C**	T	R	A	**C**	P	Y	**C**	D
B. anthracis	39-42	V	**C**	E	E	A	K	**C**	P	N	I	H	E	**C**	W	66-75	V	**C**	T	R	A	**C**	R	F	**C**	A
P. torridus	33-46	V	**C**	E	E	A	H	**C**	P	N	I	A	E	**C**	W	59-68	N	**C**	S	R	G	**C**	R	F	**C**	A
S. solfataricus	30-43	V	**C**	E	E	A	L	**C**	P	N	I	M	E	**C**	W	56-65	I	**C**	T	R	G	**C**	R	F	**C**	Y
Y. pestis	67-80	V	**C**	E	E	A	S	**C**	P	N	L	S	E	**C**	F	93-102	I	**C**	T	R	R	**C**	P	F	**C**	D
B. Suis	59-72	V	**C**	E	E	A	G	**C**	P	N	I	G	E	**C**	W	85-94	I	**C**	T	R	A	**C**	A	F	**C**	N
R. bellii	85-98	V	**C**	E	E	A	A	**C**	P	N	I	G	E	**C**	W	111-120	V	**C**	T	R	A	**C**	R	F	**C**	N
H. sapiens	105-118	V	**C**	E	E	A	R	**C**	P	N	I	G	E	**C**	W	135-144	T	**C**	T	R	G	**C**	R	F	**C**	S
S. cerevisiae	149-162	V	**C**	E	E	A	R	**C**	P	N	I	G	E	**C**	W	180-189	T	**C**	T	R	G	**C**	R	F	**C**	S
A. thaliana	102-115	V	**C**	E	E	A	K	**C**	P	N	L	G	E	**C**	W	133-142	T	**C**	T	R	G	**C**	R	F	**C**	N

Table 1.2 Alignment of FeS cluster binding amino acid sequences of LipA's from the following organisms; *Escherichia coli* (*E. coli*), *Anabaena sp.* strain PCC 7120, *Bacillus anthracis* (*B. anthracis*), *Picrophilus torridus* (*P. torridus*), *Solfolubus solfataricus* (*S. solfataricus*), *Yersinia pestis* (*Y. pestis*), *Brucella suis* (*B. suis*), *Rickettsia bellii* (*R. bellii*), *Homo sapiens (H. sapiens), Saccharomyces cerevisiae (S. cerevisiae)* and *Arabidopsis thaliana (A. thaliana).*

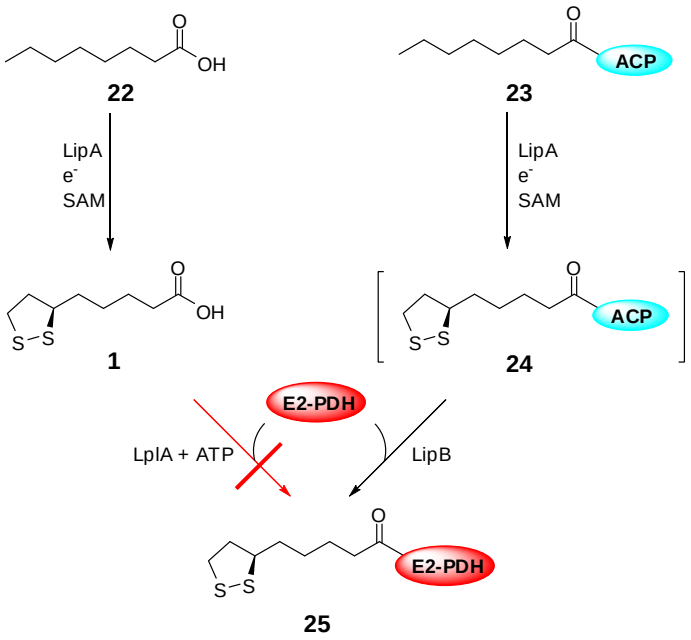

Figure 1.15 The first *in vitro* analysis of LipA, showing octanoic acid **22** was not the substrate for LipA. Formation of lipoyl-(E2-PDH) **25,** was not detected in an assay using octanoic acid **22** as the substrate, but was detected when octanoyl-ACP **23** was incubated with LipA, dithiionite, SAM, apo-PDH and LipB.

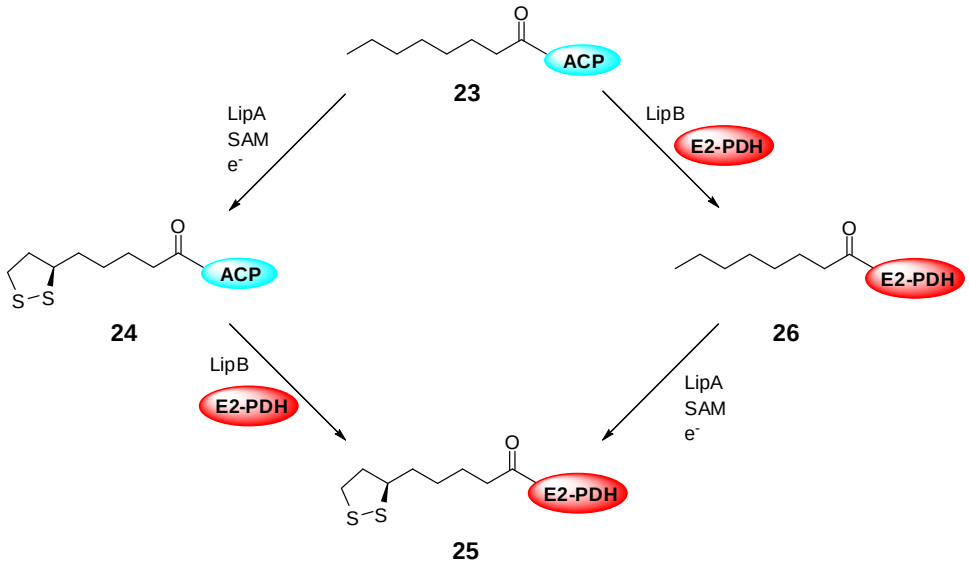

Figure 1.16 Two alternate pathways may exist, which both can occur by incubating octanoyl-ACP **23** with LipA, dithiionite, SAM, apo-PDH and LipB.

It has now been shown that the preferred substrates for LipA are the octanoylated derivatives of lipoyl accepting domains (60, 71). The conversion of these domains was demonstrated *in vivo* using *E. coli* that was lacking LipA activity supplemented with D_{15}-octanoic acid in order to accumulate an octanoyl-E2 domain which was distinguishable by mass spectrometry to endogenously-synthesised octanoate (71). Transduction of the labelled cells with phage λ particles containing a *lipA* cosmid led to LipA activity resulting in lipoylated E2 domains, observed by mass spectrometry. This preference was shown *in vitro* by following the consumption of the substrate SAM by the generation of the products AdoH and methionine in two assays; the first used octanoyl-ACP **23** as the substrate and the second using octanoyl-E2 **26** as the substrate. In the case of the octanoyl-ACP, <5 pmol SAM was consumed and no lipoylated products were detected. However, in the case of octanoyl-E2, lipoyl-E2 **25** was detected and 1050 pmol SAM was consumed (71). The formation of the octanoylated lipoyl domains can be achieved in nature using one of two independent systems (fig. 1.17) (72). The first uses LipB which catalyses the transfer of octanoyl groups from octanoyl-ACP (a product of fatty acid biosynthesis) to the E2 domain and the second uses LplA with free octanoate, requiring activation using adenosine triphosphate (ATP).

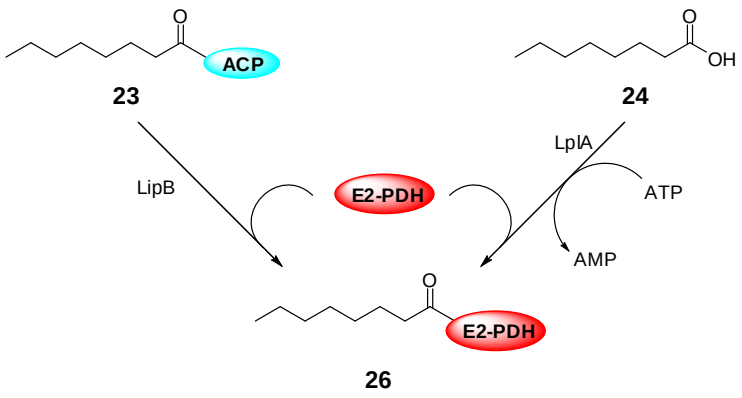

Figure 1.17 Biosynthetic pathway for octanoylated lipoyl domains **26** using LipB and octanoyl-ACP **23** or LplA and octanoic acid **22**. The E2 domain of PDH has been used as an example.

This biosynthetic pathway was further supported by the *in vitro* use of an octanoylated H-protein from the glycine cleavage system as the substrate for LipA (60). Using this protein as the substrate in the presence of SAM and flavodoxin, flavodoxin reductase and NADPH, homogenous *E. coli* LipA was able to produce the lipoyl H-protein in a

substoichemetric quantity (0.36 molar equivalents per LipA monomer). This led to speculation that either 2 equivalents of LipA were required for the formation of 1 equivalent of lipoyl product requiring release of an intermediate from the protein or that some of the LipA was not in an active configuration. Experiments that were subsequently carried out using an equimolar mixture of ^{34}S labelled LipA and ^{32}S LipA indicated that the latter hypothesis was the most likely (73). These investigations used gas chromatography – mass spectrometry (GC-MS) analysis to determine the ratio of the product masses in the absence of any other sulfur source. If a second equivalent of LipA was required for lipoyl formation, a monothiolated species would have to dissociate from the LipA monomer following the first sulfur insertion reaction and then bind to a second LipA monomer resulting in a mixture of $^{32}S/^{32}S$, $^{34}S/^{32}S$ and $^{34}S/^{34}S$ in a 1:2:1 ratio. However these reactions yielded an approximately equimolar amount of $^{34}S/^{34}S$ and $^{32}S/^{32}S$ lipoyl H-protein suggesting that both sulfur atoms were most likely derived from the same LipA monomer.

Mechanism of lipoyl group formation by LipA

The formation of lipoyl moieties from octanoylated derivatives of lipoyl accepting domains requires the regio- and stereo-selective insertion of sulfur into the unactivated C6 and C8 positions of the protein bound derivative of octanoic acid. The unreactive nature of the C-H bonds and the requirement of a radical SAM protein led to the hypothesis that the two hydrogen atoms are abstracted by Ado• radicals. The formation of AdoH and methionine upon cleavage of SAM has been demonstrated (71) and quantified using the H-protein of the glycine cleavage system as a substrate to show that at least two equivalents of SAM are used to generate one equivalent of lipoate (60). Using a deuterium labelled D_{15}-octanoyl H-protein as the substrate in the assay resulted in the detection of 5'-D-5'-deoxyadenosine (AdoD) providing evidence for the direct action of Ado• on the substrate (60). Lipoylated-H-protein was not detected in the reactions using the deuterium labelled D_{15}-octanoyl H-protein as the substrate; however a new product was detected with a mass corresponding to a monothiolated intermediate. This possibly indicates that a significant deuterium kinetic isotope effect (KIE) exists for the hydrogen abstraction at either the C6 or C8 position but failed to identify which sulfur atom is inserted first, at C8 **27**, or C6 **28** (fig. 1.18).

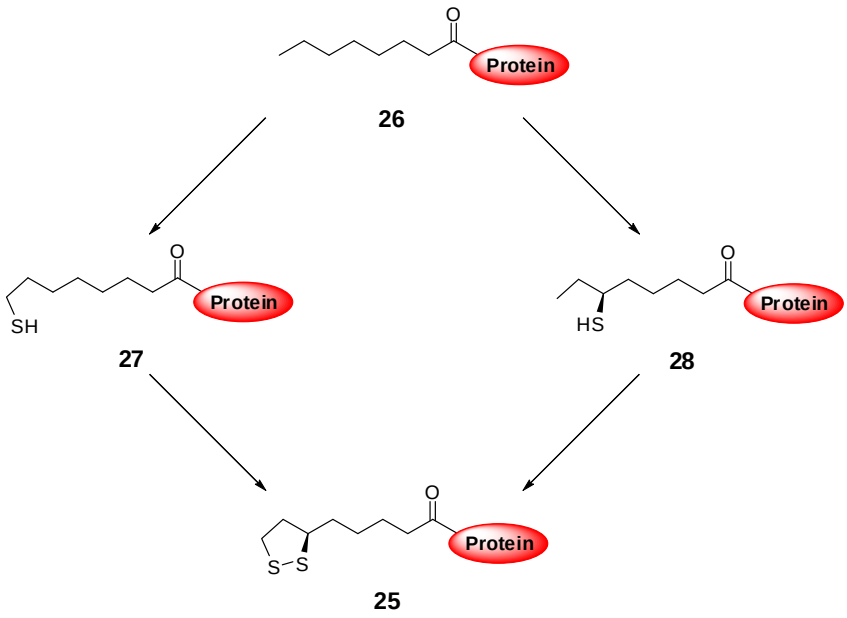

Figure 1.18 Two alternate pathways for lipoate biosynthesis. Sulfur insertion could occur first at C8 followed by C6 or *vice versa*.

Inversion of the stereochemistry at C6 was shown using octanoic acid stereospecifically tritiated at the C6 position (29) and deuterium labelled acetate (30) in feeding studies. In addition, *in vivo* feeding studies using octanoic acids specifically tritiated at the C5, C6, C7 and C8 positions indicated that lipoyl formation occurred with only the loss of hydrogen / tritium atoms from the C6 and C8 positions (28) probably ruling out the possibility of an unsaturated intermediate. It was postulated that inversion of stereochemistry could be a result of an initial hydroxylation at C6 followed by activation and substitution by sulfur derived nucleophiles (74). However, *in vivo* feeding studies using the carboxylic acids [8-$^{2}H_{2}$]-8-hydroxyoctanoic acid, [6(RS)-^{2}H]-6-hydroxyoctanoic acid and [8-$^{2}H_{2}$]-(±)-6,8-dihydroxyoctanoic indicated that none of the compounds were converted into lipoic acid and could not be intermediate species. By contrast, the carboxylic acids [8-$^{2}H_{2}$]-8-thiooctanoic and [6(RS)-^{2}H]-6-thiooctanoic acid when used *in vivo* were both converted into lipoic acid. [6(RS)-^{2}H]-6-thiooctanoic acid was only being converted 10-20% as efficiently as [8-$^{2}H_{2}$]-8-thiooctanoic acid, suggesting that 8-thiooctanoic acid was an intermediate in lipoyl biosynthesis (74).

The development of a new *in vitro* assay utilising a synthetic peptide mimic of the octanoylated derivative of the E2 subunit of PDH from *S. solfataricus* (75) could first mark

potential for the determination of the order of sulfur insertion. AdoH formation was consistent with generation of AdoH observed using other systems. The surrogate substrate for the E2 like domain led to products which are potentially easy to isolate and characterise offering improved analysis of the LipA reaction.

The source of sulfur is unknown. However, the formation of purely ^{34}S labelled or unlabelled lipoyl product in reactions containing an equimolar mix of ^{34}S labelled LipA and ^{32}S LipA suggests that the sulfur source is related to the protein (73). It has been proposed that the second cluster in LipA may act as the source of sulfur in these reactions (36).

1.3.3 Biotin synthase (BioB)

The protein BioB, the product of the *bioB* gene, is responsible for the final step in biotin biosynthesis (fig. 1.20), the formation of biotin **29** from dethiobiotin (DTB) **28** (76, 77).

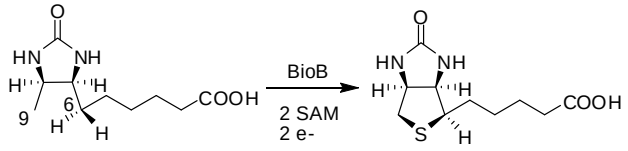

28 **29**

Figure 1.20 Conversion of DTB **28** to biotin **29** by BioB.

Like LipA, BioB is required for C-S bond formation at unactivated carbon centers (69), in the case of BioB, the insertion of a single sulfur atom between the C6 and C9 carbons of DTB **28** (fig. 1.20). SAM is required for activity (77-80) as well as a flavodoxin, flavodoxin reductase and NADPH (76, 78) or a photoreduced deazaflavin reducing system (58, 81). Experiments using isotopically labelled DTB indicate that only two hydrogen atoms are lost in biotin formation, one from the C6 and one from the C9 positions of DTB (82, 83). Unlike LipA, sulfur insertion at the C6 centre of DTB was shown to proceed with retention of configuration (84).

BioB is isolated aerobically as a red solution and ICP has shown iron to be the only metal present. Iron and sulfide has been detected in equimolar quantities and further

characterisation by UV-vis and EPR suggested the presence of a $[2Fe\text{-}2S]^{1+/2+}$ cluster (76) but this protein sample was found to be inactive. However, Mössbaurer spectroscopy studies of whole cells overexpressing BioB have found that *in vivo* the protein contains only $[2Fe\text{-}2S]^{1+/2+}$ (85) or $[4Fe\text{-}4S]^{1+/2+}$ and $[2Fe\text{-}2S]^{1+/2+}$ in a 1:3 ratio (86). The protein isolated aerobically was sacrificially made active by the anaerobic incubation of the purified protein with dithionite in 60% (v/v) glycerol, which combined two inactive $[2Fe\text{-}2S]^{1+/2+}$ clusters from separate protein monomers to form one active $[4Fe\text{-}4S]^{1+}$ cluster (51, 54). Active protein was also produced non-sacrificially by anaerobic treatment of the purified protein with exogenous iron and sulfide in the presence of DTT (76). This chemical reconstitution generated protein containing two types of clusters per monomer, a $[2Fe\text{-}2S]^{1+/2+}$ and a $[4Fe\text{-}4S]^{1+/2+}$ (87). The aerobic isolation of inactive protein containing only the inactive [2Fe-2S] clusters is most likely a result of oxidative degradation of the required [4Fe-4S] cluster during purification (69, 88). The CX_3CX_2C binding motif characteristic of radical SAM proteins is conserved in the BioB sequence (table. 1.3). The identification of this motif, the characterization of BioB as an FeS protein (76) and the requirement of SAM to generate AdoH and methionine (89, 90) has led to it's subsequent assignment as a member of the radical SAM superfamily.

Organism	**Binding Sequence (XCX_3CX_2CX)**									
	Residues	**Sequence**								
E. coli	52-61	A	**C**	P	E	D	**C**	K	Y	**C**	P
S. solfataricus	47-56	G	**C**	K	A	N	**C**	S	Y	**C**	G
Y. pestis	52-61	A	**C**	P	E	D	**C**	K	Y	**C**	P
S.cerevisiae	98-107	G	**C**	S	E	D	**C**	K	Y	**C**	A
B. subtilus	64-73	L	**C**	P	E	N	**C**	G	Y	**C**	S
A. thaliana	93-102	G	**C**	S	E	D	**C**	S	Y	**C**	P

Table 1.3 Alignment of Radical SAM FeS cluster binding amino acid sequences of BioB's from the indicated organisms.

More recent Mössbauer spectroscopy has demonstrated that BioB can harbor two distinct FeS clusters, a $[4Fe\text{-}4S]^{2+}$ and a $[2Fe\text{-}2S]^{2+}$ in a ratio of 1:0.8 by specifically incorporating ^{57}Fe into either of the two clusters (91). BioB contains six conserved cysteine residues, three are contained in the radical SAM CX_3CX_2C motif and the other three are spread over

a region 91 residues, in the case of *E. coli* they are Cys-97,128 and 188. Mutation of the cysteines residues associated with the radical SAM CX_3CX_2C motif to alanines resulted in inactive protein, which can not be reconstituted with a [4Fe-4S] cluster (32, 33, 59). Mutation of the other three cysteine residues results in protein that can be reconstituted with a [4Fe-4S] cluster but mutants are still inactive for biotin synthesis (33). These other three cysteines residues have been proposed to chelate the second [2Fe-2S] cluster (91) which is believed to be required for activity, presumably for the donation of the sulfur atom.

Crystal structure of BioB

The crystal structure of *E. coli* BioB has confirmed the binding motifs of the two clusters (43). The homodimeric apoprotein was first reconstituted with iron and sulfide before being co-crystallised with SAM and DTB and the structure solved to a 3.4 Å resolution (fig. 1.21).

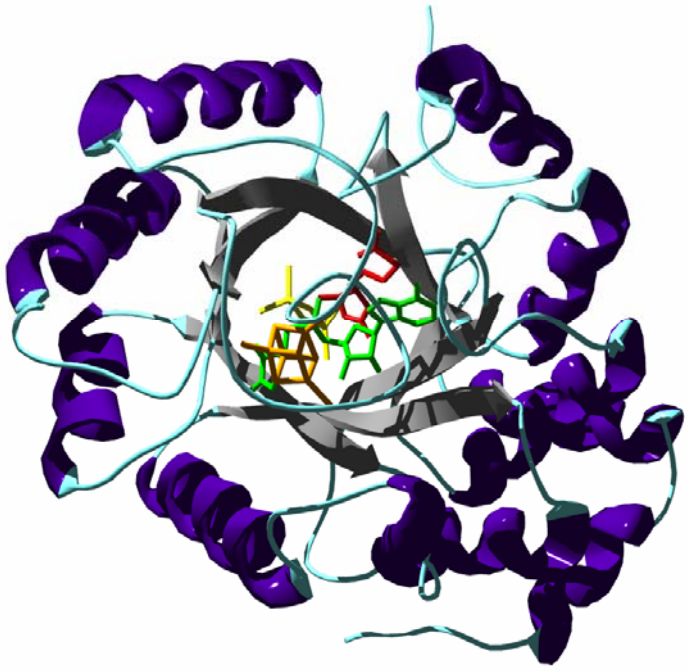

Figure 1.21 Crystal structure of *E. coli* biotin synthase homodimer showing the $[4Fe\text{-}4S]^{2+}$ clusters (orange), $[2Fe\text{-}2S]^{2+}$ clusters (yellow), SAM (green) and DTB (red) (43).

The fold of each subunit of the BioB dimer is a triosephosphate isomerase (TIM) type $(\alpha/\beta)_8$ barrel with two additional helices at the N terminus and a distorted region at the C terminus. The structure showed that each monomer binds a [4Fe-4S] cluster close to the surface of the protein, chelated by the three cysteines from the CX_3CX_2C motif, found in a 28 residue loop extending from β strand 1 to helix 1 at the C terminal end of the TIM barrel and a [2Fe-2S] cluster bound by the β strand Cys-97, 128, 188 and Arg-260 residues deep within the barrel.

The coordination of a metal by an arginine residue is rare in biology and as such was thought perhaps to have an unique catalytic or structural role (92). Mutagenesis has been used to investigate the effect of replacing Arg260 with the more conventional metal ligands histidine, cysteine or methionine and also with alanine as a control. Each of the four mutants remained capable of binding the $[2Fe\text{-}2S]^{1+/2+}$ cluster and there was no notable effect on activity. Therefore the coordination of the cluster by arginine does not appear to be essential and the reason for its coordination by this unusual ligand remains unknown. It was postulated that this residue could rearrange to bridge the two iron atoms of the [2Fe-2S] cluster if one of the sulfur atoms was donated to DTB (43) to generate biotin. It remains to be seen if a similar ligand is involved in the binding of the second [4Fe-4S] cluster of LipA.

The active site lies between the two clusters and contained SAM and DTB. SAM chelates the final iron center of the [4Fe-4S] cluster through both the amino and carboxylate groups of the methionine moiety (fig. 1.22) and this structure is consistent with changes observed in Mössbauer, resonance Raman spectroscopy (40) and UV-vis (93) that occur upon the addition of SAM.

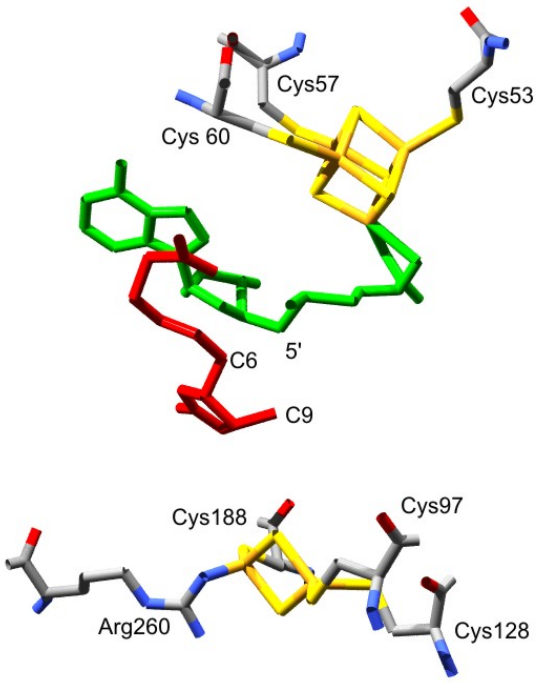

Figure 1.22 Structure of BioB showing iron sulfur cluster and substrate binding. The $[4Fe\text{-}4S]^{2+}$ cluster is coordinated by Cys53, Cys57 and C60. The final Fe site of this cluster is coordinated by SAM. The 5' position of SAM lies ~3.9 Å from C9 of DTB. The $[2Fe\text{-}2S]^{2+}$ is also found in close proximity to DTB and is coordinated by Cys97, Cys128, Cys188 and Arg260.

Within the barrel SAM is completely shielded from solvent and appears to be ideally positioned to receive an electron from the cluster to cleave SAM generating Ado•, which can, in turn, abstract a hydrogen atom from DTB. The C9 position of DTB lies ~ 4.6 Å from the nearest [2Fe-2S] cluster sulfide (fig. 1.22) which is suitably positioned to play a role in of sulfur insertion (43).

Source of sulfur in biotin biosynthesis

The debate into the source of sulfur in the final step of biotin biosynthesis has led to a number of hypothesises being put forward. For example it was reported that when assaying BioB in a reaction mixture containing whole cell extracts, sulfur was observed to be transfered from cysteine (78, 80, 94) but, when purified BioB was incubated with [^{35}S]-cysteine, transfer of the label to biotin was not observed (80). It was later reported that BioB containing only a [4Fe-4S] cluster could bind pyridoxal 5'-phosphate (PLP) and showed desulfurase activity. In these reactions alanine was formed upon incubation with

L-cysteine (95). It was proposed that the residues Cys97, and Cys128 and Cys188 were serving as a site for persulfide formation and not for binding a second [2Fe-2S] cluster. However, the crystal structure of BioB revealed that the residues Cys97, and Cys128 and Cys188 were bound to a [2Fe-2S] cluster and that the protein contained no obvious PLP binding sites (*54*). This was further supported by the lack of increased activity upon addition of PLP to reactions using purified protein (96).

The sulfur atom in SAM was considered as the source. However, this was ruled out as biotin formed using [^{35}S]-SAM failed to produce labelled biotin (80). Labelled protein grown in the presence of [^{35}S]-cysteine and [^{35}S]-sulfide resulted in significant transfer of radioactivity to biotin suggesting the protein itself could be acting as the sulfur donor (97). This was further supported by the formation of labeled biotin in reactions using *B. sphaericus* and *E. coli* BioB reconstituted with $Na_2{}^{34}S$. The biotin formed in these reactions contained 65% of the label as determined by mass spectrometry (98). Selenobiotin has also been formed by protein reconstituted with Na_2Se providing further evidence that an FeS cluster is indeed the source of sulfur in BioB (99).

Multiple turnovers of the protein have not been achieved *in vitro* (80, 96, 100) suggesting that the sulfur source is depleted during turnover, however, *in vivo* catylytic activity has been observed (101) implying that the *in vitro* experiments are lacking some component required for catalysis and the protein itself might be a reactant. A possible source of sulfur from the protein is the [2Fe-2S] cluster. The crystal structure shows that this cluster is ideally located (~4.6 Å from the C9 position of DTB) to donate a sulfur atom (43). If a cluster was indeed acting as the sulfur source one might expect that cluster degradation would accompany turnover. This was indeed observed when reactions were monitored using UV/vis and EPR spectroscopy. Changes in these spectra were characteristic to the loss of the [2Fe-2S] cluster but the [4Fe-4S] cluster remained intact (102). Regeneration of the [2Fe-2S] containing protein can be achieved by adding fresh Fe^{2+}, S^{2-} and DTT and further incubation resulted in the additional formation of 0.4 eq of biotin with respect to protein (96). Alternatively, iron sulfur cluster assembly proteins (such as NifS, or Isc) proteins which are involved in FeS cluster assembly (103, 104) can facilitate *in vitro* reconstitution of BioB and when used to reconstitute apo-BioB have resulted in the generation of [^{35}S]-biotin when the protein was incubated with either of these proteins and [^{35}S]-cysteine (100). The observed catalytic activity *in vivo* is likely to be a result of the

ability of these FeS assembly proteins to regenerate active protein. Mössbauer spectroscopy indicates that the rate of degradation of the [2Fe-2S] cluster occurs at a greater rate than biotin formation (105), leading to the belief that cluster degradation is the direct sulfur source.

Mechanism of biotin formation by BioB

The last step of biotin biosynthesis involves the insertion of a sulfur atom into the inactive methylene (C6) and methyl (C9) carbon atoms adjacent to the imidazolinone ring of DTB. Like LipA the unreactive nature of the C-H bonds and the requirement of a radical SAM protein led to the proposal that the two hydrogen atoms are abstracted by Ado• radicals. Labeling the C6 and C9 positions of DTB with deuterium has resulted in the production of AdoD (63), supporting this hypothesis.

If the biosynthesis occurs in a stepwise manner the hydrogen atom abstraction from the C6 or C9 centres of DTB would be anticipated to lead to the formation of one of two intermediates, 9-mercaptodethiobiotin **31** or 6-mercaptodethiobiotin **32** followed by a second abstraction and cyclisation to form biotin (fig. 1.23). A species that is derived form DTB not corresponding to biotin has been detected by high performance liquid chromatography (HPLC) using ^{14}C- labelled DTB, but it was not fully characterised (90). This species has characteristics of an intermediate and when isolated by HPLC could be reintroduced to an assay and converted to biotin.

9-mercaptodethiobiotin **31** can support the growth of *bioA* minus mutants, which are incapable of biosynthesising 7,8-diaminopelargonate, a precursor to DTB (106). This compound can also be converted to biotin by resting *Bacillus sphaericus* cells. However, neither 6(*R*)-mercaptodethiobiotin or 6(*S*)-mercaptodethiobiotin can serve as substrates (107) suggesting sulfur insertion happens first at C9. The crystal structure of BioB shows that SAM and DTB are in close proximity with the 5' position of SAM ~3.9 Å from C9 of DTB (43), suitably positioned to abstract a hydrogen atom from this position.

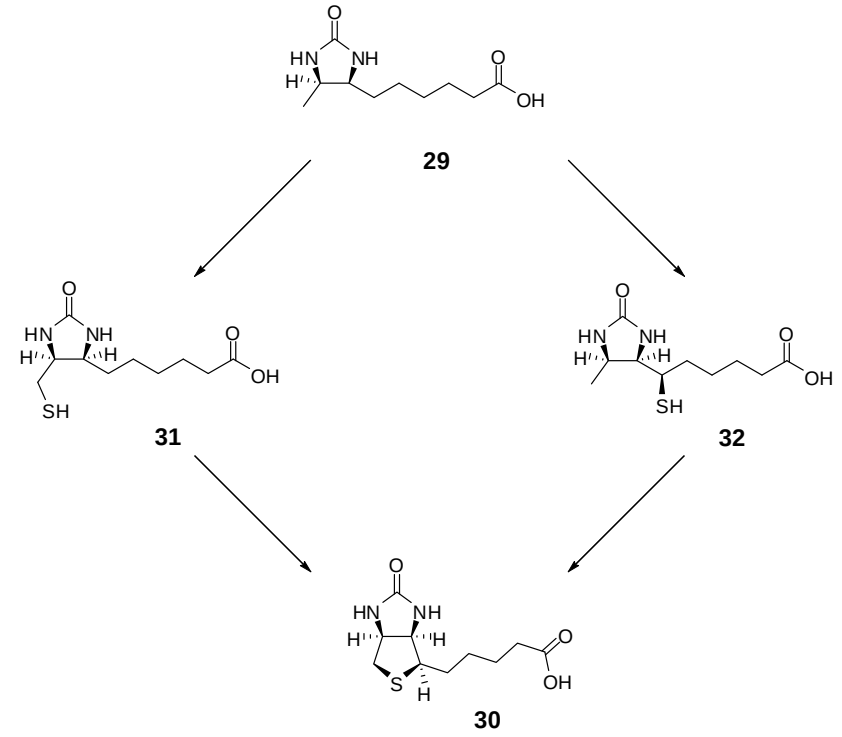

Figure 1.23 Two alternate pathways for biotin biosynthesis. Sulfur insertion can occur at C9 followed by cyclisation onto C6 or insertion at C6 followed by cyclisation onto C9.

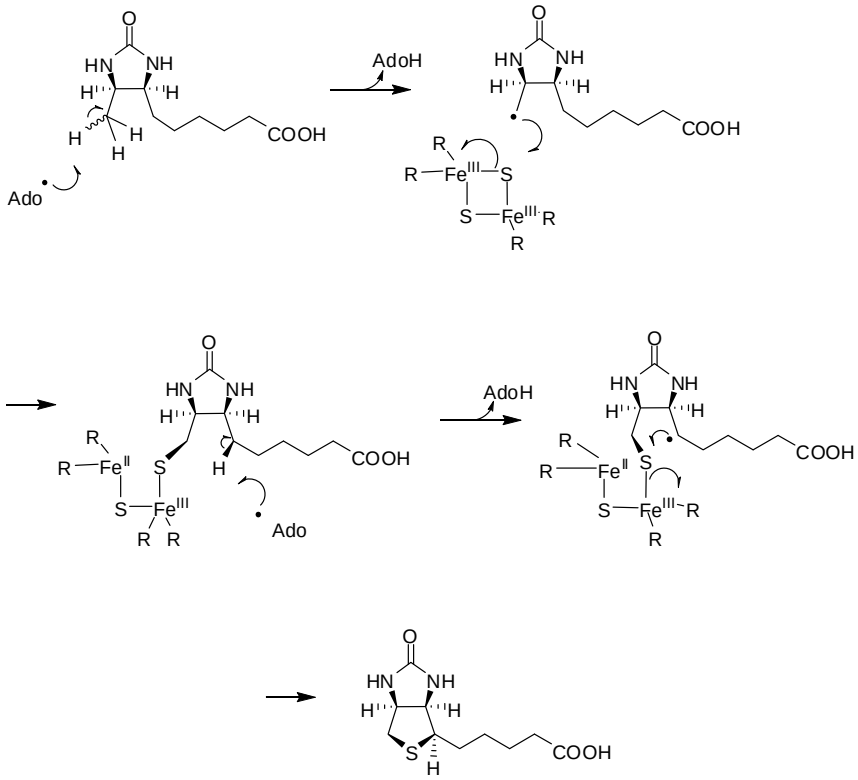

Figure 1.24 Mechanism for conversion of DTB to biotin in which the [2Fe-2S] cluster acts as the source of sulfur.

In summary although a full consensus has yet to be reached, the most widely accepted mechanism has a hydrogen atom first being abstracted from C9 and the subsequent radical being quenched by the [2Fe-2S] cluster. A second hydrogen atom is abstracted from C6 followed by cyclisation and elimination of the degraded cluster to complete the biosynthesis (fig.1.24)

1.4 Aims for this thesis

This thesis aims to describe the results collected throughout my PhD project which, initially aimed to validate a new *in vitro* assay by repeating *in vivo* feeding experiments with substrates containing an already inserted single sulfur atom. However, it soon became apparent that this assay had potential to provide a greater range of information to those previously reported due to it utilizing a simple peptide substrate. The observation of a mono-thiolated adduct by mass spectrometry was fundamental in changing the direction of the project and resulted in the aim being modified to solving the order of sulfur insertion.

Although not a trivial task, this single aim was not sufficient provide enough work for the 3 years scheduled for these investigations and as such a new aim was developed. It was considered that although a lipoyl cofactor is catalytic, the idea that the cell would form this cofactor substoichemetrically was unlikely. If this is true, the *in vitro* assay could be modified to work catalytically and this was the second aim.

The third and final aim of this project was simply to challenge the protein with alternate substrates. It was decided that a variation of one carbon atom in the substrate chain length would be investigated. A tripeptide with a heptonyl side chain was investigated by a project student under my supervision, whist reactions using a tripeptide containing a longer, nonanoyl side chain was investigated by myself.

These three aims are discussed in the three results chapters following.

1.5 References

1. Vanden Boom, T.J., K.E. Reed, and J.E. Cronan, Lipoic acid metabolism in *Escherichia coli*: isolation of null mutants defective in lipoic acid biosynthesis, molecular cloning and characterization of the *E. coli lip* locus, and identification of the lipoylated protein of the glycine cleavage system. *Journal of Bacteriology*, 1991. **173**(20): p. 6411-6420.
2. Hayden, M.A., I. Huang, D.E. Bussiere, and G.W. Ashley, The biosynthesis of lipoic acid. Cloning of *lip*, a lipoate biosynthetic locus of Escherichia coli. *Journal of Biological Chemistry* 1992. **267**(14): p. 9512-5.
3. Hayden, M.A., I.Y. Huang, G. Iliopoulos, M. Orozco, and G.W. Ashley, Biosynthesis of lipoic acid: characterization of the lipoic acid auxotrophs *Escherichia coli* W1485-lip2 and JRG33-lip9. *Biochemistry*, 1993. **32**(14): p. 3778-82.
4. Reed, K.E. and J.E. Cronan, Lipoic acid metabolism in *Escherichia coli*: sequencing and functional characterization of the *lipA* and *lipB* Genes. *Journal of Bacteriology*, 1993. **175**(5): p. 1325-1336.
5. Miller, J.R., R.W. Busby, S.W. Jordan, J. Cheek, T.F. Henshaw, G.W. Ashley, J.B. Broderick, J.E. Cronan, Jr., and M.A. Marletta, *Escherichia coli* LipA is a lipoyl synthase: *in vitro* biosynthesis of lipoylated pyruvate dehydrogenase complex from octanoyl-acyl carrier protein. *Biochemistry*, 2000. **39**(49): p. 15166-78.
6. Reed, L.J., B.B. De, I.C. Gunsalus, and C.S. Hornberger, Jr., Crystalline alpha-lipoic acid; a catalytic agent associated with pyruvate dehydrogenase. *Science*, 1951. **114**(2952): p. 93-4.
7. Malinska, D. and K. Winiarska, [Lipoic acid: characteristics and therapeutic application]. *Postepy higieny i medycyny doswiadczalnej (Online)*, 2005. **59**: p. 535-43.
8. Mislow, K. and W.C. Meluch, The configuration of (+)-α-lipoic acid. *Journal of the American Chemical Society*, 1956. **78**(10): p. 2341-2342.
9. Packer, L., K. Kraemer, and G. Rimbach, Molecular aspects of lipoic acid in the prevention of diabetes complications. *Nutrition*, 2001. **17**(10): p. 888-95.

10. Smith, A.R., S.V. Shenvi, M. Widlansky, J.H. Suh, and T.M. Hagen, Lipoic acid as a potential therapy for chronic diseases associated with oxidative stress. *Current Medicinal Chemistry*, 2004. **11**(9): p. 1135-46.
11. Holmquist, L., G. Stuchbury, K. Berbaum, S. Muscat, S. Young, K. Hager, J. Engel, and G. Munch, Lipoic acid as a novel treatment for Alzheimer's disease and related dementias. *Pharmacology & Therapeutics*, 2007. **113**(1): p. 154-64.
12. Perham, R.N., Swinging arms and swinging domains in multifunctional enzymes: catalytic machines for multistep reactions. *Annual Review of Biochemistry* 2000. **69**: p. 961-1004.
13. Perham, R.N., Domains, motifs, and linkers in 2-oxo acid dehydrogenase multienzyme complexes: a paradigm in the design of a multifunctional protein. *Biochemistry*, 1991. **30**(35): p. 8501-12.
14. Reed, L.J. and M.L. Hackert, Structure-function relationships in dihydrolipoamide acyltransferases. *Journal of Biological Chemistry* 1990. **265**(16): p. 8971-4.
15. Fujiwara, K., K. Okamura-Ikeda, and Y. Motokawa, Expression of mature bovine H-protein of the glycine cleavage system in *Escherichia coli* and in vitro lipoylation of the apoform. *Journal of Biological Chemistry* 1992. **267**(28): p. 20011-6.
16. Zhou, Z.H., D.B. McCarthy, C.M. O'Connor, L.J. Reed, and J.K. Stoops, The remarkable structural and functional organization of the eukaryotic pyruvate dehydrogenase complexes. *Proceedings of the National academy of Sciences of the United States of America* 2001. **98**(26): p. 14802-7.
17. Dardel, F., A.L. Davis, E.D. Laue, and R.N. Perham, Three-dimensional structure of the lipoyl domain from *Bacillus stearothermophilus* pyruvate dehydrogenase multienzyme complex. *Journal of Molecular Biology* 1993. **229**(4): p. 1037-48.
18. Douce, R., J. Bourguignon, D. Macherel, and M. Neuburger, The glycine decarboxylase system in higher plant mitochondria: structure, function and biogenesis. *Biochemical Society Transactions* 1994. **22**(1): p. 184-8.
19. Cohen-Addad, C., S. Pares, L. Sieker, M. Neuburger, and R. Douce, The lipoamide arm in the glycine decarboxylase complex is not freely swinging. *Nature Structural & Molecular Biology* 1995. **2**(1): p. 63-8.
20. Pares, S., C. Cohen-Addad, L.C. Sieker, M. Neuburger, and R. Douce, Refined structures at 2 and 2.2 A resolution of two forms of the H-protein, a lipoamide-

containing protein of the glycine decarboxylase complex. *Acta Crystallographica Section D: Biological Crystallography* 1995. **51**(Pt 6): p. 1041-51.

21. Faure, M., J. Bourguignon, M. Neuburger, D. MacHerel, L. Sieker, R. Ober, R. Kahn, C. Cohen-Addad, and R. Douce, Interaction between the lipoamide-containing H-protein and the lipoamide dehydrogenase (L-protein) of the glycine decarboxylase multienzyme system 2. Crystal structures of H- and L-proteins. *European Journal of Biochemistry* 2000. **267**(10): p. 2890-8.
22. Herbert, A.A. and J.R. Guest, Biochemical and genetic studies with lysine & methionine mutants of *Escherichia coli*: lipoic acid and α-ketoglutarate dehydrogenase-less mutants. *Journal of General Microbiology*, 1968. **53**(3): p. 363-81.
23. Herbert, A.A. and J.R. Guest, Lipoic acid content of *Escherichia coli* and other microorganisms. *Archives of Microbiology* 1975. **106**(3): p. 259-66.
24. Gueguen, V., D. Macherel, M. Jaquinod, R. Douce, and J. Bourguignon, Fatty acid and lipoic acid biosynthesis in higher plant mitochondria. *Journal of Biological Chemistry*, 2000. **275**(7): p. 5016-5025.
25. Thomsen-Zieger, N., J. Schachtner, and F. Seeber, Apicomplexan parasites contain a single lipoic acid synthase located in the plastid. *FEBS Letters*, 2003. **547**(1-3): p. 80-86.
26. Morikawa, T., R. Yasuno, and H. Wada, Do mammalian cells synthesize lipoic acid? Identification of a mouse cDNA encoding a lipoic acid synthase located in mitochondria. *FEBS Letters*, 2001. **498**(1): p. 16-21.
27. Yi, X. and N. Maeda, Endogenous production of lipoic acid is essential for mouse development. *Molecular and Cellular Biology*, 2005. **25**(18): p. 8387-8392.
28. Parry, R.J., Biosynthesis of lipoic acid. 1. Incorporation of specifically tritiated octanoic acid into lipoic acid. *Journal of the American Chemical Society*, 1977. **99**(19): p. 6464-6.
29. Parry, R.J. and D.A. Trainor, Biosynthesis of lipoic acid. 2. Stereochemistry of sulfur introduction at C-6 of octanoic acid. *Journal of the American Chemical Society*, 1978. **100**(16): p. 5243-4.
30. White, R.H., Stable isotope studies on the biosynthesis of lipoic acid in *Escherichia coli*. *Biochemistry*, 1980. **19**(1): p. 15-19.

31. Sofia, H.J., G. Chen, B.G. Hetzler, J.F. Reyes-Spindola, and N.E. Miller, Radical SAM, a novel protein superfamily linking unresolved steps in familiar biosynthetic pathways with radical mechanisms: functional characterization using new analysis and information visualization methods. *Nucleic Acids Research* 2001. **29**(5): p. 1097-106.

32. Hewitson, K.S., J.E. Baldwin, N.M. Shaw, and P.L. Roach, Mutagenesis of the proposed iron-sulfur cluster binding ligands in *Escherichia coli* biotin synthase. *FEBS Letters* 2000. **466**(2-3): p. 372-376.

33. Hewitson, K.S., S. Ollagnier-de Choudens, Y. Sanakis, N.M. Shaw, J.E. Baldwin, E. Munck, P.L. Roach, and M. Fontecave, The iron-sulfur center of biotin synthase: site-directed mutants. *Journal of Biological Inorganic Chemistry*, 2002. **7**(1-2): p. 83-93.

34. Layer, G., K. Verfurth, E. Mahlitz, and D. Jahn, Oxygen-independent coproporphyrinogen-III oxidase HemN from *Escherichia coli*. *Journal of Biological Chemistry* 2002. **277**(37): p. 34136-42.

35. Tamarit, J., C. Gerez, C. Meier, E. Mulliez, A. Trautwein, and M. Fontecave, The activating component of the anaerobic ribonucleotide reductase from *Escherichia coli*. An iron-sulfur center with only three cysteines. *Journal of Biological Chemistry* 2000. **275**(21): p. 15669-75.

36. Cicchillo, R.M., K.H. Lee, C. Baleanu-Gogonea, N.M. Nesbitt, C. Krebs, and S.J. Booker, *Escherichia coli* lipoyl synthase binds two distinct [4Fe-4S] clusters per polypeptide. *Biochemistry*, 2004. **43**(37): p. 11770-81.

37. Fontecave, M., E. Mulliez, and S. Ollagnier-de-Choudens, Adenosylmethionine as a source of 5'-deoxyadenosyl radicals. *Current Opinion in Chemical Biology*, 2001. **5**(5): p. 506-511.

38. Jarrett, J.T., The generation of 5'-deoxyadenosyl radicals by adenosylmethionine-dependent radical enzymes. *Current Opinion in Chemical Biology* 2003. **7**(2): p. 174-82.

39. Liu, A. and A. Graslund, Electron paramagnetic resonance evidence for a novel interconversion of $[3Fe\text{-}4S]^{+}$ and $[4Fe\text{-}4S]^{+}$ clusters with endogenous iron and sulfide in anaerobic ribonucleotide reductase activase *in vitro*. *Journal of Biological Chemistry* 2000. **275**(17): p. 12367-73.

40. Cosper, M.M., G.N. Jameson, R. Davydov, M.K. Eidsness, B.M. Hoffman, B.H. Huynh, and M.K. Johnson, The $[4Fe\text{-}4S]^{2+}$ cluster in reconstituted biotin synthase

binds S-adenosyl-L-methionine. *Journal of the American Chemical Society*, 2002. **124**(47): p. 14006-7.

41. Krebs, C., W.E. Broderick, T.F. Henshaw, J.B. Broderick, and B.H. Huynh, Coordination of adenosylmethionine to a unique iron site of the [4Fe-4S] of pyruvate formate-lyase activating enzyme: a Mössbauer spectroscopic study. *Journal of the American Chemical Society*, 2002. **124**(6): p. 912-913.
42. Walsby, C.J., W. Hong, W.E. Broderick, J. Cheek, D. Ortillo, J.B. Broderick, and B.M. Hoffman, Electron-nuclear double resonance spectroscopic evidence that S-adenosylmethionine binds in contact with the catalytically active $[4Fe\text{-}4S]^{+}$ cluster of pyruvate formate-lyase activating enzyme. *Journal of the American Chemical Society*, 2002. **124**(12): p. 3143-3151.
43. Berkovitch, F., Y. Nicolet, J.T. Wan, J.T. Jarrett, and C.L. Drennan, Crystal structure of biotin synthase, an S-adenosylmethionine-dependent radical enzyme. *Science*, 2004. **303**(5654): p. 76-9.
44. Lepore, B.W., F.J. Ruzicka, P.A. Frey, and D. Ringe, The X-ray crystal structure of lysine-2,3-aminomutase from *Clostridium subterminale. Proceedings of the National academy of Sciences of the United States of America* 2005. **102**(39): p. 13819-24.
45. Layer, G., J. Moser, D.W. Heinz, D. Jahn, and W.D. Schubert, Crystal structure of coproporphyrinogen III oxidase reveals cofactor geometry of radical SAM enzymes. *EMBO Journal* 2003. **22**(23): p. 6214-24.
46. Hanzelmann, P. and H. Schindelin, Binding of 5'-GTP to the C-terminal FeS cluster of the radical S-adenosylmethionine enzyme MoaA provides insights into its mechanism. *Proceedings of the National academy of Sciences of the United States of America* 2006. **103**(18): p. 6829-34.
47. Padovani, D., F. Thomas, A.X. Trautwein, E. Mulliez, and M. Fontecave, Activation of class III ribonucleotide reductase from E. coli. The electron transfer from the iron-sulfur center to S-adenosylmethionine. *Biochemistry*, 2001. **40**(23): p. 6713-9.
48. Henshaw, T.F., J. Cheek, and J.B. Broderick, The [4Fe-4S](1+) cluster of pyruvate formate-lyase activating enzyme generates the glycyl radical on pyruvate formate-lyase: EPR-detected single turnover. *Journal of the American Chemical Society*, 2000. **122**(34): p. 8331-8332.

49. Lieder, K.W., S. Booker, F.J. Ruzicka, H. Beinert, G.H. Reed, and P.A. Frey, S-Adenosylmethionine-dependent reduction of lysine 2,3-aminomutase and observation of the catalytically functional iron-sulfur centers by electron paramagnetic resonance. *Biochemistry*, 1998. **37**(8): p. 2578-85.

50. Krebs, C., T.F. Henshaw, J. Cheek, B.H. Huynh, and J.B. Broderick, Conversion of 3Fe-4S to 4Fe-4S clusters in native pyruvate formate-lyase activating enzyme: Mössbauer characterization and implications for mechanism. *Journal of the American Chemical Society*, 2000. **122**(50): p. 12497-12506.

51. Ugulava, N.B., B.R. Gibney, and J.T. Jarrett, Iron-sulfur cluster interconversions in biotin synthase: dissociation and reassociation of iron during conversion of [2Fe-2S] to [4Fe-4S] clusters. *Biochemistry*, 2000. **39**(17): p. 5206-14.

52. Broderick, J.B., T.F. Henshaw, J. Cheek, K. Wojtuszewski, S.R. Smith, M.R. Trojan, R.M. McGhan, A. Kopf, M. Kibbey, and W.E. Broderick, Pyruvate formate-lyase-activating enzyme: strictly anaerobic isolation yields active enzyme containing a $[3Fe\text{-}4S]^{+}$ cluster. *Biochemical and Biophysical Research Communications* 2000. **269**(2): p. 451-6.

53. Imlay, J.A., Iron-sulphur clusters and the problem with oxygen. *Molecular Microbiology* 2006. **59**(4): p. 1073-82.

54. Duin, E.C., M.E. Lafferty, B.R. Crouse, R.M. Allen, I. Sanyal, D.H. Flint, and M.K. Johnson, [2Fe-2S] to [4Fe-4S] cluster conversion in *Escherichia coli* biotin synthase. *Biochemistry*, 1997. **36**(39): p. 11811-20.

55. Ifuku, O., N. Koga, S. Haze, J. Kishimoto, and Y. Wachi, Flavodoxin is required for conversion of dethiobiotin to biotin in *Escherichia coli*. *European Journal of Biochemistry* 1994. **224**(1): p. 173-8.

56. Mulliez, E., D. Padovani, M. Atta, C. Alcouffe, and M. Fontecave, Activation of class III ribonucleotide reductase by flavodoxin: a protein radical-driven electron transfer to the iron-sulfur center. *Biochemistry*, 2001. **40**(12): p. 3730-6.

57. Bianchi, V., R. Eliasson, M. Fontecave, E. Mulliez, D.M. Hoover, R.G. Matthews, and P. Reichard, Flavodoxin is required for the activation of the anaerobic ribonucleotide reductase. *Biochemical and Biophysical Research Communications* 1993. **197**(2): p. 792-7.

58. Mejean, A., B. Tse Sum Bui, D. Florentin, O. Ploux, Y. Izumi, and A. Marquet, Highly purified biotin synthase can transform dethiobiotin into biotin in the

absence of any other protein, in the presence of photoreduced deazaflavin. *Biochemical and Biophysical Research Communications* 1995. **217**(3): p. 1231-7.

59. Ollagnier-de Choudens, S., Y. Sanakis, K.S. Hewitson, P. Roach, E. Munck, and M. Fontecave, Reductive cleavage of S-adenosylmethionine by biotin synthase from *Escherichia coli*. *Journal of Biological Chemistry*, 2002. **277**(16): p. 13449-13454.
60. Cicchillo, R.M., D.F. Iwig, A.D. Jones, N.M. Nesbitt, C. Baleanu-Gogonea, M.G. Souder, L. Tu, and S.J. Booker, Lipoyl synthase requires two equivalents of S-adenosyl-L-methionine to synthesize one equivalent of lipoic acid. *Biochemistry*, 2004. **43**(21): p. 6378-86.
61. Moss, M. and P.A. Frey, The role of S-adenosylmethionine in the lysine 2,3-aminomutase reaction. *Journal of Biological Chemistry* 1987. **262**(31): p. 14859-62.
62. Frey, M., M. Rothe, A.F. Wagner, and J. Knappe, Adenosylmethionine-dependent synthesis of the glycyl radical in pyruvate formate-lyase by abstraction of the glycine C-2 pro-S hydrogen atom. Studies of [2H]glycine-substituted enzyme and peptides homologous to the glycine 734 site. *Journal of Biological Chemistry* 1994. **269**(17): p. 12432-7.
63. Escalettes, F., D. Florentin, B.T.S. Bui, D. Lesage, and A. Marquet, Biotin synthase mechanism: Evidence for hydrogen transfer from the substrate into deoxyadenosine. *Journal of the American Chemical Society*, 1999. **121**(15): p. 3571-3578.
64. Knappe, J. and A.F. Wagner, Stable glycyl radical from pyruvate formate-lyase and ribonucleotide reductase (III). *Advances in Protein Chemistry* 2001. **58**: p. 277-315.
65. Ollagnier, S., E. Mulliez, P.P. Schmidt, R. Eliasson, J. Gaillard, C. Deronzier, T. Bergman, A. Graslund, P. Reichard, and M. Fontecave, Activation of the anaerobic ribonucleotide reductase from *Escherichia coli*. The essential role of the iron-sulfur center for S-adenosylmethionine reduction. *Journal of Biological Chemistry* 1997. **272**(39): p. 24216-23.
66. Moss, M.L. and P.A. Frey, Activation of lysine 2,3-aminomutase by S-adenosylmethionine. *Journal of Biological Chemistry* 1990. **265**(30): p. 18112-5.
67. Busby, R.W., J.P.M. Schelvis, D.S. Yu, G.T. Babcock, and M.A. Marletta, Lipoic acid biosynthesis: LipA is an iron-sulfur protein. *Journal of the American Chemical Society*, 1999. **121**(19): p. 4706-4707.

68. Ollagnier-de Choudens, S. and M. Fontecave, The lipoate synthase from *Escherichia coli* is an iron-sulfur protein. *FEBS Letters* 1999. **453**(1-2): p. 25-8.
69. Ollagnier-De Choudens, S., Y. Sanakis, K.S. Hewitson, P. Roach, J.E. Baldwin, E. Munck, and M. Fontecave, Iron-sulfur center of biotin synthase and lipoate synthase. *Biochemistry*, 2000. **39**(14): p. 4165-73.
70. Jordan, S.W. and J.E. Cronan, Jr., A new metabolic link. The acyl carrier protein of lipid synthesis donates lipoic acid to the pyruvate dehydrogenase complex in *Escherichia coli* and mitochondria. *Journal of Biological Chemistry* 1997. **272**(29): p. 17903-6.
71. Zhao, X., J.R. Miller, Y. Jiang, M.A. Marletta, and J.E. Cronan, Assembly of the covalent linkage between lipoic acid and its cognate enzymes. *Chemistry and Biology*, 2003. **10**(12): p. 1293-302.
72. Cronan, J.E., X. Zhao, and Y. Jiang, Function, attachment and synthesis of lipoic acid in *Escherichia coli*. *Advances in microbial physiology*, 2005. **50**: p. 103-46.
73. Cicchillo, R.M. and S.J. Booker, Mechanistic investigations of lipoic acid biosynthesis in *Escherichia coli*: both sulfur atoms in lipoic acid are contributed by the same lipoyl synthase polypeptide. *Journal of the American Chemical Society*, 2005. **127**(9): p. 2860-1.
74. White, R.H., Biosynthesis of lipoic acid - extent of incorporation of deuterated hydroxyoctanoic and thiooctanoic acids into lipoic acid. *Journal of the American Chemical Society*, 1980. **102**(21): p. 6605-6607.
75. Bryant, P., M. Kriek, R.J. Wood, and P.L. Roach, The activity of a thermostable lipoyl synthase from *Sulfolobus solfataricus* with a synthetic octanoyl substrate. *Analytical Biochemistry* 2006. **351**(1): p. 44-9.
76. Sanyal, I., G. Cohen, and D.H. Flint, Biotin synthase: purification, characterization as a [2Fe-2S] cluster protein, and *in vitro* activity of the *Escherichia coli bioB* gene product. *Biochemistry*, 1994. **33**(12): p. 3625-31.
77. Ifuku, O., J. Kishimoto, S. Haze, M. Yanagi, and S. Fukushima, Conversion of dethiobiotin to biotin in cell-free extracts of *Escherichia coli*. *Bioscience Biotechnology and Biochemistry* 1992. **56**(11): p. 1780-5.
78. Birch, O.M., M. Fuhrmann, and N.M. Shaw, Biotin Synthase From Escherichia-Coli, an Investigation of the Low- Molecular-Weight and Protein-Components Required For Activity in- Vitro. *Journal of Biological Chemistry*, 1995. **270**(32): p. 19158-19165.

79. Ohshiro, T., M. Yamamoto, Y. Izumi, B.T. Bui, D. Florentin, and A. Marquet, Enzymatic conversion of dethiobiotin to biotin in cell-free extracts of a *Bacillus sphaericus bioB* transformant. *Bioscience Biotechnology and Biochemistry* 1994. **58**(9): p. 1738-41.

80. Sanyal, I., K.J. Gibson, and D.H. Flint, Escherichia coli biotin synthase: an investigation into the factors required for its activity and its sulfur donor. *Archives of Biochemistry and Biophysics* 1996. **326**(1): p. 48-56.

81. Ohshiro, T., T. Kishimoto, M. Arase, and Y. Izumi, Characterization of the biotin synthase reaction from *Bacillus sphaericus* using the photoreduced deazaflavin system. *Journal of Fermentation and Bioengineering*, 1998. **86**(5): p. 446-450.

82. Parry, R.J. and M.G. Kunitani, Letter: Biotin biosynthesis. 1. The incorporation of specifically tritiated dethiobiotin into biotin. *Journal of the American Chemical Society* 1976. **98**(13): p. 4024-6.

83. Guillerm, G., F. Frappier, M. Gaudry, and A. Marquet, On the mechanism of conversion of dethiobiotin to biotin in *Escherichia coli*. *Biochimie*, 1977. **59**(1): p. 119-21.

84. Trainor, D.A., R.J. Parry, and A. Gitterman, Biotin Biosynthesis .2. stereochemistry of sulfur introduction at C-4 of dethiobiotin. *Journal of the American Chemical Society*, 1980. **102**(4): p. 1467-1468.

85. Cosper, M.M., G.N. Jameson, M.K. Eidsness, B.H. Huynh, and M.K. Johnson, Recombinant *Escherichia coli* biotin synthase is a $[2Fe\text{-}2S]^{2+}$ protein in whole cells. *FEBS Letters* 2002. **529**(2-3): p. 332-6.

86. Benda, R., B. Tse Sum Bui, V. Schunemann, D. Florentin, A. Marquet, and A.X. Trautwein, Iron-sulfur clusters of biotin synthase in vivo: a Mössbauer study. *Biochemistry*, 2002. **41**(50): p. 15000-6.

87. Ugulava, N.B., B.R. Gibney, and J.T. Jarrett, Biotin synthase contains two distinct iron-sulfur cluster binding sites: chemical and spectroelectrochemical analysis of iron-sulfur cluster interconversions. *Biochemistry*, 2001. **40**(28): p. 8343-51.

88. Tse Sum Bui, B., D. Florentin, A. Marquet, R. Benda, and A.X. Trautwein, Mössbauer studies of *Escherichia coli* biotin synthase: evidence for reversible interconversion between $[2Fe\text{-}2S]^{2+}$ and $[4Fe\text{-}4S]^{2+}$ clusters. *FEBS Letters* 1999. **459**(3): p. 411-4.

89. Guianvarc'h, D., D. Florentin, B. Tse Sum Bui, F. Nunzi, and A. Marquet, Biotin synthase, a new member of the family of enzymes which uses S-

adenosylmethionine as a source of deoxyadenosyl radical. *Biochemical and Biophysical Research Communications* 1997. **236**(2): p. 402-6.

90. Shaw, N.M., O.M. Birch, A. Tinschert, V. Venetz, R. Dietrich, and L.A. Savoy, Biotin synthase from *Escherichia coli*: isolation of an enzyme- generated intermediate and stoichiometry of S-adenosylmethionine use. *Biochemical Journal*, 1998. **330**(Pt3): p. 1079-1085.
91. Ugulava, N.B., K.K. Surerus, and J.T. Jarrett, Evidence from Mössbauer spectroscopy for distinct $[2Fe\text{-}2S]^{2+}$ and $[4Fe\text{-}4S]^{2+}$ cluster binding sites in biotin synthase from *Escherichia coli*. *Journal of the American Chemical Society* 2002. **124**(31): p. 9050-1.
92. Broach, R.B. and J.T. Jarrett, Role of the $[2Fe\text{-}2S]^{2+}$ cluster in biotin synthase: mutagenesis of the atypical metal ligand arginine 260. *Biochemistry*, 2006. **45**(47): p. 14166-14174.
93. Ugulava, N.B., K.K. Frederick, and J.T. Jarrett, Control of adenosylmethionine-dependent radical generation in biotin synthase: a kinetic and thermodynamic analysis of substrate binding to active and inactive forms of BioB. *Biochemistry*, 2003. **42**(9): p. 2708-2719.
94. DeMoll, E. and W. Shive, The origin of sulfur in biotin. *Biochemical and Biophysical Research Communications*, 1983. **110**(1): p. 243-249.
95. Ollagnier-de-Choudens, S., E. Mulliez, K.S. Hewitson, and M. Fontecave, Biotin synthase is a pyridoxal phosphate-dependent cysteine desulfurase. *Biochemistry*, 2002. **41**(29): p. 9145-9152.
96. Tse Sum Bui, B., M. Lotierzo, F. Escalettes, D. Florentin, and A. Marquet, Further investigation on the turnover of *Escherichia coli* biotin synthase with dethiobiotin and 9-mercaptodethiobiotin as substrates. *Biochemistry*, 2004. **43**(51): p. 16432-41.
97. Gibson, K.J., D.A. Pelletier, and I.M. Turner, Sr., Transfer of sulfur to biotin from biotin synthase (BioB protein). *Biochemical and Biophysical Research Communications* 1999. **254**(3): p. 632-5.
98. Tse Sum Bui, B., D. Florentin, F. Fournier, O. Ploux, A. Mejean, and A. Marquet, Biotin synthase mechanism: on the origin of sulphur. *FEBS Letters* 1998. **440**(1-2): p. 226-30.
99. Tse Sum Bui, B., T.A. Mattioli, D. Florentin, G. Bolbach, and A. Marquet, *Escherichia coli* biotin synthase produces selenobiotin. Further evidence of the

involvement of the $[2Fe\text{-}2S]^{2+}$ cluster in the sulfur insertion step. *Biochemistry*, 2006. **45**(11): p. 3824-34.

100. Tse Sum Bui, B., F. Escalettes, G. Chottard, D. Florentin, and A. Marquet, Enzyme-mediated sulfide production for the reconstitution of [2Fe-2S] clusters into apo-biotin synthase of *Escherichia coli*. Sulfide transfer from cysteine to biotin. *European Journal of Biochemistry* 2000. **267**(9): p. 2688-94.
101. Choi-Rhee, E. and J.E. Cronan, Biotin synthase is catalytic *in vivo*, but catalysis engenders destruction of the protein. *Chemistry and Biology*, 2005. **12**(4): p. 461-8.
102. Ugulava, N.B., C.J. Sacanell, and J.T. Jarrett, Spectroscopic changes during a single turnover of biotin synthase: destruction of a [2Fe-2S] cluster accompanies sulfur insertion. *Biochemistry*, 2001. **40**(28): p. 8352-8.
103. Zheng, L., R.H. White, V.L. Cash, and D.R. Dean, Mechanism for the desulfurization of L-cysteine catalyzed by the *nifS* gene product. *Biochemistry*, 1994. **33**(15): p. 4714-20.
104. Zheng, L.M., V.L. Cash, D.H. Flint, and D.R. Dean, Assembly of iron-sulfur clusters - Identification of an *iscSUA- hscBA-fdx* gene cluster from *Azotobacter vinelandii*. *Journal of Biological Chemistry*, 1998. **273**(21): p. 13264-13272.
105. Jameson, G.N., M.M. Cosper, H.L. Hernandez, M.K. Johnson, and B.H. Huynh, Role of the [2Fe-2S] cluster in recombinant *Escherichia coli* biotin synthase. *Biochemistry*, 2004. **43**(7): p. 2022-31.
106. Baxter, R.L., D.J. Camp, A. Coutts, and N. Shaw, Synthesis and biological activity of 9-mercaptodethiobiotin - a putative Biotin precursor in *Escherichia coli*. *Journal of the Chemical Society-Perkin Transactions 1*, 1992(2): p. 255-258.
107. Marquet, A., F. Frappier, G. Guillerm, M. Azoulay, D. Florentin, and J.C. Tabet, Biotin biosynthesis - synthesis and biological evaluation of the putative intermediate thiols. *Journal of the American Chemical Society*, 1993. **115**(6): p. 2139-2145.

Chapter 2. Characterisation of an intermediate from lipoic acid biosynthesis

2.1 Introduction

The mechanism of lipoyl biosynthesis has been widely investigated. The natural substrate has been identified as a protein bound octanoyl moiety (1, 2) and it is understood that this conversion requires 2 equivalents of SAM to abstract a hydrogen atom from each the C6 and C8 positions of this group. The order of sulfur insertion has not yet been conclusively determined. However, a species corresponding to a monothiolated intermediate has been observed in *in vitro* reactions which used fully labeled octanoic acid (2) but did not identify if sulfur was first inserted at C6 or C8 (fig. 1.18).

In vivo feeding studies have suggested that sulfur is first inserted at the terminal C8 position (3) and these studies have also eliminated the possibility of an hydroxylated intermediate, which would have accounted for the observed inversion of stereochemistry at C6 (4, 5).

The conversion of a synthetic octanoyl tetra-peptide **32** or tri-peptide **33** (fig. 2.1) mimicking the E2-PDH domain *S. solfataricus* and the equivalent *E. coli* peptides (6, 7) to their corresponding lipoyl and DHL peptides has also been observed by HPLC. Reactions using *E. coli* protein and peptide substrates have been analysed by LCMS, confirming the formation of lipoyl, DHL and interestingly, a peptide corresponding to a single sulfur inserted product (6).

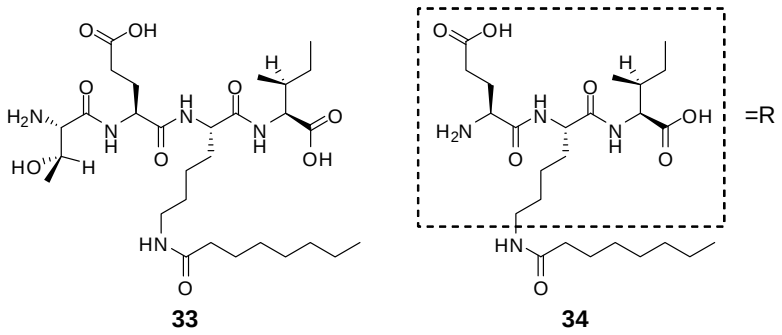

Figure 2.1 The structure of the tetra- **33** and tri-peptide mimic **34** of the octanoylated derivative of the lipoyl accepting domain from *S. solfataricus* PDH

The development of this *in vitro* assay offers the first real possibility of isolating this monothiolated species and determining the site of primary sulfur insertion in lipoyl biosynthesis. This chapter describes the use of this assay to characterise the structure of the intermediate in lipoyl formation.

2.2 An assay for LipA Activity

The development of an *in vitro* assay by Bryant *et al.* (6, 7) for measuring LipA activity using a synthetic peptide mimic of the PDH-E2 domain from *S. solfataricus* can also be used to investigate the biosynthesis of lipoyl groups by this protein. Under these conditions no catalytic activity is observed and an excess of LipA was used and is not recoverable. Therefore, large quantities of the protein were required, hence LipA was expressed and purified regularly from *E. coli*. Due to the oxygen sensitivity of LipA, all manipulations were carried out in a glovebox maintained under an oxygen free nitrogen atmosphere. All buffers and reagents were degassed inside the glovebox for 24 h prior to use.

2.2.1 Expression and purification of *S. solfataricus* LipA

S. solfataricus LipA was co-expressed with the proteins encoded by the *E. coli isc* operon (8) in *E. coli* strains BL21(DE3) or LMG 194 from the plasmid pMK024 (fig. 2.2), constructed by Dr. M. Kriek. The *E. coli isc* operon encodes proteins which have been shown to improve iron and sulfide content of the expressed protein (9).

Figure 2.2 pMK024, constructed by Dr. M .Kriek for the co-expression of *S. solfataricus* LipA and proteins encoded by the *E. coli isc* operon

Cells were grown in 2YT medium on a 5 L scale in a New Brunswick Scientific BioFlo 110 ® fermentor maintained at 37 °C. At a late log phase (OD_{600} ~ 1.0), Cells were induced by the addition of arabinose and protein was expressed for 3-4 h at 27 °C. Cells

were harvested by centrifugation and yielded 12 - 16 g wet cell paste during a typical growth.

LipA from this plasmid is expressed containing an N-terminal His_6-tag and was purified using Ni affinity chromatography (fig. 2.3, A) followed by size exclusion chromatography (fig. 2.3, B) by a method that is analogous to that described for the purification of *E. coli* LipA (6, 9).

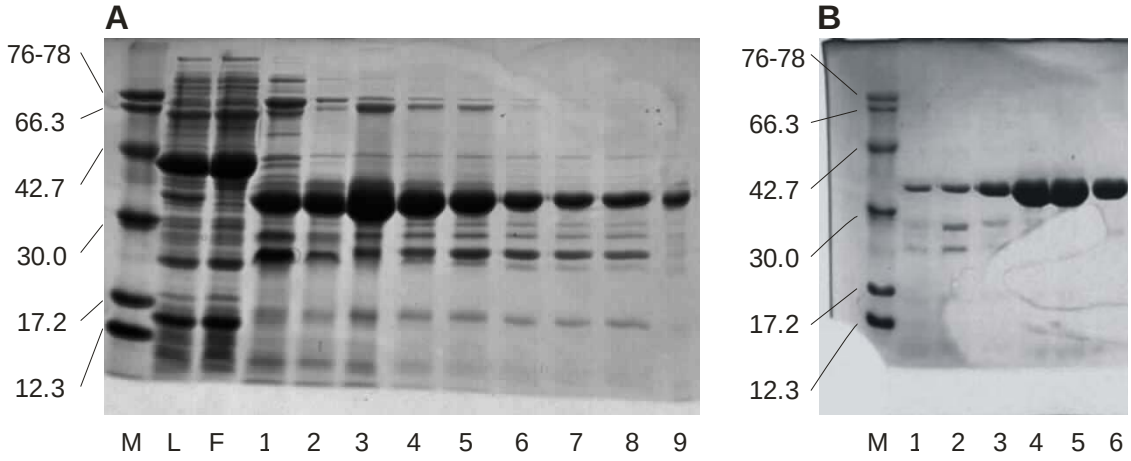

Figure 2.3 SDS–PAGE (15%) of LipA purification: **(A)** Ni affinity chromatography. Lanes indicate the following samples; **M-** molecular weight markers (kDa); **L-** cleared lysate; **F-** Ni column flow through; **1-9-** LipA containing fractions which were combined prior to size exclusion chromatography: (**B)** S-75 gel filtration. Lanes indicate the following samples; **M-** molecular weight markers (kDa); **1-6-** LipA containing fractions.

LipA was purified anaerobically from *E. coli* LMG 194 (30 - 50 g) with a typical yield of 13 - 18 mgL^{-1}. Purified protein was stored at -80 °C until required.

2.2.2 Substrate peptide 34 synthesis

The tripeptide substrate **34** was synthesised manually according to standard solid-phase protocols, using a sintered glass bubbler device (scheme 2.1) (10). The peptide was prepared on Wang resin with 9-fluorenylmethyloxycarbonyl (Fmoc) protected amino acids using diisopropylcarbodiimide (DIC) and hydroxybenzotriazole (HOBt) coupling chemistry.

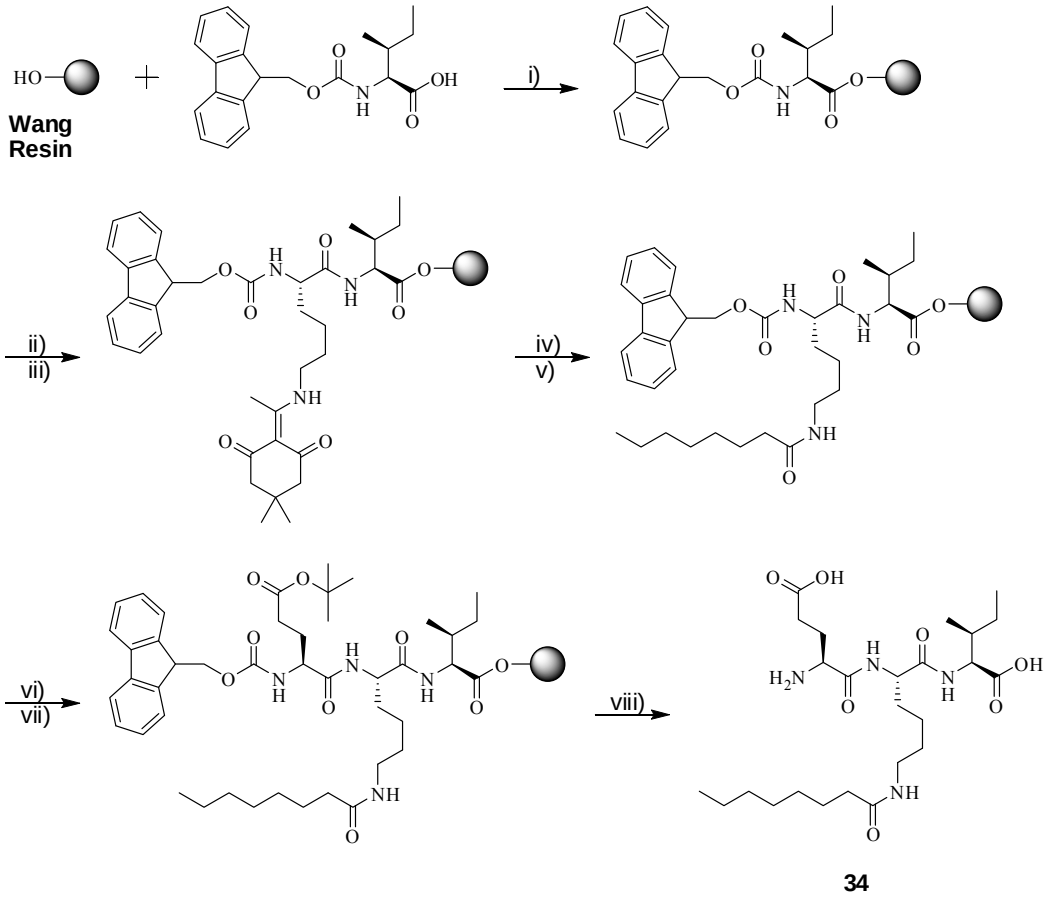

Scheme 2.1 Preparation of substrate peptide **34** for *S. solfataricus* LipA assays. *Reagents and conditions*: (i) DIC, DMAP, DMF, 3 h; (ii) 20% (v/v) piperidine, DMF, 30 min; (iii) Fmoc-Lys(Dde)-OH, DIC/HOBt, DMF, 1 h; (iv) $NH_2OH.HCl$, imidazole, NMP, 3 h; (v) octanoic acid, PyBOP, DIPEA, 1 h; (vi) 20% (v/v) piperidine, DMF, 30 min; (vii) Fmoc-Glu(O^{t}Bu)-OH, DIC, HOBt, DMF, 1 h; (viii) TFA, anisole, H_2O, 2 h.

Reagents were selected due to their compatibility with solid phase peptide chemistry using the Wang linker. PyBop was used to couple the octanoyl side group as poor activation was observed when HOBt and DIC was used (6). Orthogonality was introduced at the ε-amino group on the lysine side chain using the Dde protecting group (scheme 2.1) which is stable under Fmoc deprotection conditions (20% piperidine in DMF). The Dde protecting group can be selectively removed by using a mixture of $NH_2OH.HCl$ and imidazole in *N*-methylpyrrolidone (NMP) since the Fmoc group is completely stable under these conditions (11). Coupling of octanoic acid to the deprotected lysine N^{ε} amine was achieved using benzotriazole-1-yl-oxy-tris-pyrrolidino-phosphonium hexafluorophosphate (PyBOP) in the presence of N,N-diisopropylethylamine (DIPEA) as this has been found to be the most efficient method (6).

The substrate peptide **34** was cleaved from the resin using a mixture of trifluoroacetic acid (TFA), anisole and water with a typical crude yield of 90-100%. The peptide was purified on a 5 or 50 mg scale using pre-packed reverse phase chromatography which gave a final yield of 65 ± 5% on separate occasions with a purity >95% when analysed by HPLC, MS and NMR.

2.2.3 Turnover of the substrate peptide 34 by LipA

For maximum activity, *S. solfataricus* LipA first requires chemical reconstitution with exogenous iron and sulfide in the presence of DTT to reform degraded iron sulfur clusters (7). Reactions were carried out anaerobically with an excess of protein due to not all the protein being in an active form (6) and also contained SAM, sodium dithionite and substrate peptide **34** (table. 2.1)

Constituent	Final concentration (μM)
Reconstituted LipA	300
SAM	1000
Sodium dithionite	1000
Substrate peptide **34**	150

Table 2.1 Reactions to show LipA activity were prepared using the concentrations of protein, SAM, sodium dithionite and substrate outlined above. Reactions were prepared with an end volume of 500 μL.

Initial reactions were incubated at 37 °C for 2 h before the reaction was stopped by acidic precipitation of the protein by TFA.

2.2.4 Confirmation of LipA activity by LCMS

LCMS analysis of the reaction using *S. solfataricus* LipA and peptide substrate **34** (fig. 2.4) gave the same pattern of peaks that was previously observed for the reaction using *E.* coli protein and peptide substrate (6).

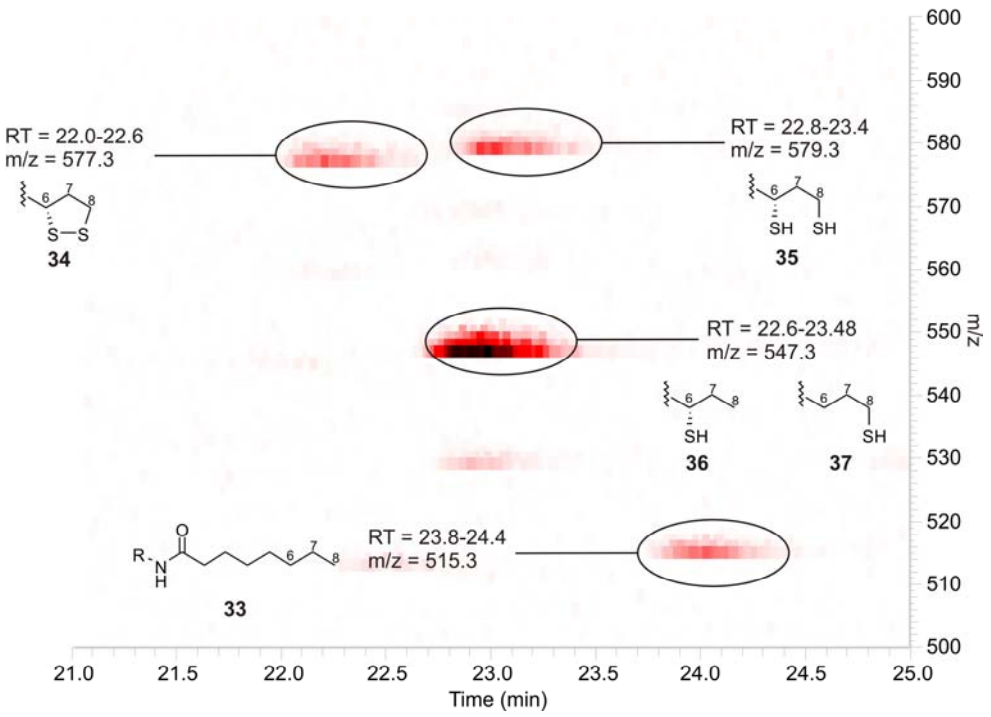

Figure 2.4 LCMS trace showing the products formed in an *in vitro* assay using *S. solfataricus* LipA, SAM, sodium dithionite and the tripeptide **34** as the substrate. Substrate peptide **34** appears at ~24 min, with new species appearing at ~23 min (m/z 579.3, 547.3) **36** and **37** or **38** and ~22 min (m/z 577.3) **35**.

On the basis of the mass ions observed, the following could be identified (fig. 2.5), lipoyl peptide **35** eluted at 22.0 - 22.6 min, the DHL peptide **36** and single sulfur inserted peptide **37** or **38** co-eluted at 22.6 - 23.4 min and the substrate peptide **34** was eluted at 23.8-24.4 min. The product eluted at 22.6 - 23.4 min, m/z = 547.3, was consistent with the starting peptide having undergone a single sulfur insertion reaction to form either the 6- **37** or 8- **38** monothiolated peptide which are indistinguishable by mass spectrometry (MS).

2.3 Characterisation of the single sulfur inserted product

In vivo feeding studies using [8-$^{2}H_2$]-8-thiooctanoic and [6(RS)-^{2}H]-6-thiooctanoic acids have shown that [8-$^{2}H_2$]-8-thiooctanoic acid was more readily converted into lipoic acid, suggesting that sulfur was inserted primarily into the terminal C-H bond (3). The order of

sulfur insertion was further investigated *in vitro* and the results are discussed within this section.

2.3.1 Investigating sulfur insertion using labeled substrates

Isotopic labelling can be used to follow atoms through reaction pathways and has been used to probe lipoyl formation by LipA (2, 3, 5, 12-14). The *in vivo* turnover of octanoic acids specifically tritiated at the C5, C6, C7 and C8 positions has shown that hydrogen atoms are only abstracted from the C6 and C8 positions (13). Commercially available 8,8,8 - D_3 - octanoic acid (Qmx Laboratories, Thaxted) and synthesised 6,6 - D_2 - octanoic acid were coupled to the tripeptide backbone (R) to generate the peptides **39** and **40** (fig. 2.5).

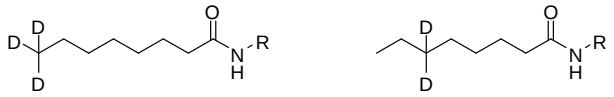

39 **40**

Figure 2.5 Structure of the two labeled peptides used to investigate the order of sulfur insertion in lipoic acid biosynthesis.

Single sulfur insertion into one of the C6 or C8 centres of either of these peptides, would result in the formation of monothiolated adducts which would be distinguishable by MS depending on where sulfur insertion has occurred. This would identify which hydrogen atom is abstracted first providing insight into the mechanism of lipoyl formation.

Reactions using 8,8,8-D_3 peptide 38

Incubation of 8,8,8- D_3- octanoyl peptide **39** with LipA could lead to the formation of either the 6- thiol **41** (Pathway A) or the 8- thiol **42** peptides (Pathway B) (fig. 2.6). These monothiolated adducts have a mass difference of 1 Da, **41** an expected m/z = 550.3 and **42** a m/z = 549.3 making them distinguishable by our MS system which is capable of resolving this 1 Da mass difference.

8,8,8- D_3- peptide **39** was incubated with LipA, SAM and sodium dithionite at 37 °C for 2 h before being quenched by acidification and analysed by LCMS (fig. 2.7).

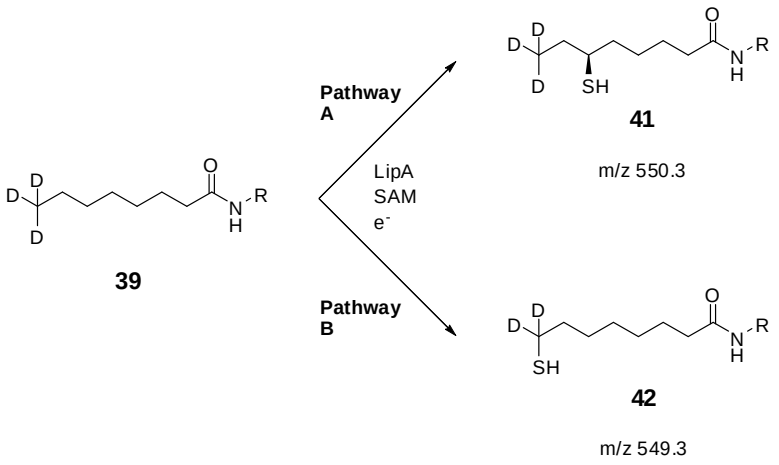

Figure 2.6 The insertion of a single sulfur atom into the 8,8,8- D_3 peptide **39** could result in the formation of one or both or two distinguishable monothiolated peptides **41** or **42.**

The 8-thiol peptide **42** is not observed to be formed in this experiment, suggesting that sulfur insertion occurs first at C6. However, the data is not conclusive due to the possibility that a deuterium isotope effect is present at C8 forcing selective insertion at C6. The presence of this isotope effect does not eliminate any of the three reaction pathways that could exist:

1) Ordered insertion with C6 first (supported by this observation).
2) Ordered insertion with C8 first (reaction might proceed via an alternate pathway due to a KIE present at C8 preventing hydrogen atom abstraction).
3) Random order of sulfur insertion (would expect a mixture of **41** and **42** to be detected but **42** was not observed due to KIE for C8 hydrogen abstraction).

A large kinetic isotope effect (KIE) for hydrogen abstraction has previously been associated with lipoyl formation using a fully deuterated substrate (2). Using this substrate, lipoyl formation was greatly reduced, but the hydrogen atom which was linked to the KIE could not be identified. Using the 8,8,8- D_3 labelled peptide **39,** a low quantity of DHL and lipoyl peptide are formed (fig. 2.8) in comparison with the unlabelled substrate **34**. A KIE is the ratio of the initial reaction rates for the two substrates. However, using the ratio of the products formed, an approximation of the KIE for the C8 hydrogen abstraction can be reached. This method is not conclusive, as the two reactions are expected to progress at different rates and as time increases the ratio of products formed in each reaction would decrease.

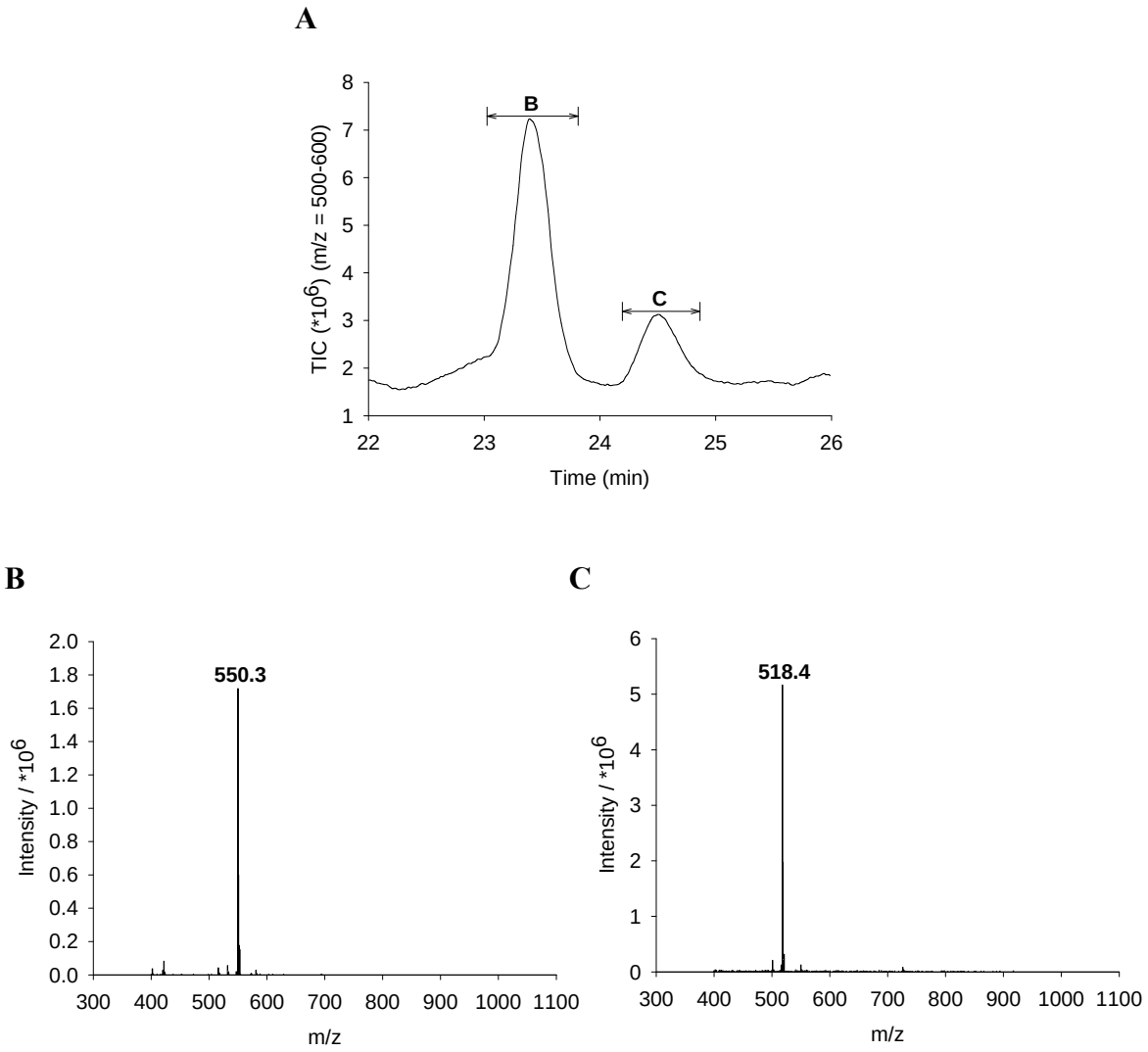

Figure 2.7 (A) TIC and mass spectra of an assay using 8,8,8- D_3 peptide **39** after incubation at 37 °C for 2 h. Protein was removed by acid precipitation followed by centrifugation; **(B)** mass ion of single sulfur inserted product, m/z = 550.3 showing exclusive formation of only the 6-thio peptide **41** only (expected m/z for protonated adduct = 550.3); **(C)** mass ion of starting peptide, m/z = 518.4 (expected m/z for protonated adduct = 518.4).

The expected KIE for hydrogen/deuterium abstraction is 1 - 7 (15). However, the ratio of the calculated areas for double sulfur inserted products formed after 2 h at 37 °C suggests a much larger KIE of 14.5 applies to hydrogen atom abstraction from C8. This approximate KIE was supported by calculating the ratio of the products formed after 20 min, which was found to be 15.0. However, a large error can be expected in the quantification of the double sulfur inserted products as the peaks observed is close to the detection threshold of the mass spectrometer. A complete kinetic analysis of the two substrates would be required to accurately quantify this KIE. Previously KIE's outside the expected range have been

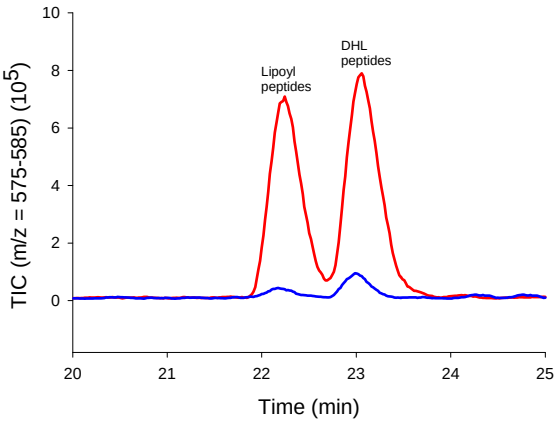

Figure 2.8 TIC trace of an assay comparing 8,8,8- D_3 peptide **39** (Blue) after incubation at 37 °C for 2 h with one using the unlabelled octanoyl peptide **34** (Red). Selected ion monitoring (SIM) (m/z = 575-585) is used to detect only lipoyl and DHL peptides.

observed in other systems (16, 17) and is believed to be a result of quantum tunneling. The presence of a KIE at C8 suggests that this hydrogen atom abstraction is a rate determining (RDS) step in lipoyl formation.

Reactions using 6,6-D_2 peptide 40

To investigate whether the KIE at C8 was hindering hydrogen atom abstraction at this centre and altering the reaction pathway, the reaction of the 6,6-D_2 labeled peptide was also investigated. Incubation of 6,6- D_2- octanoyl peptide **40** with LipA could lead to the formation of either the 6- thiol **43** (Pathway A) or the 8- thiol **44** (Pathway B) peptides (fig. 2.9). These monothiolated adducts should be distinguishable by MS due to an m/z difference of 1 Da, **43** has an expected m/z value of 548.3 and **44** has an expected m/z value of 549.3.

Synthesis of C6-D_2- octanoyl peptide 40

6,6- D_2- octanoic acid was not commercially available and first had to be prepared as outlined in scheme 2.2 before it could be attached to the peptide backbone. Regioselective deuterated fatty acids can be prepared by the reduction of an oxo group at the required position in the chain (18). A method for the synthesis of the 6-oxo-octanonic acid

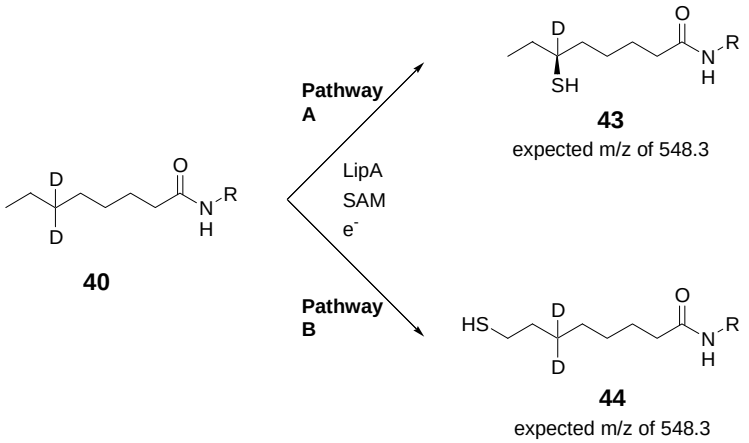

Figure 2.9 The insertion of a single sulfur atom into the 6,6- D_2 peptide **40** could result in the formation of one or both or two distinguishable monothiolated peptides **43** or **44**.

precursor **47** has been previously reported (3).

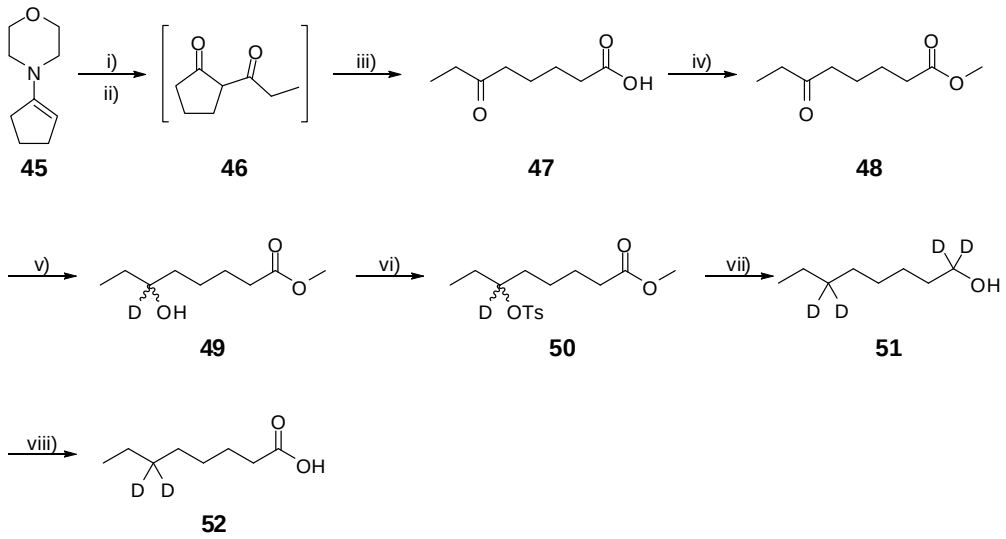

Scheme 2.2 Synthetic pathway for the formation of 6,6- D_2- octanoic acid **52**. *Reagents and conditions*: i) EtCOCl, Et_3N, DCM, RT, 16 h; ii) 20% $HCl_{(aq)}$, 50 °C, 16 h; iii) 5M NaOH, DCM, 50 °C, 16 h, 49%; iv) MeOH, H_2SO_4, DCM, 50 °C, 16 h, 99%; v) $NaBD_4$, THF, D_2O, 0 °C, 1 h, 91%; vi) TsCl, pyridine, RT, 16 h, 49%; vii) $LiAlD_4$, THF, 0 °C, 5 h, 69%; viii) CrO_3, H_2SO_4, H_2O, acetone, RT, 5 h, 28%.

Formation of 6-oxo octanoic acid **47** from 1-morpholinocyclopentene **45** was achieved by propylation using propionyl chloride followed by acid hydrolysis to form a mixture of the diketone **46** and the desired ketoacid **47**. Conversion of residual diketone to the ketoacid was achieved by refluxing the mixture under basic conditions to form the retro-Claison condensation product. Esterification of the ketoacid produced **48** followed by selective

reduction of the ketone using sodium borodeuteride incorporated the first deuterium atom at C6 forming the hydroxyl ester **49**. Conversion to the tosylate **50** followed by substitution and reduction to the alcohol **51** using lithium aluminium deuteride inserted the second deuterium atom at C6. Oxidation using Jones reagent completed the synthesis of the labeled octanoic acid **52**. This acid was coupled to the tripeptide by the method of Bryant *et al.* (7) forming the labeled substrate **40** which was purified by HPLC to >95%.

LCMS analysis of reactions using a C6-D_2 octanoyl peptide

6,6- D_2 peptide **40** was incubated with SAM and sodium dithionite at 23 °C for 60 min before being quenched by acid precipitation of the protein. LCMS analysis of the supernatant revealed the exclusive formation of the 6- thiooctanoyl peptide **43** (fig. 2.10) without any evidence of the 8- thiooctanoyl peptide **44**.

Experiments using labeled substrates **39** and **40** provide evidence that sulfur insertion is occurring in a stepwise manner with insertion at C6 preceding that at C8. Experiments using the 6,6-D_2 peptide **40** failed to detect initial sulfur insertion at C8 suggesting that the observed large KIE was not forcing selective insertion at C6 when using the 8,8,8- D_3 peptide **39**. It is clear there is a difference between thiooctanoic acid groups added to the growth medium (3) and those formed in *in vitro* experiments. The *in vitro* experiments described here have demonstrated exclusive sulfur insertion at C6 regardless of the position of deuterium atoms on the octanoyl chain. It can therefore be concluded that using the preferred octanoyl substrate, sulfur insertion occurs in a stepwise manner first at C6 followed by insertion of sulfur at C8. This observation suggests that the 8-thiooctanoyl groups are not, as previously thought an intermediate species, but are more easily accommodated in the active site of LipA than 6-(*RS*)-thiooctanoyl groups and can undergo sulfur insertion at C6 forming the lipoyl product.

Assuming that lipoyl formation proceeds in a stepwise manner with sulfur insertion first at C6, the progress of the initial step can be easily followed by monitoring the exhaustion of the starting peptide. A comparison between the rate of depletion of the 6,6-D_2-peptide **40** and the unlabelled peptide **34** has allowed the estimation of a KIE associated with this hydrogen atom abstraction (fig. 2.11). The depletion of starting peptide was followed by incubating each of the substrates with LipA in the presence of SAM and sodium dithionite.

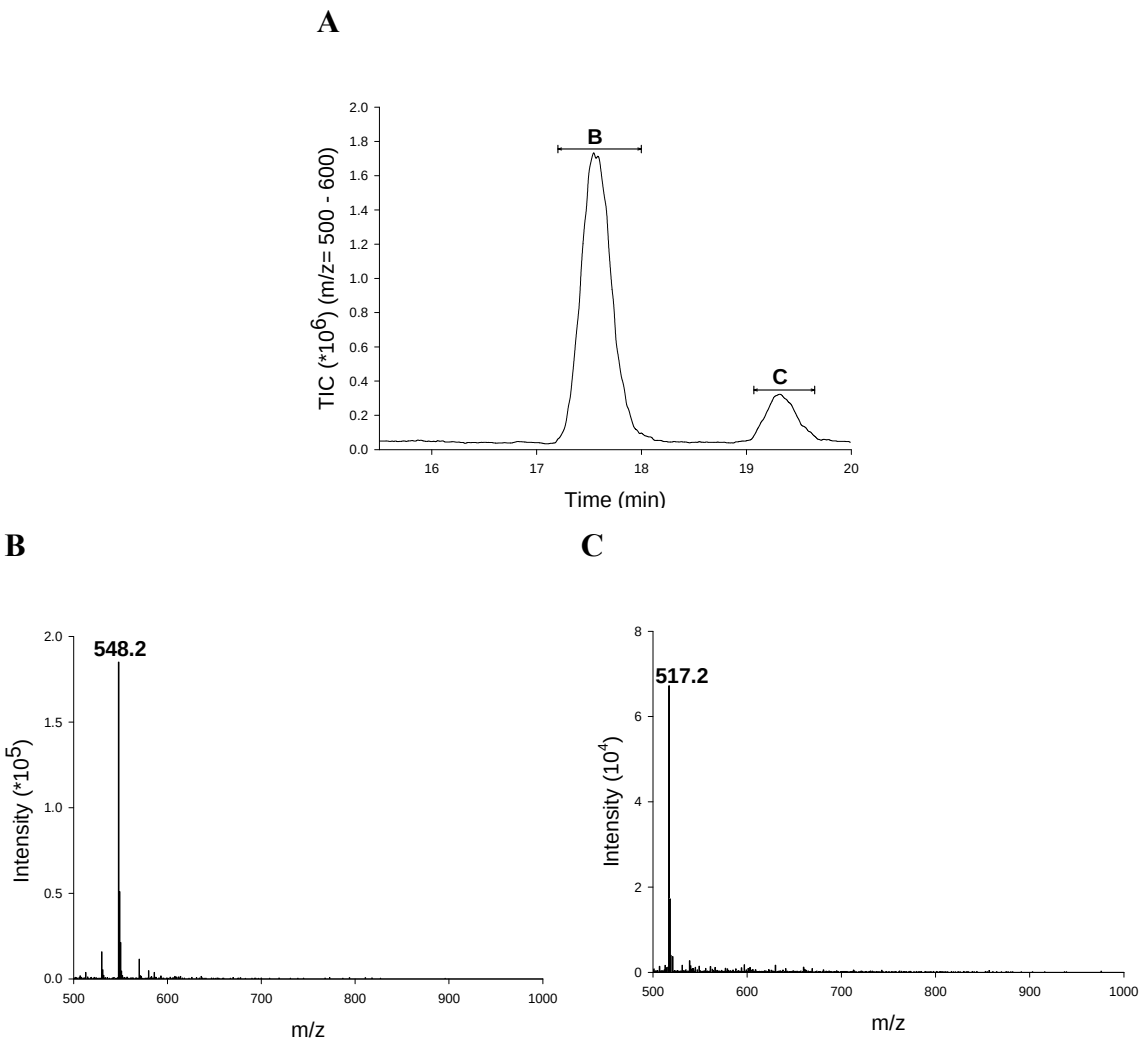

Figure 2.10 (A) TIC and mass spectra of an assay using 6,6- D_2 peptide **40** after incubation at 23 °C for 60 min; **(B)** mass ion of the protonated single sulfur inserted product, m/z = 548.2 showing exclusive formation of only the 6-thio peptide **43**; **(C)** mass ion of the protonated starting peptide, m/z = 517.2.

Reactions were carried out on a 2.5 mL scale with gentle stirring to facilitate mixing and were maintained at 23 ° to inhibit the second sulphur insertion. 250 µL aliquots were removed and quenched by the addition to previously measured TFA at varying timepoints. The 0 s time point was taken from an assay mixture lacking SAM. Supernatants were analysed by LCMS with SIM set to detect ions in the mass range of 510-520. Peak areas were intergrated using the Xcalibur® software and their values plotted against time.

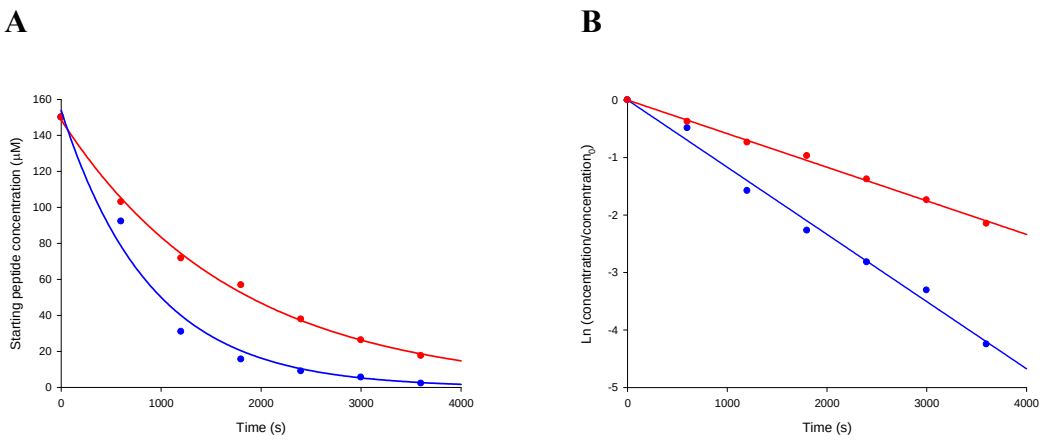

Figure 2.11 (A) Graph comparing the exhaustion of the 6,6-D_2-peptide **40** (**Red**) compared to the unlabeled peptide **34** (**Blue**); **(B)** Plot for calculating the rate constants for the insertion of the first sulfur atom, using the 6,6-D_2-peptide **34** ($k = 6 \times 10^{-4}\ s^{-1}$) and the unlabeled peptide **34** ($k = 12 \times 10^{-4}\ s^{-1}$). Using these rate constants a KIE of ~2 is estimated for hydrogen atom abstraction from C6.

The depletion of the starting peptides can be used to estimate the rate constant for the initial step in lipoyl formation any products formed are thought to result from this initial hydrogen atom abstraction. The ratio of the observed rate constants for the formation of the monothiolated species suggests a KIE of ~2 which is within the range expected for a Hydrogen atom abstraction. Observing KIE's at the C6 and C8 centers of the octanoyl group implies that Hydrogen atom abstraction and not sulfur insertion is the rate determining steps for both sulfur atoms inserted by LipA. If sulfur insertion was the rate determining step, a KIE would not be expected to affect the formation of any detected products.

2.3.2 Characterisation of the monothiolated peptide using NMR

Monothiolated product **37** was further characterised by ^1H NMR. A sample of monothiolated peptide was isolated by HPLC (fig. 2.12) from fourteen 0.5 mL reactions using the unlabelled substrate **34**. However although the NMR confirmed the MS observations from the labeled experiments that sulfur was inserting at C6, there was some residual DHL peptide **36** contaminating the spectrum due to co-elution with the desired peak.

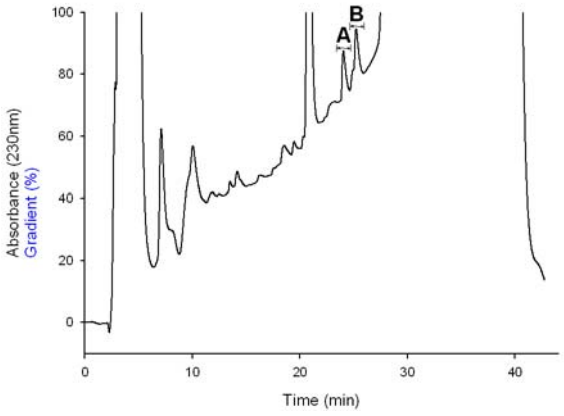

Figure 2.12 HPLC analysis with UV detection (230 nm) for purification of a single sulfur inserted product from a *S. solfataricus* LipA assay at 23 °C using tripeptide **34**. Peaks were identified using MS. **A** had an observed mass ion of547.6 and 579.6 whilst peak **B** had an observed mass ion of 515.6.

Characterisation of the alkylated monothiolated peptide

To allow separation and therefore isolation of the C6 monothiolated peptide **37** from the contaminating DHL peptide **36** without potentially confusing disulfide formation, the crude products from fourteen 0.5 mL reactions using the unlabelled substrate **34** were combined and treated with an excess of tris(2-carboxyethyl)phosphine hydrochloride (TCEP) to reduce any formed disulfides. The reduced mixture was treated with the alkylating agent iodoacetamide, generating the more stable polar thioethers **54** and **55** (fig. 2.13).

The increased range in polarity from the addition of the acetamide groups was sufficient to allow separation the alkylated single sulfur inserted peptide **53** from the alkylated double sulfur inserted peptides **54** by HPLC (fig. 2.14).

The improved separation achieved by the alkylation of the reaction mixture facilitated the purification of the alkylated 6-thiooctanoyl peptide **53** (<100 μg) from the reaction mixture. Fractions containing the monothiolated peptide were pooled, lyophilised and proton NMR collected. A COSY spectrum (fig. 2.15) allowed identification of the protons attached at C6, C7 and C8 of the monothiolated octanoyl group confirming that sulfur insertion at C6 precedes C8.

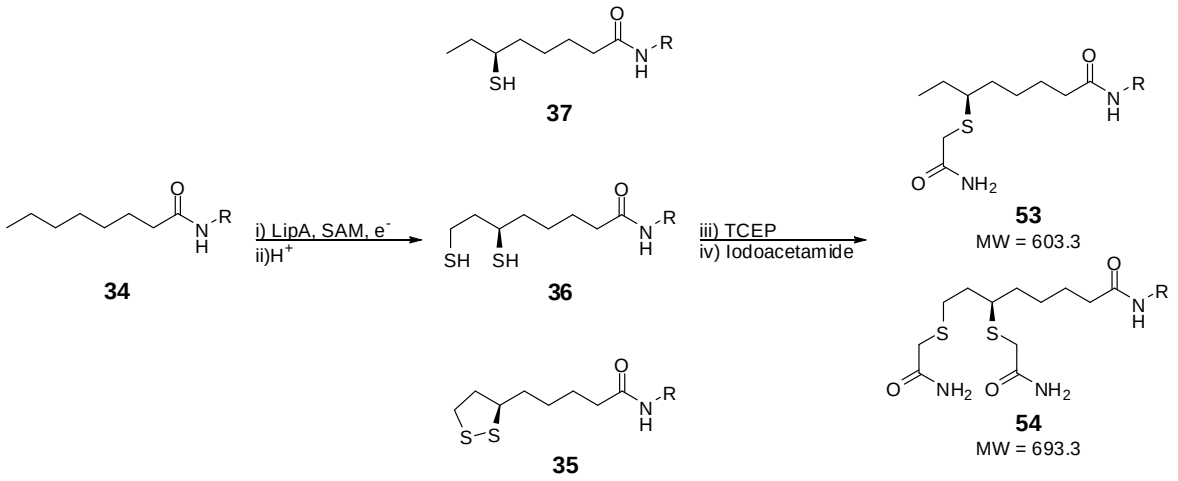

Figure 2.13 Treatment of a reaction using LipA and substrate peptide **34** converting suspected products **35**, **36** and **37** with TCEP and iodoacetamide results in the formation of the two new peptide species **54** and **55**.

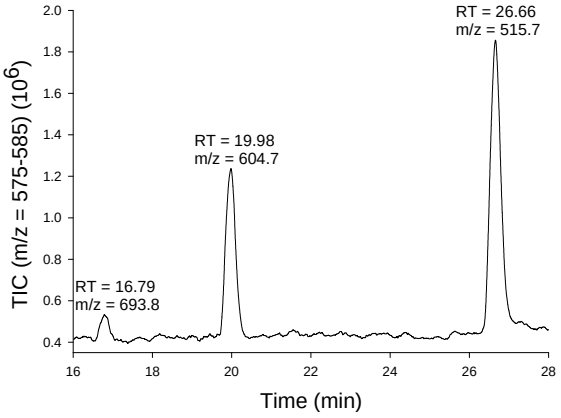

Figure 2.14 The TIC of an assay after reduction and alkylation with iodoacetamide. The peak at 26.66 min corresponds to protonated starting peptide **34** (expected m/z =515.3), the peak at 19.98 min corresponds to protonated alkylated monothiolated peptide **53** (expected m/z = 604.3) and the peak at 16.79 corresponds to protonated alkylated DHL peptide **54** (expected m/z = 693.3).

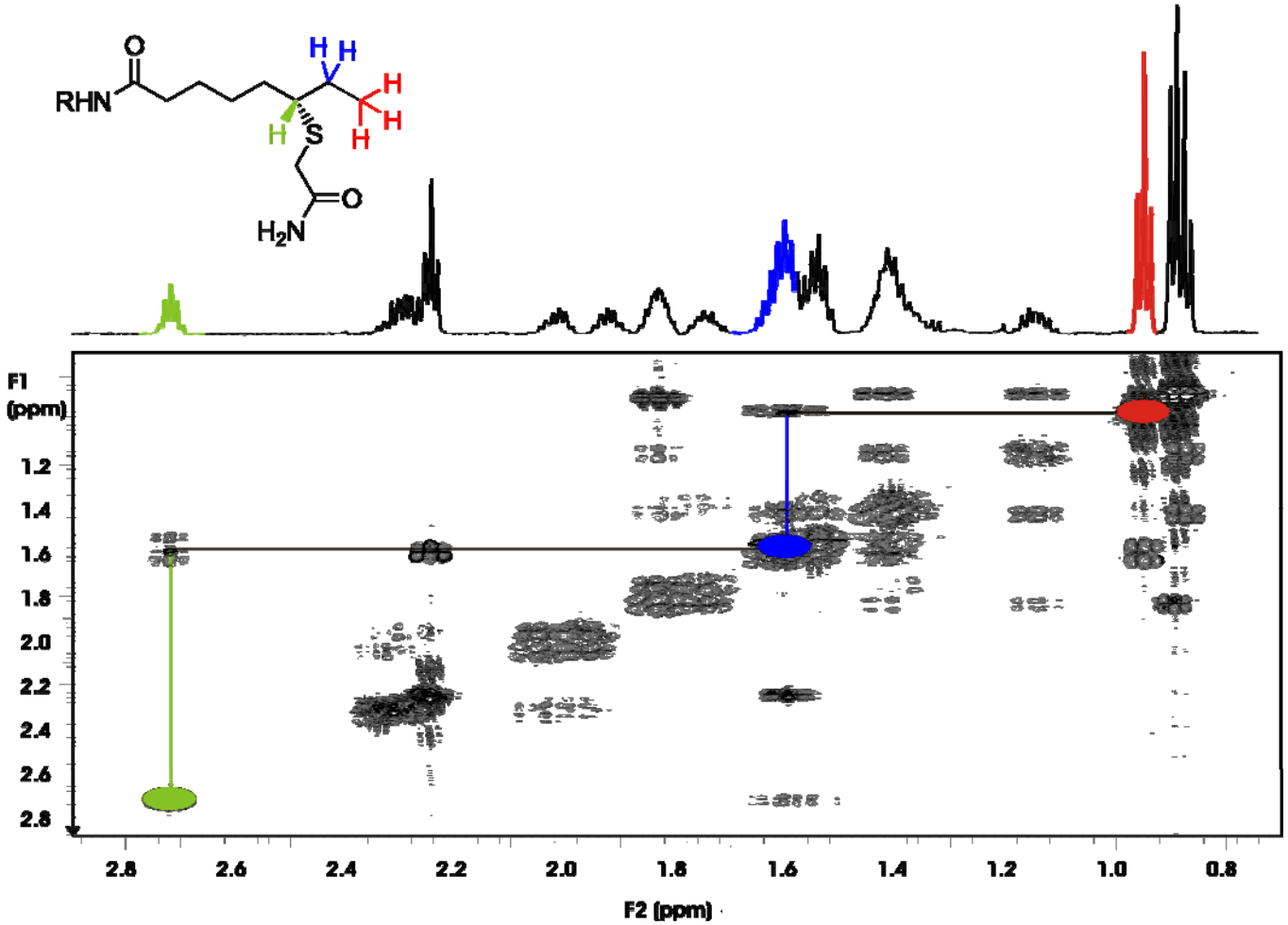

Figure 2.15 HH NMR (600 MHz) of the isolated functionlised monothiolated peptide **53**. Correlations are marked between C8-C7-C6. The Signal at C6 is characteristic of an α-CH of a thiol group.

2.4 Investigating whether the single sulfur product is protein bound

It has been shown that both sulfur atoms in lipoic acid are derived from the same protein molecule (12). This observation raises the possibility that the monothiolated intermediate formed after the first sulfur insertion remains bound to LipA. Feeding studies show the 8-thioctanoic acid is more readily incorporated into lipoic acid (3) but an 8- thiooctanoyl derivative is not detected *in vitro*. The detection of the 6-thiooctanoyl derivative and the evidence that both sulfur atoms come from the same protein molecule suggests that the intermediate is bound to the protein, not free in solution. This was investigated by modifying the reaction protocol to separate the protein from any free peptide material within the reaction mixture.

2.4.1 Removal of the protein using molecular weight cut off (MWCO) filters

The assay protocol was modified to include the use of a 5 kDa MWCO spin filter to separate the LipA and any bound products from any material free in solution, effectively quenching the reaction. LCMS analysis of the filtrate, compared to the supernatant isolated from a reaction using TFA precipitation detected a decrease in the total quantity of peptides isolated. However, there was a two fold increase in the proportion of starting peptide recovered. This increase in signal strength is likely to arise from an increase in concentration rather than reduced activity as not all the buffer was recoverable using this method. The peak containing the monothiolated peptide was greatly reduced (< 6%) as was the peak corresponding to the lipoyl peptide (30%) reflecting the decrease in isolated peptides (fig. 2.16).

The decrease in detection of 6-thiooctanoyl peptide **37** suggested that the intermediate species remained bound to the protein. However, using this method, monothiolated adducts were detected. This may have been due to the protein denaturing as precipitate was observed to form during filtration.

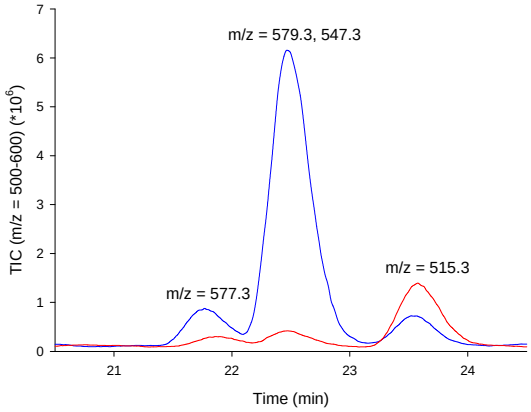

Figure 2.16 TIC of a reaction incubated for 2 h at 37 °C quenched by TFA precipitation (Blue) compared with removal of the protein using a 5 kDa MWCO spin filter (Red) corrected by -0.477 min showing a decrease in detection of sulfur inserted peptides.

2.4.2 Partial purification of the bound intermediate by size exclusion chromatography

A second modified protocol utilised a PD-10 desalting column (Amersham Biosciences) to remove any free low molecular weight molecules (M/W < 1000) eg. starting peptide, from the large molecular weight molecules (M/W > 5000) eg. proteins. After separation of the reaction mixture, the protein was precipitated by the addition of acid and removed by centrifugation and the supernatant analysed by LCMS. The only peptide species observed in the reaction mixture was the monothiolated species **37** which had remained bound to the protein (fig. 2.17, A).

A sample of the PD-10 filtered protein was incubated at 60 °C for 1 h (fig. 2.17, B) and a second sample incubated with fresh SAM and sodium dithionite (fig. 2.17, C). The sample containing fresh SAM and sodium dithionite was capable of converting the bound intermediate peptide to lipoyl peptide suggesting that the intermediate for lipoyl formation is the protein bound 6- thiooctanoyl peptide **55**.

Both experiments to determine if the single sulfur inserted peptide remains bound to the protein have shown that strongly denaturing conditions are required for the release of the intermediate species from LipA (fig. 2.18), in this case acidic precipitation of the protein.

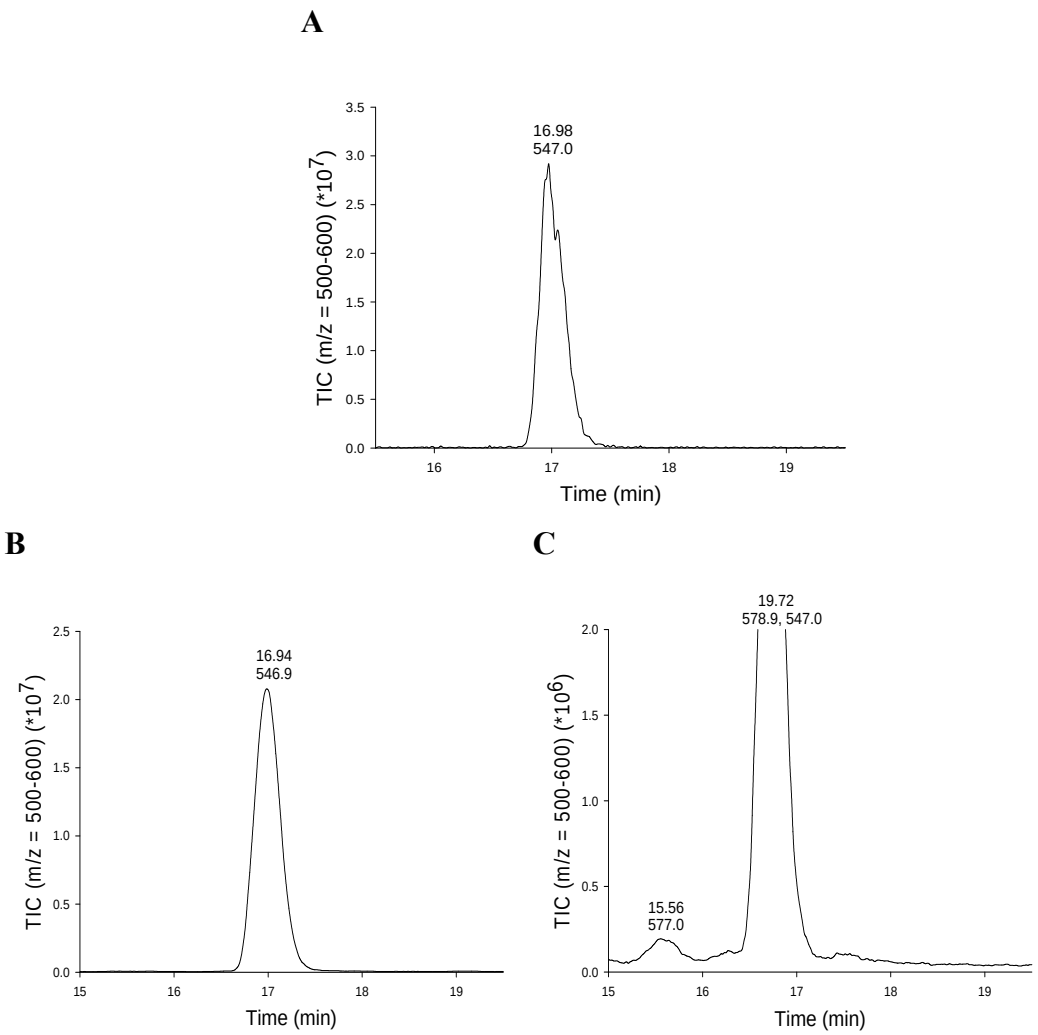

Figure 2.17 (A) TIC of the supernatant of protein from a reaction that after 1 h at 37 °C has been stopped by PD-10 filtration; **(B)** TIC of the supernatant of the protein which after PD-10 filtration had been further incubated for 1 h at 60 °C; **(C)** TIC of the supernatant of the protein which after PD-10 filtration had been further incubated for 1 h at 60 °C with fresh SAM and sodium dithionite.

The observation that the intermediate remains tightly bound to the protein and is not in rapid equilibrium with the bulk solution is consistent with the observation that both sulfur atoms are derived from the same LipA monomer (12). These results show that one intermediate for lipoyl formation is protein bound 6-thiooctanoyl derivatives. The observation that 8-thiooctanoyl derivatives are more readily incorporated into lipoic acid than the 6 thiooctanoyl derivatives (3), suggests that the protein is more capable of accommodating a longer substrate than a branched alkyl chain.

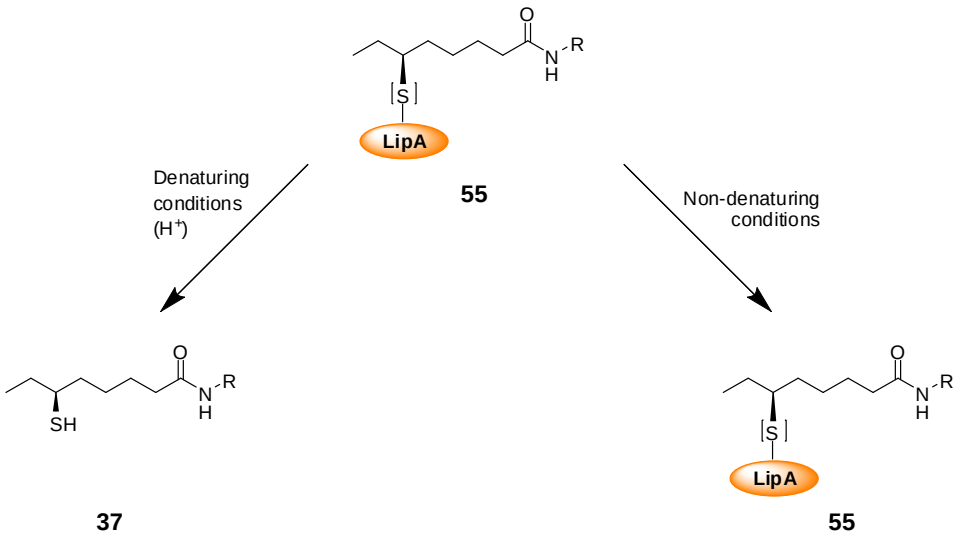

Figure 2.18 Denaturing conditions are required for the efficient release of a monothiolated species from LipA.

2.5 Proposed mechanism of lipoyl formation by LipA

The observed formation of a monothiolated peptide and its subsequent characterisation as the 6-monothiooctanoyl species by NMR and MS has offered insight into the biosynthesis of lipoyl groups. Further insight was gained by the determination that the detected single sulfur inserted peptide remains bound to the protein, presumably through the second iron sulfur cluster during the reaction. However this assumption will require crystallisation of the protein bound intermediate to be confirmed. The results discussed in this chapter are consistent with a mechanism where a hydrogen atom is first abstracted from C6 and sulfur, presumably from the second cluster in LipA, is inserted in a stepwise manner to form the protein bound intermediate **55**. In a subsequent rate determining step a second sulfur atom is inserted at C8 (fig. 2.19).

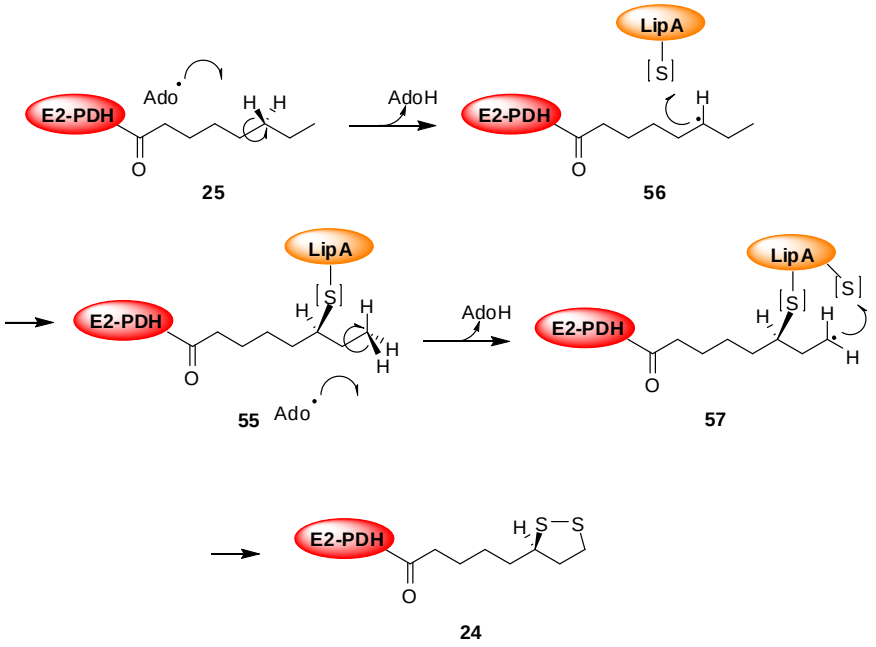

Figure 2.19 Proposed Mechanism of sulfur insertion by LipA. The sulfur source (depicted as [S]) is unknown but believed to be associated with the protein, presumably the second [4Fe-4S] cluster.

2.6 References

1. Zhao, X., J.R. Miller, Y. Jiang, M.A. Marletta, and J.E. Cronan, Assembly of the covalent linkage between lipoic acid and its cognate enzymes. *Chemistry and Biology*, 2003. **10**(12): p. 1293-302.
2. Cicchillo, R.M., D.F. Iwig, A.D. Jones, N.M. Nesbitt, C. Baleanu-Gogonea, M.G. Souder, L. Tu, and S.J. Booker, Lipoyl synthase requires two equivalents of S-adenosyl-L-methionine to synthesize one equivalent of lipoic acid. *Biochemistry*, 2004. **43**(21): p. 6378-86.
3. White, R.H., Biosynthesis of lipoic acid - extent of incorporation of deuterated hydroxyoctanoic and thiooctanoic acids into lipoic acid. *Journal of the American Chemical Society*, 1980. **102**(21): p. 6605-6607.
4. Parry, R.J. and D.A. Trainor, Biosynthesis of lipoic acid. 2. Stereochemistry of sulfur introduction at C-6 of octanoic acid. *Journal of the American Chemical Society*, 1978. **100**(16): p. 5243-4.
5. White, R.H., Stable isotope studies on the biosynthesis of lipoic acid in *Escherichia coli*. *Biochemistry*, 1980. **19**(1): p. 15-19.
6. Bryant, P., Investigations into the Biosynthesis of Lipoic Acid, University of Southampton, Ph.D Thesis, 2008
7. Bryant, P., M. Kriek, R.J. Wood, and P.L. Roach, The activity of a thermostable lipoyl synthase from *Sulfolobus solfataricus* with a synthetic octanoyl substrate. *Analytical Biochemistry* 2006. **351**(1): p. 44-9.
8. Zheng, L.M., V.L. Cash, D.H. Flint, and D.R. Dean, Assembly of iron-sulfur clusters - Identification of an *iscSUA- hscBA-fdx* gene cluster from *Azotobacter vinelandii*. *Journal of Biological Chemistry*, 1998. **273**(21): p. 13264-13272.
9. Kriek, M., L. Peters, Y. Takahashi, and P.L. Roach, Effect of iron-sulfur cluster assembly proteins on the expression of *E. coli* lipoic acid synthase. *Protein Expression and Purification*, 2003. **28**: p. 241-245.
10. Atherton, E., Sheppard, R. C., *Solid phase peptide synthesis a practicle approach*. 1989: IRL Press at Oxford University Press.
11. Diaz-Mochon, J.J., L. Bialy, and M. Bradley, Full orthogonality between Dde and Fmoc: the direct synthesis of PNA--peptide conjugates. *Organic Letters* 2004. **6**(7): p. 1127-9.

12. Cicchillo, R.M. and S.J. Booker, Mechanistic investigations of lipoic acid biosynthesis in *Escherichia coli*: both sulfur atoms in lipoic acid are contributed by the same lipoyl synthase polypeptide. *Journal of the American Chemical Society*, 2005. **127**(9): p. 2860-1.
13. Parry, R.J., Biosynthesis of lipoic acid. 1. Incorporation of specifically tritiated octanoic acid into lipoic acid. *Journal of the American Chemical Society*, 1977. **99**(19): p. 6464-6.
14. Parry, R.J. and M.G. Kunitani, Letter: Biotin biosynthesis. 1. The incorporation of specifically tritiated dethiobiotin into biotin. *Journal of the American Chemical Society* 1976. **98**(13): p. 4024-6.
15. Smith, M.B., J. March, and J.A.o.c. March, *March's advanced organic chemistry : reactions, mechanisms, and structure*. 5th ed. / Michael B. Smith, Jerry March. ed. 2001, New York ; Chichester: Wiley. xviii, 2083 p.
16. Lewis, E.S. and L. Funderburk, Rates and isotope effects in the proton transfers from 2-nitropropane to pyridine bases. *Journal of the American Chemical Society*, 1967. **89**(10): p. 2322-2327.
17. Reinsch, J., A. Katz, J. Wean, G. Aprahamian, and J.T. McFarland, The deuterium isotope effect upon the reaction of fatty acyl-CoA dehydrogenase and butyryl-CoA. *Journal of Biological Chemistry*, 1980. **255**(19): p. 9093-9097.
18. Bragina, N.A. and V.V. Chupin, Methods of synthesis of deuterium labelled lipids. *Uspekhi Khimii*, 1997. **66**(11): p. 1077-1090.

Chapter 3. Investigation of inhibition of LipA by methionine and AdoH

3.1 Introduction

Under the conditions tested using *S. solfataricus* LipA, the measured yield of lipoyl peptide with respect to octanoyl peptide was observed as 55% (1). Proteins are commonly inhibited by their products, for example 5'-methylthioadenosine (MTA) acts as a strong feedback inhibitor of polyamine biosynthesis (2, 3) and *S*-adenosylhomocysteine (SAH) can act as a strong feedback inhibitor of SAM dependant methyltransferase reactions (4, 5). It was hypothesised that the low activity observed for LipA resulted from the inhibition of the reaction by products formed during lipoyl formation.

Radical SAM proteins reductively cleave SAM to generate methionine **11** and the highly reactive Ado• radical (6, 7). The reactions that follow the formation of this radical are controlled by the protein. In the case of lipoyl biosynthesis, the Ado• radical abstracts hydrogen atoms from the C6 and C8 centres of a protein bound octanoyl group (8, 9) followed by insertion of sulfur atoms at these positions. Abstraction of the hydrogen atoms results in reduction of the Ado• radical generating AdoH **58** (fig. 3.1). As each lipoyl moiety **24** formed requires the cleavage of two C-H bonds by Ado•, two molecules of SAM are required and in turn two molecules of methionine **11** and AdoH **58** are produced.

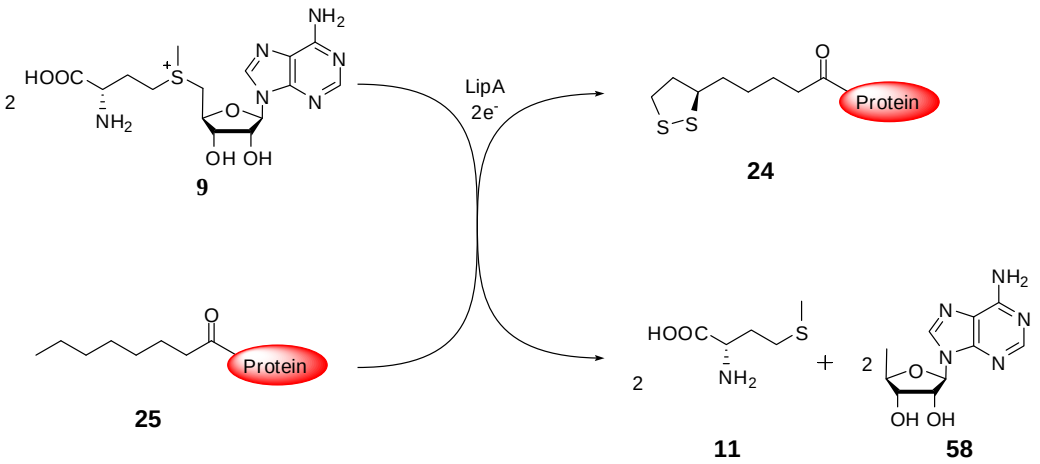

Figure 3.1 Lipoyl group formation generates the side products methionine **11** and AdoH **58**.

The *in vitro* inhibition of the radical SAM sulfur insertion protein BioB by its side product AdoH has been investigated in a range of systems. Reactions containing BioB (35 μM), DTB (400 μM), DTT (1 mM), SAM (150 μM) flavodoxin (Fldx) (20 μM), Fldx reductase (4 μM), NADPH (1 mM) cysteines (2 mM) and PLP (35 μM) with increasing AdoH concentration has shown that complete inhibition occurs at a concentration of 52.5 μM (10). However, in another system containing BioB (9 μM), DTB (100 μM), SAM (100 μM), NADPH (2 mM), Fldx (2 μM), Fldx reductase (0.05 μM), DTT (2 mM) and $Fe(NH_4)_2(SO_4)_2$ (200 μM) and increasing AdoH concentration no inhibition was observed (11). The conflicting results reported by different research groups has been sugested to be a result of subtle differences in the preparation of the protein prior to testing activity (12).

The inhibition of BioB by its products AdoH and methionine was investigated in a simpler third *in vitro* system which contained only BioB (30 μM), DTB (200 μM), SAM (500 μM), Fldx (10 μM), Fldx reductase (4 μM) and $NADP^+$ (1 mM) with increasing inhibitor concentration. Under these conditions it was observed that although a limited inhibition was achieved by AdoH (half maximal inhibitory concentration (IC_{50}) = 400 μM) or methionine (IC_{50} = 700 μM) independently, a stronger synergistic inhibition was present in reactions which contained both AdoH and methionine (IC_{50} = 150 μM) (13).

5'-methylthioadenosine/*S*-adenosylhomocysteine nucleosidase (Pfs), the product of the *Pfs* gene (14) has been shown to hydrolyse the glycosidic bond between adenosine and ribose in AdoH *in vivo* (12) and *in vitro* (13) (fig 3.2) and is involved in the recycling of *S*-adenosylhomocysteine (SAH) **59** and MTA **62** in bacteria (15).

E. coli strains lacking the *Pfs* gene were found to be deficient in biotin production due to the accumulation of AdoH, whereas cells containing the *Pfs* gene were fully capable of converting DTB to biotin (12). The synergistic inhibition of BioB *in vitro* is also reversed by the addition of the Pfs protein to the reaction mixture (13).

The objective of the experiments described in this chapter was to determine if the observed low activity of LipA *in vitro* is a result of inhibition due to the side products methionine **11** and AdoH **58** and to investigate if Pfs can reverse any observed inhibition.

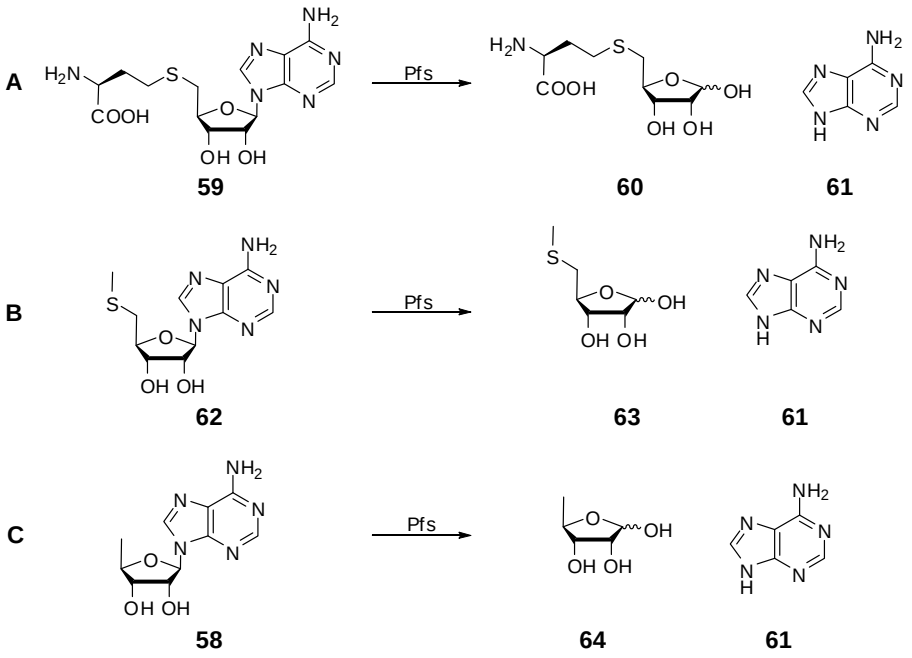

Figure 3.2 Reactions catalysed by Pfs: (A) hydrolysis of *S*-adenosylhomocysteine **59** to form *S*-ribosyl-homocysteine **60** and adenine **61**; (B) MTA **62** to form methylthiolribose **63** and adenine **61**; (C) hydrolysis of AdoH **58** to form 5'deoxyribose **64** and adenine **61**.

3.2 Peptide quantification using TIC

The quantification of substrate peptides **34** and **39** (fig. 3.3) using HPLC analysis coupled with UV-detection (230 nm) in the concentration range present under the reaction conditions of a LipA assay (0-150 μM) results in a weak signal peak due to a lack of a strong chromophore within the peptides. Peptides assembled with fluorescein attached at the C-terminus have been turned over by LipA *in vitro*, however the fluorescence of the peptides that were in the reaction mixture was greatly decreased, perhaps as a result of a reaction with the excess sodium dithionite in the assay (16).

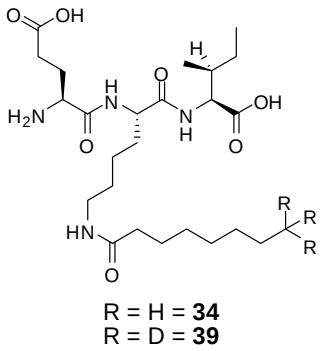

Figure 3.3 Structure of substrate peptides **34** and **39**.

MS has been used as a quantitative technique using a range of ionisation methods. GC-MS analysis using electron impact ionisation (EI) with SIM has been used to quantify manufacturing by-products from malathion formulations (17) and of constituents of bacterial lipids and glycoconjugates (18). Electrospray ionisation (ESI) has been used to quantify structurally diverse analytes (19) and also apolipoproteins in human serum (20). The suitability of ESI coupled with SIM for the determination of peptide species was therefore investigated. Known concentrations of peptides **34** and **39** in the expected experimental range (0-150 μM) were analysed using LCMS with SIM and their peaks integrated (fig. 3.4).

Samples of octanoyl peptide **34** and 8,8,8-D_3-octanoyl peptide **39** were prepared using a series of dilutions. When analysed by LCMS it was found that linear trends (Sigma plot) relating peak area to concentration could be fitted to each dataset. However, the linear gradients observed for the two peptides showed a large variation in the apparent

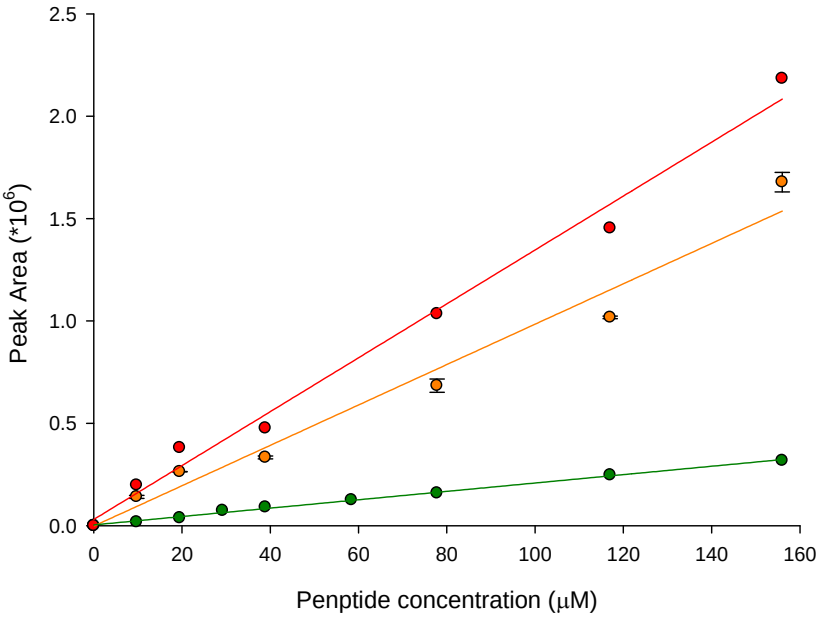

Figure 3.4 Standard curves of octanoyl peptide **34** and 8,8,8-D_3-octanoyl peptide **39**. Peptide **34** is shown in green (R^2 = 0.997) (single measurements) and peptide **39** is shown in red (R^2 = 0.987) (single measurements) and orange (R^2 = 0.974) (average of a duplicate measurements).

concentrations of these samples. The two peptides differ only by deuterium labelling and, as such, samples of the same concentration should result in identical peak areas. An explanation for the observed variation in signal strength is that the samples were not the same concentration as a result of inaccurate measurement of the sample weight. This error could arise as the peptides after lyophilisation are susceptible to static electricity interactions with the sample vial and are hydroscopic resulting in a lower than measured mass for the sample. A sample of the deuterated peptide **39** was analysed on a second occasion and resulted in a linear trend with a gradient which was different from the one previously measured for this sample. A likely explanation for this variance is that the buffers used in the chromatography were prepared with a slight variation in the final acid concentration. These differing acid concentrations would affect the relative ionisation of the two samples and result in inconsistency between datasets analysed on separate occasions.

Quantification by TIC allows clear detection of peptides at low concentrations. However, the integrations observed are not consistent outside each dataset and as a result a standard

curve is not valid. Within each dataset a direct correlation was observed. For subsequent studies a control reaction will be analysed in each case to define 55% conversion of the starting peptide to the double sulfur inserted product. The peaks were identified using SIM (m/z = 570-580) after incubation of the substrate for 2 h at 37 °C with LipA, SAM and sodium dithionite.

3.3 Testing inhibition of LipA by its products, methionine and AdoH

3.3.1 Investigations into the inhibition of LipA by methionine

The inhibition of LipA by methionine was investigated by incubating LipA (300 μM) with SAM (1 mM), sodium dithionite (1 mM), substrate peptide **34** (150 μM) and a known concentration of methionine **11** (50, 100, 250, 500, 750, 1000 μM) for 2 h at 37 °C and measuring the lipoyl peptides formed as a percentage ratio of activity compared to assays containing no inhibitor using SIM (fig. 3.5).

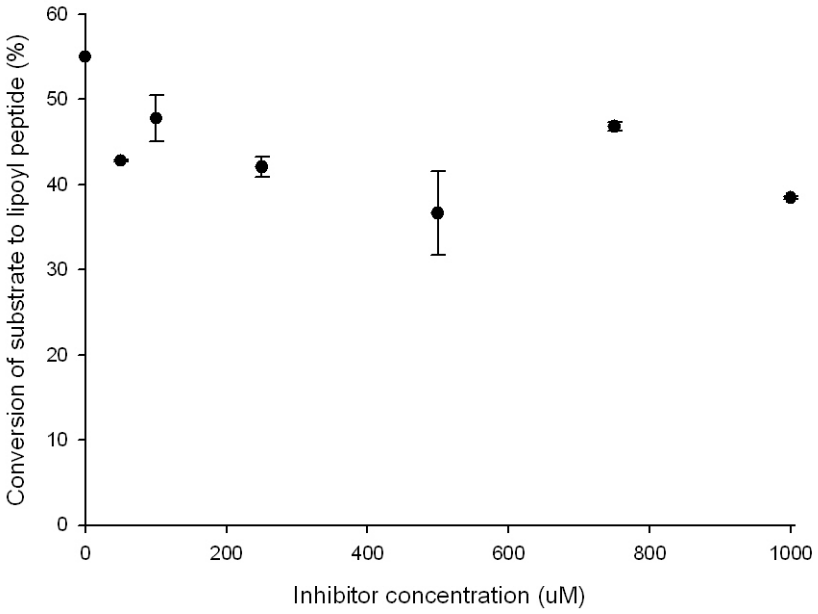

Figure 3.5 Plot comparing LipA activity against methionine concentration. Points are the average of duplicate measurements.

Although the activity appears to gradually decrease with increasing methionine concentration the effect is marginal and no clear relationship could not be elucidated (R^2

values for linear and an exponential decay were both <0.320). Complete turnover of substrate **34** to the lipoyl product **35** should result in a final concentration of methionine of 300 μM. However, under conditions of maximum LipA turnover *in vitro* using the synthetic peptide substrate **34** (observed to be 55%) (1), a yield of 165 μM methionine would be anticipated. At this concentration there was no significant inhibition of LipA observed. Whereas, in the case of BioB, methionine has shown a weak inhibitionary effect (IC_{50} = 700 μM) (13).

3.3.2 Investigations into the inhibition of LipA by AdoH

The inhibition of LipA by AdoH was investigated by incubating LipA (300 μM) with SAM (1 mM), sodium dithionite (1 mM), substrate peptide **34** (150 μM) and increasing concentration of AdoH **58** (50, 100, 250, 500, 750, 1000 μM) for 2 h at 37 °C and measuring the lipoyl peptides formed in comparison to assays containing no inhibitor using SIM (fig. 3.6).

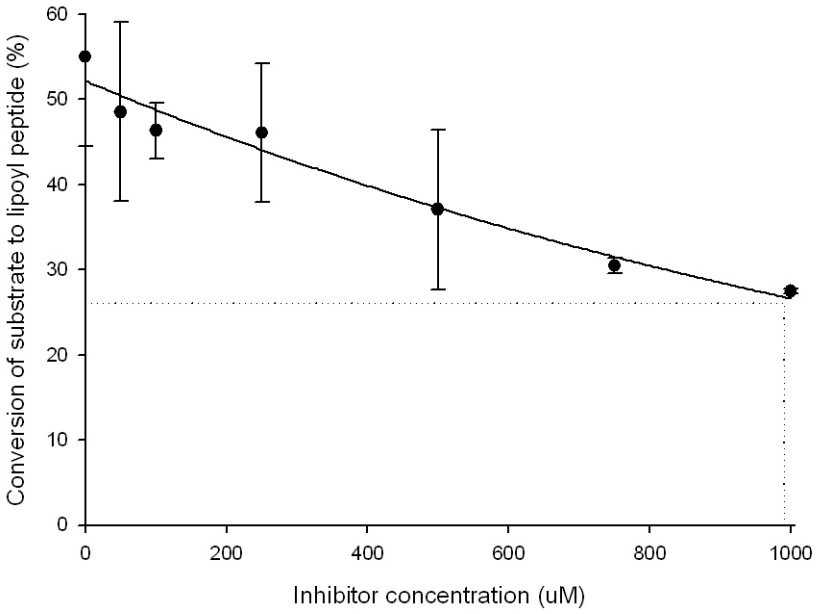

Figure 3.6 Plot comparing LipA activity against AdoH concentration. Points are the average of duplicate measurements. The data was fitted to an exponential decay function with a goodness of fit (R^2) of 0.9616. AdoH has a calculated IC_{50} of 990 ± 83 μM and is shown as a (····) line.

The results closely follow those observed for BioB, as AdoH is a more potent inhibitor than methionine (13). The IC_{50} of AdoH for LipA inhibition under these conditions was found to be 990 μM, whereas for BioB it was 400 μM. It is anticipated that the

concentration of AdoH present after maximum LipA turnover (observed to be 55% conversion of the starting peptide **33**) (1) would be 165 μM. From the results shown in figure 3.6, this concentration of AdoH would give a very modest reduction in LipA activity (<11%). A much higher AdoH concentration of around 850 μM, which is not reached under these conditions, would be required in order to be solely responsible for the low activity observed.

3.3.3 Investigations into the synergistic inhibition of LipA by methionine and AdoH

The inhibition of LipA by methionine or AdoH alone is not sufficient to account for the low activity observed *in vitro* under these conditions. The possibility of synergistic inhibition of LipA by methionine and AdoH acting together was investigated using the same method with a varying inhibitor mixture concentration (50, 100, 250, 500, 750, 1000 μM of each compound) and measuring the lipoyl peptides formed in comparrison to assays containing no added inhibitors using SIM (fig. 3.7) after incubation for 2 h at 37 °C.

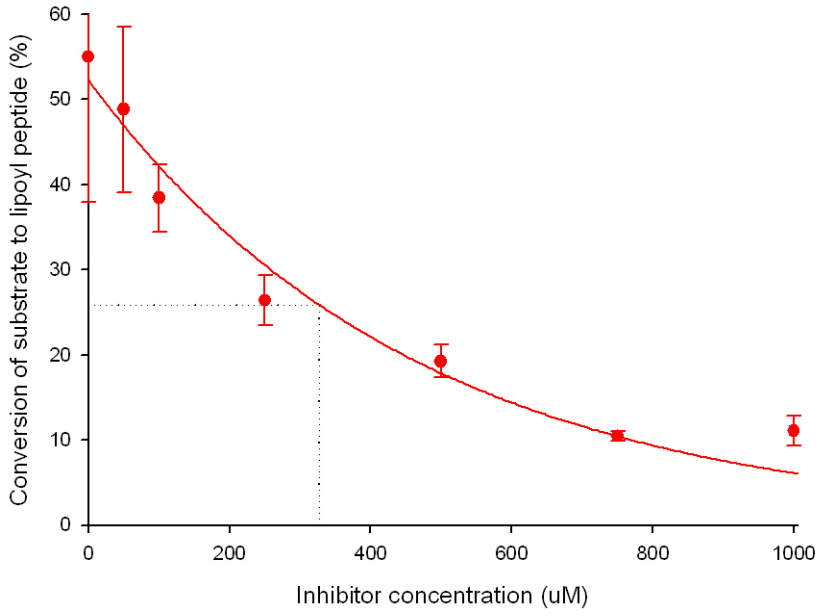

Figure 3.7 Plot showing the activity of LipA reactions containing a known quantity of methionine and AdoH, points are the average of a duplicate measurements. The data was fitted to an exponential decay function with a goodness of fit (R^2) of 0.964. Methionine and AdoH has a calculated IC_{50} of 327 ± 22 μM and is shown as a (····) line.

When added to the reaction mixture together, a strong synergistic inhibition is observed. The IC_{50} was found to equal 327 ± 22 μM compared to 150 μM for BioB. Under conditions of maximum LipA turnover, the expected yield of AdoH and methionine (165 μM) would result in 29% inhibition. It is anticipated that complete conversion of the octanoyl substrate **33** to lipoyl peptide **34** by LipA would generate 300 μM AdoH and methionine, which would result in 47% inhibition. The inhibition observed was 45% and clearly there has not been sufficient turnover to generate the quantity of AdoH and methionine implied by the observed inhibition. An alternative explanation for the low *in vitro* activity observed is therefore required and might be that:

1) Not all the protein contains the required [4Fe-4S] cluster (16, 21), possibly due to incomplete reconstitution of the [Fe-S] cluster.
2) A contaminant is present within the reaction mixture which could inhibit LipA. The SAM and sodium dithionite used in the assays are low purity (~75% and ≥85% respectively). A contaminant in one of these chemicals could be acting as an inhibitor of LipA, for example SAM is known to undergo two spontaneous degradation pathways under physiological conditions (22) (fig 3.8) and one of these products could be acting as another inhibitor.

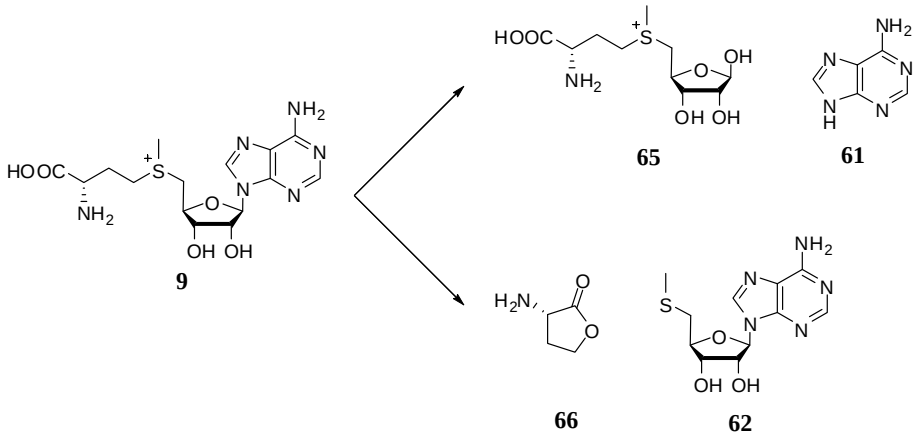

Figure 3.8 The two known SAM degradation pathways.

3.4 Preventing product inhibition by the addition of Pfs

Pfs catalyses the hydrolysis of AdoH *in vivo* (12) and has been shown to increase BioB activity *in vitro* (13) and *in vivo* (12). The effect of adding Pfs to the LipA reaction mixture

was investigated by repeating the synergistic inhibition experiments with and without the addition of Pfs. The formation of lipoyl peptides formed as a percentage ratio of activity was monitored using SIM (fig. 3.9) after 2 h at 37 °C.

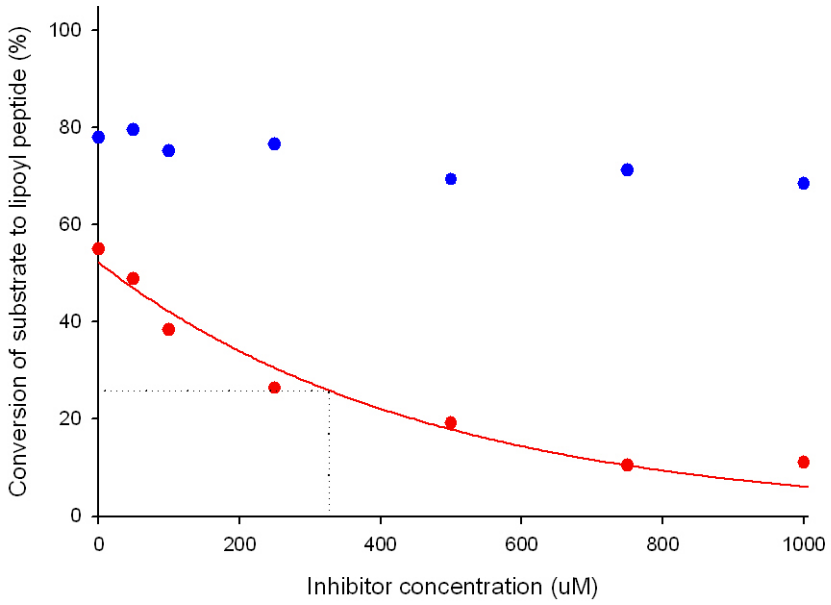

Figure 3.9 Plot comparing the activity of LipA reactions containing a known quantity of AdoH and methionine (Red) to reactions containing the same quantity of AdoH and methionine with the addition of Pfs (1 μM) (Blue). Points are the average of double measurements. An exponential decay was fitted to the data for the reactions containing no Pfs whereas in the case of reactions containing Pfs no expontial trend was observed.

In control reactions without any added inhibitor, a 1.4 fold increase in the total quantity of lipoyl **35** and DHL **36** peptides was observed after the addition of Pfs. The level of inhibition removed can partially be attributed to the synergistic inhibition by AdoH and methionine formed during the reaction. However, the level of increased activity, if it is a result of synergistic inhibition suggests an inhibitor concentration of 187 μM is present in the reaction mixture prior to hydrolysis of AdoH by Pfs. This concentration is marginally greater than the quantity of AdoH and methionine formed for the maximum turnover previously observed (1) (165 μM) but could be the result of AdoH and methionine from the formation of the single sulfur inserted product **37**.

Alternatively, as Pfs removes this extra inhibition, it appears likely that this extra inhibition could be the result of an alternate Pfs substrate. The SAM degradation products were

considered as potential LipA inhibitors. Adenine **61** can be eliminated, as it is a product of Pfs hydrolysis of AdoH and therefore, its concentration would be increased upon addition of Pfs. S-ribosylmethionine **65** and homoserine lactone **66** are not known substrates for Pfs, so their presence within the reaction mixture would also not be affected by its addition. MTA **62** is hydolysed by Pfs (15) and would be effectively removed from the reaction mixture by the addition of this protein. This SAM degradation product could be competing with SAM for the SAM binding site resulting in competitive inhibition of LipA and has been observed within our SAM samples.

3.5 Requirements for achieving catalytic activity *in vitro*

The observed increased activity observed by the addition of Pfs is a step towards achieving catalytic activity of LipA *in vitro*. However, other components are clearly missing from this system to achieve multiple turnovers. The negative trend observed in reactions containing AdoH, methionine and Pfs could be a result of the products of the AdoH hydrolysis, adenine **61** and 5'deoxyribose **64**. Increasing methionine concentration has shown a slight negative trend in activity but no clear relationship has been established. However, the removal of methionine can be facilitated by the addition of methionine adenosyltransferase (MAT) and ATP which would generate SAM *in situ* (23) (fig. 3.10).

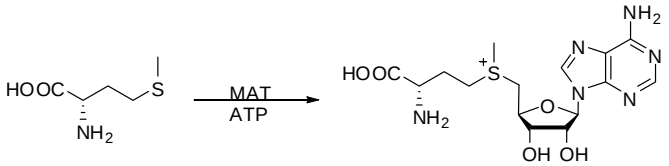

11 **9**

Figure 3.10 Generation of SAM from methionine using MAT and ATP.

The source of sulfur in biotin biosynthesis by BioB is thought to be the second [Fe-S] cluster and cluster degradation has been observed during a single turnover of the protein (24). Similarly if cluster degradation is involved in the mechanism of LipA, catalytic activity could only be achieved if the cluster was regenerated *in situ*. NifS or Isc type proteins which are involved in FeS cluster assembly (25, 26) could facilitate *in vitro* reconstitution of BioB, these proteins could also potentially be used to reconstitute LipA *in vitro* in principle leading to catalytic activity.

3.6 References

1. Bryant, P., M. Kriek, R.J. Wood, and P.L. Roach, The activity of a thermostable lipoyl synthase from *Sulfolobus solfataricus* with a synthetic octanoyl substrate. *Analytical Biochemistry* 2006. **351**(1): p. 44-9.
2. Pajula, R.L., A. Raina, and T. Eloranta, Polyamine synthesis in mammalian tissues. Isolation and characterization of spermine synthase from bovine brain. *European Journal of Biochemistry*, 1979. **101**(2): p. 619-26.
3. Cacciapuoti, G., M. Porcelli, M. Carteni-Farina, A. Gambacorta, and V. Zappia, Purification and characterization of propylamine transferase from Sulfolobus solfataricus, an extreme thermophilic archaebacterium. *European Journal of Biochemistry*, 1986. **161**(2): p. 263-71.
4. Pugh, C.S., R.T. Borchardt, and H.O. Stone, Inhibition of Newcastle disease virion messenger RNA (guanine-7-)-methyltransferase by analogues of S-adenosylhomocysteine. *Biochemistry*, 1977. **16**(17): p. 3928-32.
5. Wood, R.J., M.D. Maynard-Smith, V.L. Robinson, P.C.F. Oyston, R.W. Titball, and P.L. Roach, Kinetic Analysis of Yersinia pestis DNA Adenine Methyltransferase Activity Using a Hemimethylated Molecular Break Light Oligonucleotide. *PLoS ONE*, 2007. **2**(8): p. e801.
6. Fontecave, M., E. Mulliez, and S. Ollagnier-de-Choudens, Adenosylmethionine as a source of 5'-deoxyadenosyl radicals. *Current Opinion in Chemical Biology*, 2001. **5**(5): p. 506-511.
7. Jarrett, J.T., The generation of 5'-deoxyadenosyl radicals by adenosylmethionine-dependent radical enzymes. *Current Opinion in Chemical Biology* 2003. **7**(2): p. 174-82.
8. Cicchillo, R.M., D.F. Iwig, A.D. Jones, N.M. Nesbitt, C. Baleanu-Gogonea, M.G. Souder, L. Tu, and S.J. Booker, Lipoyl synthase requires two equivalents of S-adenosyl-L-methionine to synthesize one equivalent of lipoic acid. *Biochemistry*, 2004. **43**(21): p. 6378-86.
9. Zhao, X., J.R. Miller, Y. Jiang, M.A. Marletta, and J.E. Cronan, Assembly of the covalent linkage between lipoic acid and its cognate enzymes. *Chemistry and Biology*, 2003. **10**(12): p. 1293-302.

10. Ollagnier-de-Choudens, S., E. Mulliez, and M. Fontecave, The PLP-dependent biotin synthase from *Escherichia coli*: mechanistic studies. *FEBS Letters*, 2002. **532**(3): p. 465-468.
11. Tse Sum Bui, B., M. Lotierzo, F. Escalettes, D. Florentin, and A. Marquet, Further investigation on the turnover of *Escherichia coli* biotin synthase with dethiobiotin and 9-mercaptodethiobiotin as substrates. *Biochemistry*, 2004. **43**(51): p. 16432-41.
12. Choi-Rhee, E. and J.E. Cronan, A nucleosidase required for *in vivo* function of the S-adenosyl-L-methionine radical enzyme, biotin synthase. *Chemistry & Biology*, 2005. **12**(5): p. 589-593.
13. Ziegert, T., Investigations of the Last Step in Biotin Biosynthesis, the Conversion of Dethiobiotin to Biotin, University of Southampton, Ph.D Thesis, 2003
14. Cornell, K.A. and M.K. Riscoe, Cloning and expression of Escherichia coli 5 '-methylthioadenosine/S-adenosylhomocysteine nucleosidase: Identification of the pfs gene product. *Biochimica Et Biophysica Acta-Gene Structure and Expression*, 1998. **1396**(1): p. 8-14.
15. Duerre, J.A., A Hydrolytic Nucleosidase Acting on S-Adenosylhomocysteine and on 5'-Methylthioadenosine. *Journal of Biological Chemistry* 1962. **237**(12): p. 3737-3741.
16. Bryant, P., Investigations into the Biosynthesis of Lipoic Acid, University of Southampton, Ph.D Thesis, 2008
17. Lin, Y.-W. and S.S. Que Hee, Simultaneous gas chromatographic-mass spectrometric quantitation of the alkylbenzene inert components, pesticide manufacturing by-products and active ingredient in two malathion formulations. *Journal of Chromatography A*, 1998. **814**(1-2): p. 181-186.
18. Bohin, A., F. Bouchart, C. Richet, O. Kol, Y. Leroy, P. Timmerman, G. Huet, J.-P. Bohin, and J.-P. Zanetta, GC/MS identification and quantification of constituents of bacterial lipids and glycoconjugates obtained after methanolysis as heptafluorobutyrate derivatives. *Analytical Biochemistry*, 2005. **340**(2): p. 231-244.
19. Yu, K., L. Di, E. Kerns, S.Q. Li, P. Alden, and R.S. Plumb, Ultra-performance liquid chromatography/tandem mass spectrometric quantification of structurally diverse drug mixtures using an ESI-APCI multimode ionization source. *Rapid Commun Mass Spectrom*, 2007. **21**(6): p. 893-902.
20. Kay, R.G., B. Gregory, P.B. Grace, and S. Pleasance, The application of ultra-performance liquid chromatography/tandem mass spectrometry to the detection and

quantitation of apolipoproteins in human serum. *Rapid Commun Mass Spectrom*, 2007. **21**(16): p. 2585-93.

21. Cicchillo, R.M., K.H. Lee, C. Baleanu-Gogonea, N.M. Nesbitt, C. Krebs, and S.J. Booker, *Escherichia coli* lipoyl synthase binds two distinct [4Fe-4S] clusters per polypeptide. *Biochemistry*, 2004. **43**(37): p. 11770-81.
22. Iwig, D.F. and S.J. Booker, Insight into the Polar Reactivity of the Onium Chalcogen Analogues of S-Adenosyl-L-methionine. *Biochemistry*, 2004. **43**(42): p. 13496-13509.
23. Markham, G.D., J. DeParasis, and J. Gatmaitan, The sequence of metK, the structural gene for S-adenosylmethionine synthetase in Escherichia coli. *Journal of Biological Chemistry*, 1984. **259**: p. 14505-14507.
24. Ugulava, N.B., C.J. Sacanell, and J.T. Jarrett, Spectroscopic changes during a single turnover of biotin synthase: destruction of a [2Fe-2S] cluster accompanies sulfur insertion. *Biochemistry*, 2001. **40**(28): p. 8352-8.
25. Zheng, L., R.H. White, V.L. Cash, and D.R. Dean, Mechanism for the desulfurization of L-cysteine catalyzed by the *nifS* gene product. *Biochemistry*, 1994. **33**(15): p. 4714-20.
26. Zheng, L.M., V.L. Cash, D.H. Flint, and D.R. Dean, Assembly of iron-sulfur clusters - Identification of an *iscSUA- hscBA-fdx* gene cluster from *Azotobacter vinelandii*. *Journal of Biological Chemistry*, 1998. **273**(21): p. 13264-13272.

Chapter 4. Formation of unexpected products from LipA using a nonanoyl substrate analogue

4.1 Introduction

The control of reactive intermediates by enzymes yielding a single product has been postulated to involve the closing off of reaction pathways leading to alternate products (1). Although proteins are highly specific, small variations in the substrate can often be accommodated within the active site. By using modified substrates, insight into to the enzyme mechanism can be gained by blocking the desired pathway resulting in inhibition of the protein and/or the detection of alternative reaction pathways.

Substrate analogues are commonly used as protein inhibitors as they closely resemble the natural substrate. An example of this is the drug penicillin, which inhibits the formation of the peptidoglycan cross-links in the bacterial cell wall by mimicking the D- alanine D-alanine substrate of the transpeptidase in the active site and reacting irreversibly with the enzyme (2).

The use of modified substrates has identified alternate reaction pathways for a number of biological reactions (fig. 4.1, **A-C**). Some of the reactions which have been investigated include the conversion of δ-(L-α-aminoadipoyl)-L-cysteinyl-D-valine (ACV) **67** to isopenicillin N **68** by isopenicillin N synthase (IPNS) (3-5), squalene **69** to hopene **70** by squalene- hopene cyclase (SHC), oxidosqualene **71** to lanosterol **72** by oxidosqualene-lanosterol cyclase (OCS) (6) and the conversion of proclavaminic acid **73** to clavaminic acid **74** by clavaminic synthase (CAS) (7). Mechanisms which are thought to proceed using a radical mediated pathway are often investigated using cyclopropyl radical clocks for example cytochrome p450 hydroxylation of hydrocarbons (8). In addition, an allylic SAM analogue **19** has been used to detect the formation of a resonance stabilised radical species **20** in reactions with KAM, a member of the radical SAM family (fig. 4.1, **D**).

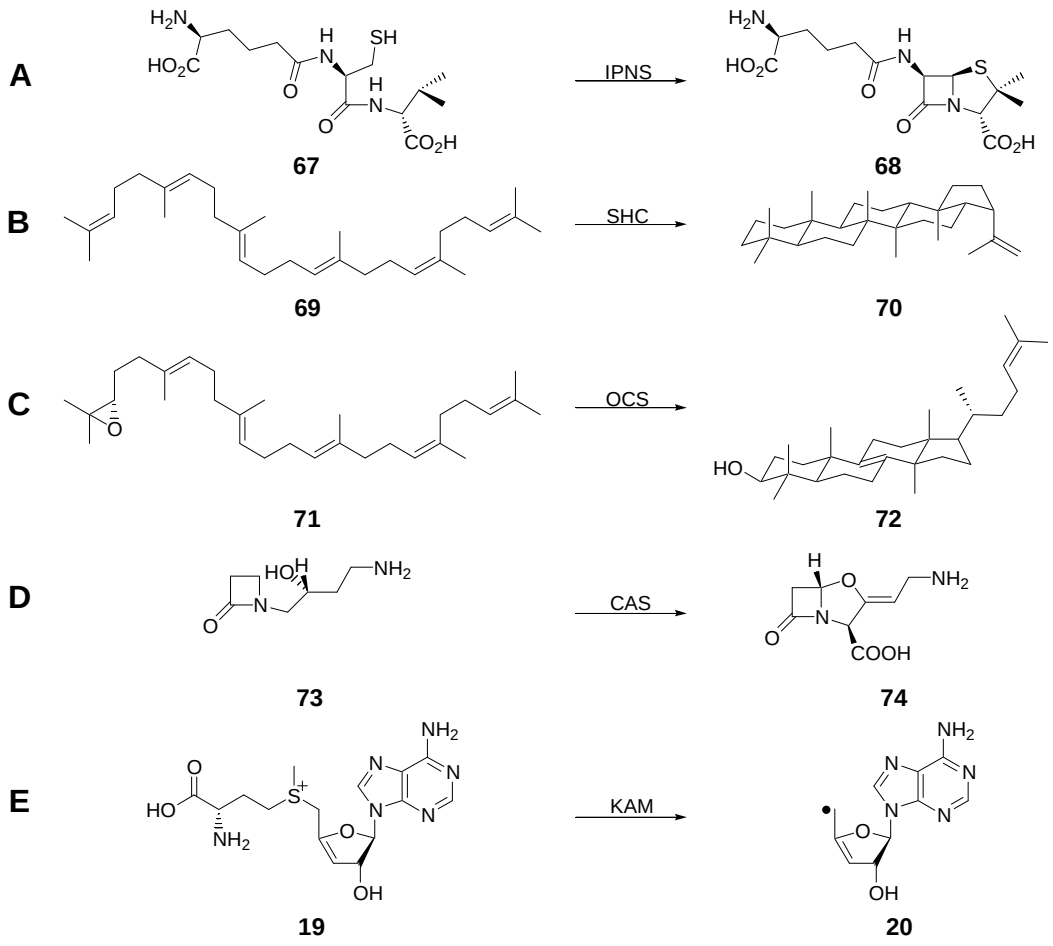

Figure 4.1 Examples of biological transformations which have been investigated using substrate analogues: (A) conversion of ACV **67** to isopenicillin N **68** by IPNS; (B) conversion of squalene **69** to hopene **70** by SHC; (C) conversion of oxidosqualene **71** to lanosterol **72** by oxidosqualene-lanosterol cyclase (OCS); (D) conversion of proclavaminic acid **73** to clavaminic acid **74** by clavaminic acid synthase CAS; (E) formation of an allylic radical by KAM using a SAM analogue.

Substrate analogues have been used to investigate the mechanism of lipoic acid biosynthesis by LipA. *In vivo* experiments with labelled octanoic acid (9-11), [8-$^2H_2$]-8-hydroxyoctanoic acid, [6(RS)-^{2}H]-6-hydroxyoctanoic acid, [8-$^2H_2$]-(±)-6,8-dihydroxyoctanoic, [8-$^2H_2$]-8-thiooctanoic acid and [6(RS)-^{2}H]-6-thiooctanoic acid have all provided insight into lipoyl formation (12). The most prominent was utilization of [8-$^2H_2$]-8-thiooctanoic acid for lipoic acid biosynthesis which led White to conclude that sulfur was inserted into the terminal C-H first due to the more efficient conversion of the 8-thiooctanoic acid (table. 4.1) to lipoic acid than the 6-thiooctanoic acid.

Octanoic acid	Percentage of isolated lipoic acid derived from substrate analogue
[6(RS)-^{2}H]-6-thiooctanoic acid	5.1
[8-$^{2}H_2$]-8-thiooctanoic acid	27.9

Table 4.1 Results from *in vivo* feeding studies using [8-$^{2}H_2$]-8-thiooctanoic acid and [6(RS)-^{2}H]-6-thiooctanoic acid. These results suggest that the intermediate was the C8 monothiolated octanoic acid.

However, the development of an *in vitro* assay utilizing a peptide mimic of the octanoyl protein substrate (13) has shown that sulfur is actually inserted at the C6 center first (14) contradicting the tentative conclusions drawn from *in vivo* feeding experiments. This conflicting observation could be attributed to the linear C8 thiol being more readily accommodated in the active site of the protein than the branched C6 thiol in the feeding experiments.

A sample of a smaller heptanoyl tripeptide substrate analogue was prepared in our laboratory by M. R. Challand. LCMS was used to provide a preliminary analysis of the turnover of this substrate after two time points. After 20 mins, the predominant mass ion (m/z = 533 $(M+H)^{+}$) observed was consistent with the starting peptide having undergone a single sulfur insertion. After prolonged incubation of LipA with this substrate the predominant product mass ion observed (m/z = 498 $(M+H)^{+}$) was consistent with a loss of two hydrogen atoms from the starting peptide. These results were interpreted as an initial sulfur insertion reaction followed by an elimination generating the desaturated product.

This chapter aims to investigate the ability of the protein to accommodate a longer nonanoyl substrate and to characterise any peptidyl products detected from this reaction and to rationalise their formation in terms of a radical mediated reaction mechanism for LipA.

4.2 LCMS analysis of a LipA reaction using a nonanoyl substrate

The nonanoyl peptide substrate **75** (fig. 4.2) was prepared using methods analogous to those previously described for the octanoyl peptide **34** (Section 2.2.2).

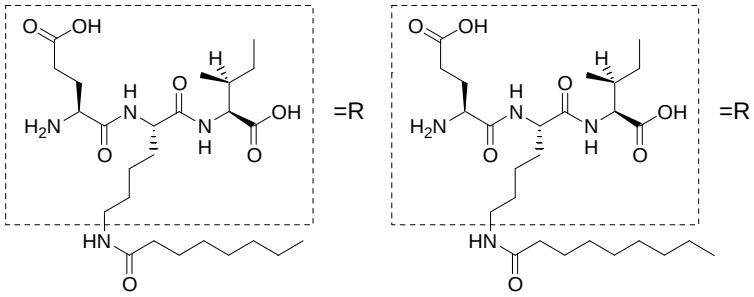

Figure 4.2 Structures of the octanoyl **34** and nonanoyl **75** peptides used to investigate LipA activity.

4.2.1 Turnover of the nonanoyl substrate 75 by LipA

Reactions of *S. solfataricus* LipA with the nonanoyl peptide **75** were carried out anaerobically and also contained SAM and sodium dithionite (table. 4.1). The reactions were incubated for 30 min at 37 °C then the protein was precipitated with acid and removed by centrifugation. Control reactions using the octanoyl peptide **34** resulted in detection of mass ions corresponding to the monothiolated peptide, dihydrolipoyl peptide and the lipoyl peptide (13, 14).

Constituent	Final concentration (μM)
Reconstituted LipA	300
SAM	1000
Sodium dithionite	1000
Substrate analogue peptide **73**	150

Table 4.2 Reaction of LipA with the nonanoyl peptide **75** were prepared using the concentrations of protein, SAM, sodium dithionite and substrate analogue outlined above. Reactions were prepared with a final volume of 500 μL.

100 μL of the supernatant was analysed by LCMS (fig. 4.3).

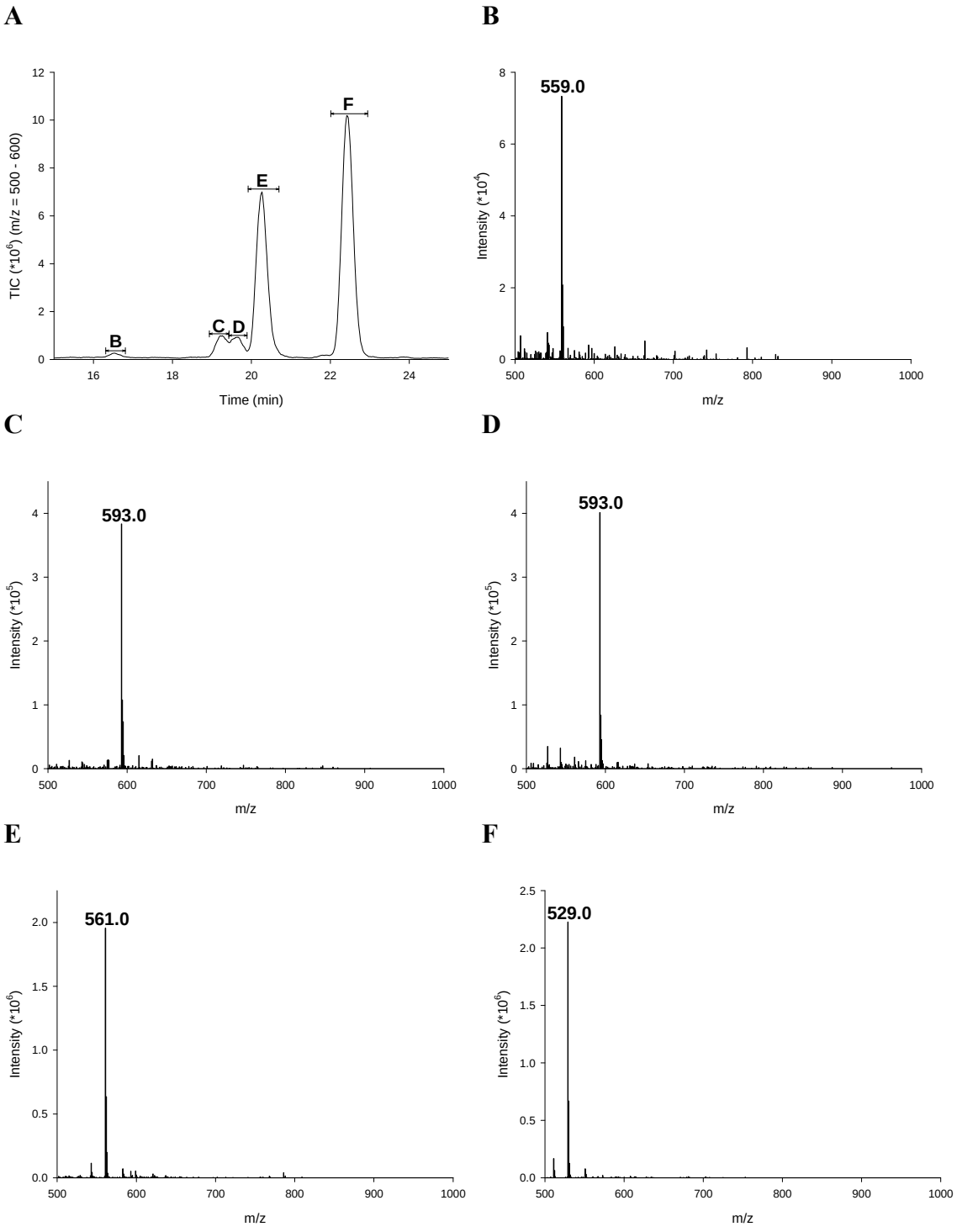

Figure 4.2 (**A**) TIC Chromatagram of an assay using nonanoyl peptide **75** after incubation at 37 °C for 30 min with SIM = 500-600; (**B**) Mass ion of unknown $(M+X+H)^+$, m/z = 559.0; (**C**) mass ion of unknown reduced double sulfur inserted product$(M+2S+H)^+$, m/z = 593.0; (**D**) mass ion of unknown reduced double sulfur inserted product $(M+2S+H)^+$, m/z = 593.0; (**E**) mass ion of unknown single sulfur inserted product $(M+S+H)^+$, m/z = 561.0; (**F**)- mass ion of starting peptide $(M+H)^+$, m/z = 529.0.

Using the nonanoyl peptide **75** resulted in the detection of five major peaks. One corresponded to the starting nonanoyl peptide **75** and the other four are believed to have been derived from the substrate that has undergone a range of modifications (table. 4.3).

Peak	Retention time (min)	Major ion	Change in mass from nonanoyl peptide 73 (Da)	Propossed transformation from substrate
B	16.3 - 16.7	559.0	30	+S -2H
C	19.0 - 19.3	593.0	64	+2S
D	19.4-19.7	593.0	64	+2S
E	19.9 - 20.5	561.0	32	+S
F	22.0 - 23.0	529.0	0	None
G (Not Detected in this sample)	N/a	527.0	- 2	-2H

Table 4.3 Major mass peaks detected from a LipA reaction with nonanoyl substrate **75**. The proposed transformations is the simplest chemical modifications to the substrate using only transformations known to be associated with this protein, hydrogen atom abstraction and sulfur insertion, which accounts for the mass change. Peak G- observed ion 527.0 was detected in other reactions using this substrate.

Peak E eluting at 19.9 - 20.5 min is consistant with the monothiol peak from reactions using the octanoyl peptide **34**. Peaks C and D eluting at 19.0 - 19.7 min are consistent with the substrate having undergone two sulfur insertions and is thought to resemble the dihydrolipoyl peptide **36** although alternate products with the addition of two sulfur atoms might account for this change. Peaks B and G correspond to transformations which were thought to be present only using the nonanoyl substrate. However, upon closer inspection, peaks corresponding to these mass changes were found in reactions using the octanoyl peptide **34** (fig. 4.3 and table. 4.4). These signals relative to the other products were much weaker that, may indicate a lower concentration.

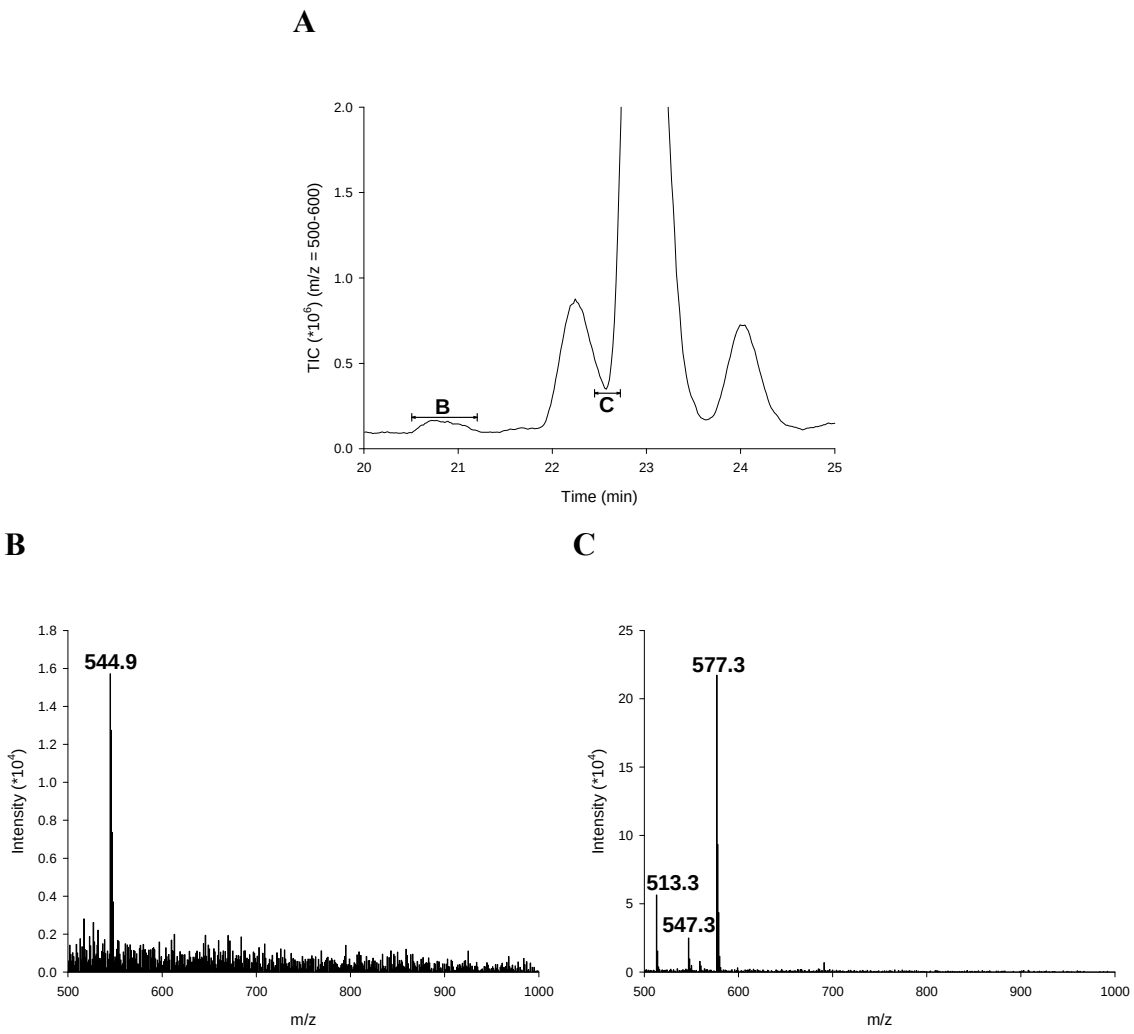

Figure 4.3 A- TIC of an assay using octanoyl peptide **34** after incubation at 37 °C for 2 h with SIM = 500-600: **B**- Mass ion of unknown, m/z = 544.9: **C**- mass ion of unknown, m/z = 513.3 and monothiol peptide **37**, m/z = 547.3 and DHL peptide **36**, m/z= 577.3.

Peak	Retention time (min)	Major ion	ΔM from nonanoyl peptide 73 (Da)	Propossed transformation from substrate
B	20.4 - 21.2	544.9	30	+S -2H
C	22.2 - 22.7	513.3	-2	-2H

Table 4.4 Unknown peaks detected from a LipA reaction with octanoyl substrate **34** analogous with unknown peaks listed in table 4.3.

Partial purification of a bound intermediate using size exclusion chromatography

Both sulfur atoms in lipoic acid are donated from the same protein molecule (15) and a protein bound intermediate has been characterised (Section 2.4.2). As analogous

transformations are observed for the octanoyl **34** and the nonanoyl **75** peptides when incubated with LipA in the presence of SAM and a reducing agent, it was anticipated that these reactions using the nonanoyl peptide would proceed similarly, resulting initially in a protein bound intermediate.

The existence of this protein bound intermediate was investigated by using PD-10 desalting column (Amersham Biosciences) to separate two fractions: a higher MW fraction containing the protein and any bound species and a lower MW fraction containing any unbound peptides and other small molecules within the assay. After separation of the reaction mixture, the protein was denatured and precipitated with acid and removed by centrifugation. The supernatant was analysed by LCMS and the results closely resembled observations with the octanoyl peptide (section 2.4.2). Only one peptidyl species was detected in the supernatant from the precipitated protein sample which, corresponded to the substrate having undergone single sulfur atom insertion (fig. 4.4).

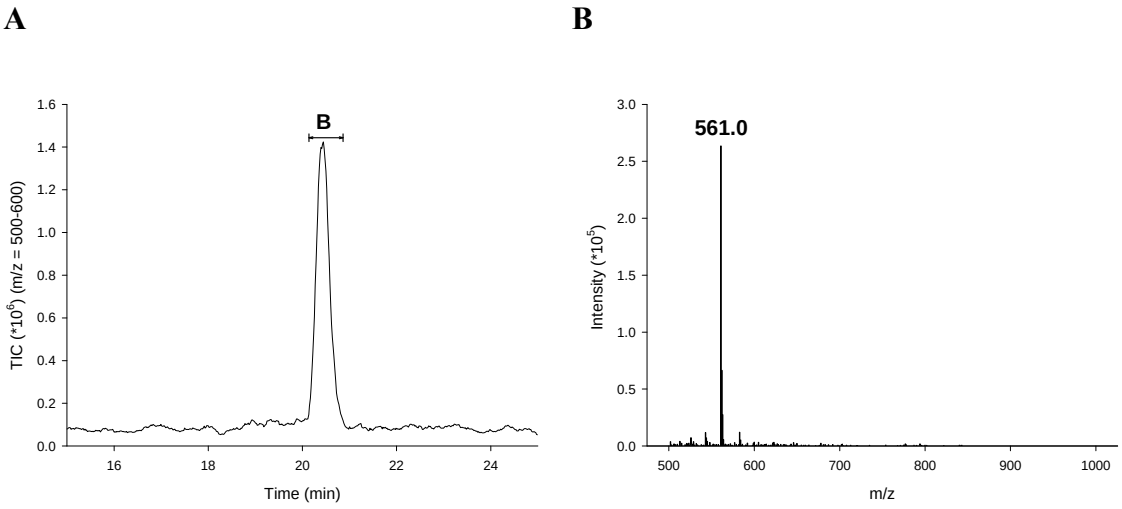

Figure 4.4 (**A**) TIC of the supernatant of protein from a reaction that after 30 min at 37 °C has been stopped by PD-10 filtration; (**B**) Mass spectrum of the supernatant corresponding to a single sulfur inserted product $(M+S+H)^+$, m/z = 561.0.

A protein sample partially purified by PD-10 filtration was incubated at 60 °C for 1 h prior to removal of the protein by acid precipitation and centrifugation. Analysis of this supernatant using LCMS revealed that, under these conditions the bound monothiolated species was stable. This observation is consistent with results using the octanoyl peptide

34. A second sample of protein isolated from PD-10 filtration was incubated in the presence of SAM and sodium dithionite at 60 °C for 1 h then the protein was removed by acid precipitation followed by centrifugation. Subsequent LCMS analysis of the supernatant revealed that the quantity of the monothiolated species was greatly reduced. However there were no obvious new signals in the chromatogram. Analysis using SIM (M ± 5) corresponding to the mass ions observed in a reaction without intermediate purification (table 4.3) facilitated the detection of all the expected signals apart from the M-2 species. The relative intensity of the intermediate species from reactions using the nonanoyl peptide compared to those utilizing the octanoyl peptide suggest that the octanoyl intermediate is present at a higher concentration (table 4.5). It follows that any products formed from the nonanoyl intermediate species would also result in weak signal detection and could explain the low levels observed and the absence of the expected M-2 species.

ΔM from substrate,	**Substrate relative intensity**	
[proposed transformation]	**Octanoyl peptide 34**	**Nonanoyl peptide 75**
+32, [+S][a]	343741629	24318111
+32, [+S][b]	21567477	1199362
+64, [+2S][b]	2254135	454813
+62, [+2S-2H][b]	34494015	Not detected
+30, [+S-2H][b]	Not detected	1628714
-2, [-2H][b]	Not detected	Not detected

Table 4.5 Comparison between the relative signal strengths of mass ions of products formed after isolation of the protein bound intermediate in reactions using the octanoyl **34** and nonanoyl **75** substrate analogues.

4.3 Isolation and characterisation of products formed in a LipA reaction using a nonanoyl substrate

Although the transformations proposed seem likely to account for the mass ions observed, further characterisation of the products formed in this reaction was required. This section discusses the use of chemical alkylation and proton NMR to determine the structure of the products.

4.3.1 Alkylation of products formed in a LipA reaction using the nonanoyl substrate

To allow isolation of sufficient material to allow NMR characterization, the reaction conditions were modified to promote turnover of the starting peptide. This was achieved by increasing the reaction time from 30 min to 2 h and by elevating the incubation temperature to that of optimal *S. solfataricus* LipA turnover, 60 °C (13). Alkylation of the reaction mixture using iodoacetamide was used to provide chemical insight into the nature of any sulfur atoms present in the structures and to improve the separation of the product peaks. This was achieved following treatment of the reaction products with an excess of TCEP to convert any disulfides present in the reaction mixture into free thiols. Increasing the duration of the HPLC gradient also increased separation of the product peaks. A 100 µL aliquot of this alkylated mixture was analysed by LCMS (fig. 4.5) using an elongated gradient.

The peaks thought to correspond to single (M+32) and double (M+64) sulfur inserted peptides were alkylated as anticipated by iodoacetamide. This suggests these signals probably correspond to thiol compounds arising from one or two sulfur insertion reactions respectively. However, although the change in the chemical constitution implied in the mass change (M+S) and (M+2S) probably corresponds to formation of a thiol for each sulphur insertion, the regiochemistry of the inserted sulfur atom(s) can not be deduced using this method. The peak corresponding to the M -2H was not alkylated by iodoacetamide and was thought likely to result from a desaturated species. The peak corresponding to the M +S -2H was not alkylated by iodoacetamide suggesting that a free thiol is not present within this structure.

4.3.2 ^{1}H Proton NMR characterisation of products formed in a nonanoyl reaction.

By combining and alkylating the supernatants from fifty-four 0.5 mL reactions using the nonanoyl substrate **75**, sufficient quantities of the new products were collected to obtain proton NMR spectra. After freeze drying, the alkylated products of the reaction were redisolved in the minimum quantity of water and purified using preparative HPLC (fig. 4.6). Fractions containing the purified products were identified using LCMS, pooled, lyophilized and characterised using proton NMR.

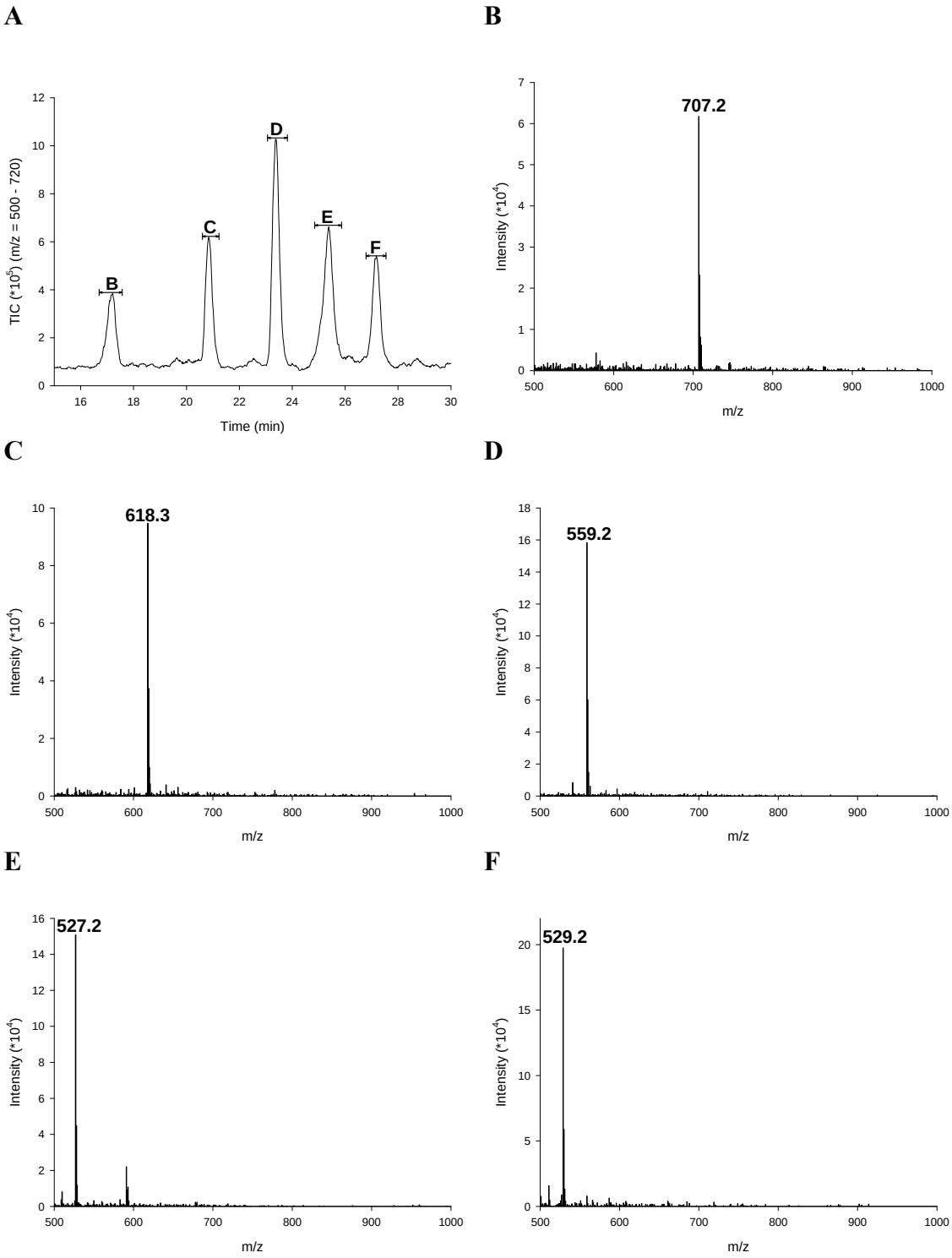

Figure 4.5 (**A**) TIC of an assay using nonanoyl peptide **75** after incubation at 60 °C for 2 h with SIM = 500-720. Treatment with TCEP and iodoacetamide followed removal of the protein by acid precipitation and centrifugation; (**B**) Mass ion of a double sulfur inserted product $(M+2S+H)^+$, m/z = 707.2; (**C**) mass ion of single sulfur inserted product $(M+S+H)^+$, m/z = 618.3; (**D**) mass ion of unknown$(M+X+H)^+$, m/z = 559.2; (**E**) mass ion of unknown, m/z = 527.2: **F-** mass ion of starting peptide **75** $(M+H)^+$, m/z = 529.2.

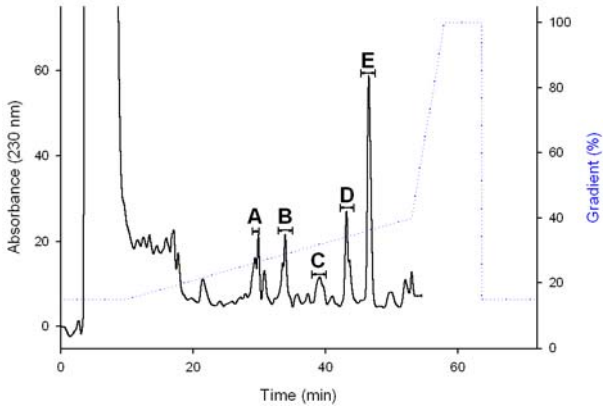

Figure 4.6 HPLC trace from the purification of products from reactions using the nonanoyl substarte. Peak (**A**) from MS m/z = 707.2 could not be identified; Peak (**B**) from MS m/z = 618.2 (alkylated mono thiol peptide +H)$^+$; Peak (**C**) unknown product from MS m/z = 559.2; Peak (**D**) unknown product from MS m/z = 527.2; Peak (**E**) from MS m/z = 529.2 starting peptide **75** **(M+H)**$^+$. Organic buffer gradient is shown (…….).

The product thought to result from the insertion of two sulfur atoms was not detected after preparative HPLC.

Proton NMR characterisation of unknown peak C: observed m/z = 618.3.

The characterisation of a monothiolated nonanoyl peptide formed in the reaction could provide insight into how the substrate is recognised in the active site. The exclusive primary insertion of sulfur into the C6 C-H bond of an octanoyl substrate suggests that the protein has to recognise the correct carbon centre by "counting" from one end of the substrate to form the specific sulfur inserted product. The protein could recognises the substrate by the peptidyl residues and/or the amide connecting the alkyl chain to the peptide, sulfur insertion would be expected to occur at the C6 centre **76** (fig. 4.7), independent of the carbon chain length. However, if the substrate was recognised from the terminal end, sulfur would be anticipated to insert 2 carbons away from this methyl group, C6 in the case of the octanoyl peptide **34** or at C7 in the case of the nonanoyl peptide **77** (fig. 4.7).

76 **77**

Figure 4.7 Possible structures of the monothiolated peptide formed in the reaction formed in a reaction of LipA with the nonanoyl peptide **75**. **76** is formed by sulfur insertion at C6. **77** is formed by sulfur insertion at C7.

A COSY spectrum (fig. 4.8) and TOCSY (Appendix A) facilitated the characterisation of the protons attached to the C9, C8, C7 and C6 centres of the monothiolated nonanoyl group confirming sulfur insertion occurs only at the C6 centre. It seems likely that the stereochemistry of the C6 sulfur inserted product follows the natural octanoyl products

The observed formation of a monothiolated peptide and its subsequent characterisation as the 6-monothiononanoyl species by NMR offers insight into the chemistry undertaken by LipA. Like the octanoyl substrate **34**, the nonanoyl peptide **75** appears to undergo a single sulfur insertion to form a protein bound intermediate, presumably bound to the protein through the second iron sulfur cluster during the reaction. The mechanism proposed for this transformation is analogous to the first two steps proposed for lipoyl formation (section. 2.5) (14) where a hydrogen atom is first abstracted from C6 to form a carbon centred radical **79** and a sulfur source is used to quench the radical formed to generate a protein bound intermediate **80**. The monothiolated peptide **76** is released upon denaturation of the protein by acidification of the reaction (fig. 4.9).

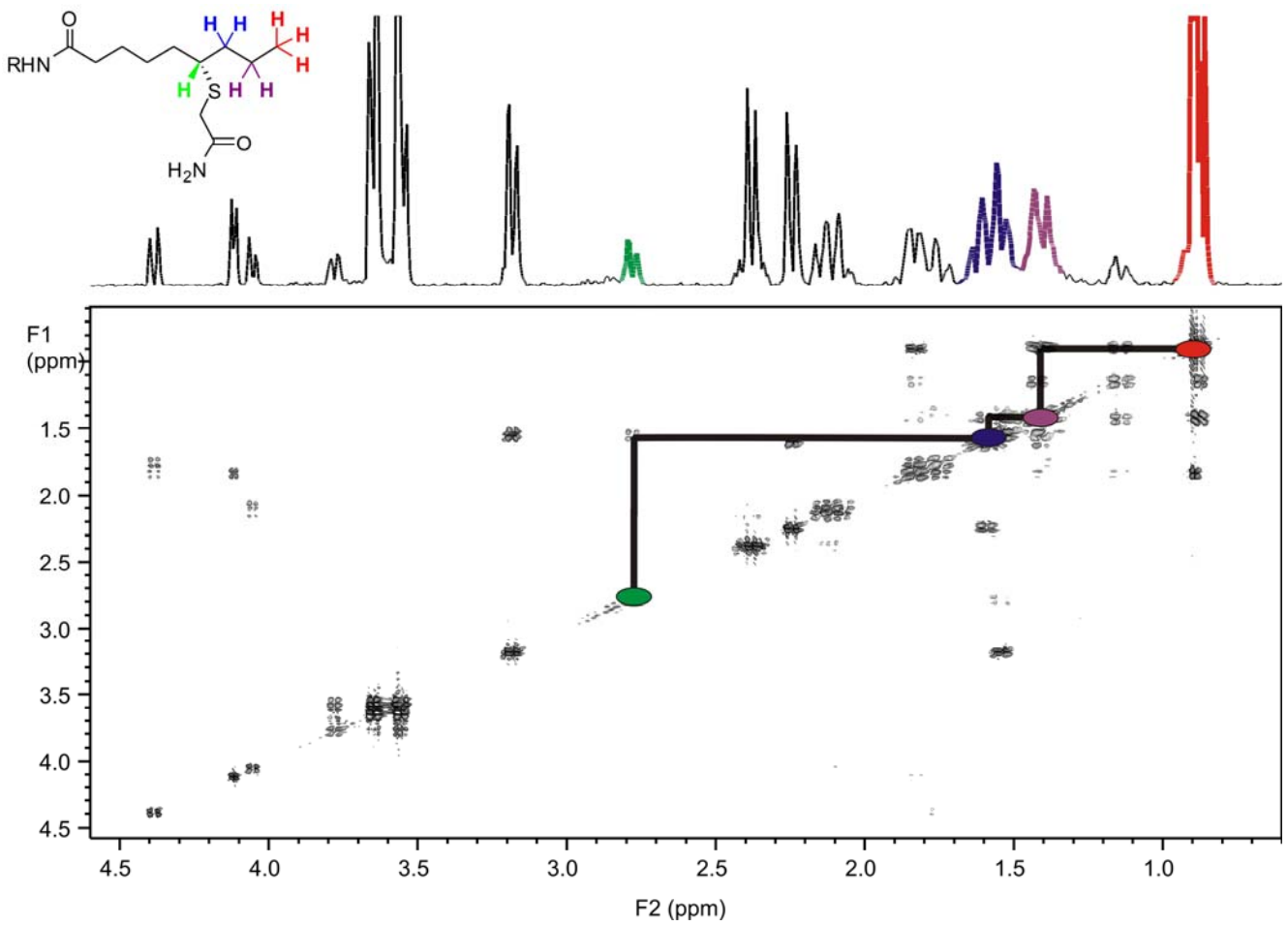

Figure 4.8 COSY NMR (600 MHz) of the isolated functionlised monothiolated peptide **76**. Correlations are marked between C9-C8-C7-C6. The signal at C6 is characteristic of an α-CH of a thiol group.

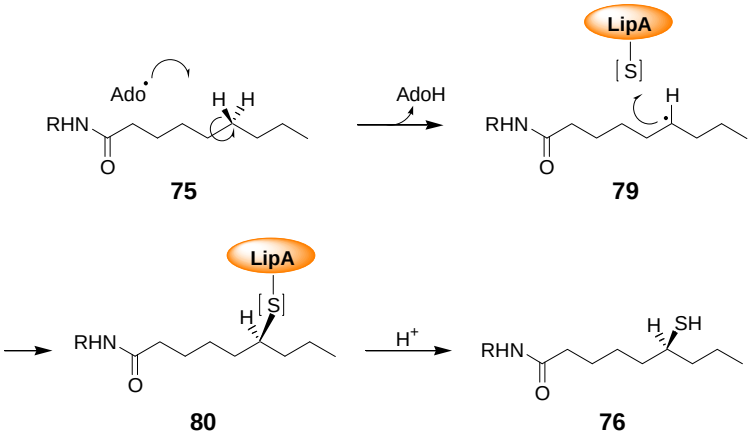

Figure 4.9 Proposed mechanism for the formation of the monothiolated peptide **76.** The sulfur source (depicted as [S]) is unknown but believed to be associated with the protein, presumably the second [4Fe-4S] cluster.

^{1}H Proton NMR characterisation of unknown peak D: observed m/z = 559.2.

The mass change from the substrate observed for this product (m/z = 559.2; M + 30.0 Da + H) is consistent with the insertion of sulfur and the loss of two hydrogen atoms. Iodoacetamide failed to alkylate the product eliminating the possibility of a free thiol containing species. Assuming this compound is derived from the proposed protein bound intermediate **80**; the formation of a thioketone would explain the mass ion observed, but was considered unlikely. One of a series of heterocyclic thioether containing peptides were thought more likely to account for the observed transformation and include the thiiranes **81** or **82**, the thietanes **83** or **84** or a tetrahydrothiophene **85** (fig. 4.10).

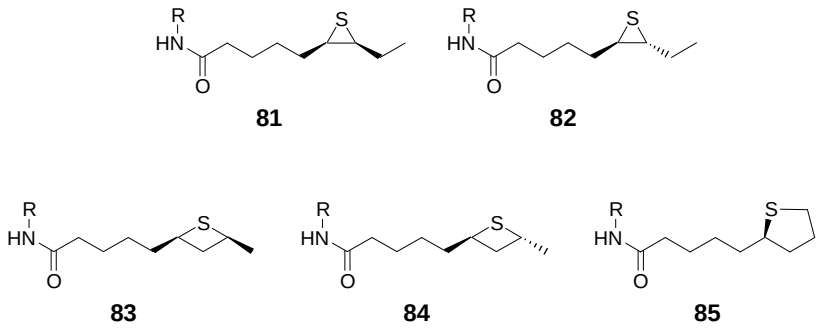

Figure 4.10 Possible structures of the peptide with the transformation (M +S -2H) formed in the reaction LipA with the nonanoyl peptide **75**.

The observations that an analogous reaction can occur for the octanoyl peptide **34** but was not observed in reactions using the 8,8,8- D_3 labeled **39** or an heptanoyl peptide analogue, suggesting that the formation of this product is dependant on a hydrogen atom abstraction from C8 or C9. This would discount the possibilities of thiiranes **81** or **82** leaving thietane or tetrahydothiophene formation as the likely candidates.

A COSY spectrum (fig. 4.11) with a Total Correlation Spectroscopy (TOCSY) (Appendix B) showed the presence of at least two diastereomerically related thietanes **83** and **84** in this sample but provided no evidence for tetrahydothiophene formation.

As thietanes are formed from the protein bound intermediate, it can be assumed that only the *R* stereocentre is present at C6. Correlations of the C9, C8, C7 and C6 centres of each of the two diastereomers can be observed and fit with the literature examples (16) of cis and trans thietanes (fig. 4.12). However, the absolute configuration at the two stereocentres (C6 and C8) could not be determined. By comparing the integrals of the C9 methyl protons with literature examples, it can be deduced that the two heterocyclic peptides are formed in a 1.8:1.2 ratio (*cis:trans*).

Thietanes do not commonly occur in natural products and little is known about their biosynthesis. However, simple thietanes are found in mixtures of small molecules produced from the scent glands of several small animals from the mustelidae family including Serbian weasels, Steppe polecats, ferrets, minks and zorillas (17-19). Often also contained within these mixtures are the 1,2-dithiolanes which share the same carbon backbone as the thietanes observed (table 4.6). This correlation of thietane and 1,2-dithiolane structures may suggest a common biosynthetic origin. Moreover, the observed ability of LipA to insert both of these functional groups into common unfunctionalized precursors (octanoyl amido and nonanoyl amido) suggests the speculative hypothesis that a radical SAM enzyme may be involved in the biosynthesis of the mustelidae scent molecule.

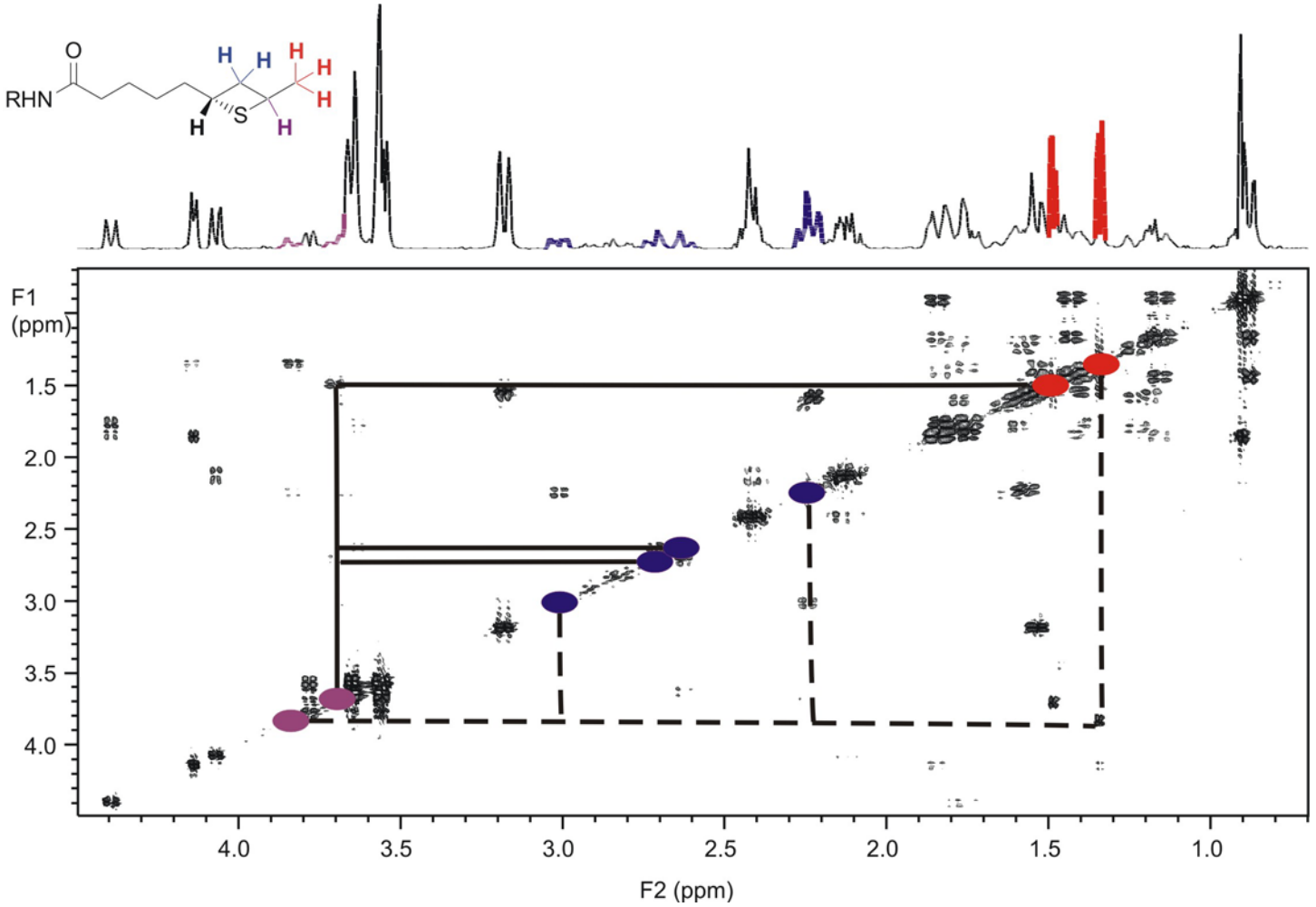

Figure 4.11 COSY NMR (600 MHz) of the isolated thietanes **83** and **84**. Correlations are marked between C9-C8-C7. The signal at C6 is in the region 2.2 - 2.5 ppm and was assigned using a TOCSY spectrum.

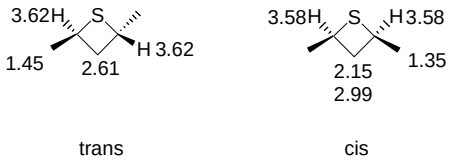

Figure 4.12 Literature examples of proton shifts observed in synthetic *cis* and *trans* thietanes.

Organism	Minks and Polecats	Ferrets			
Thietanes			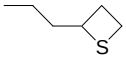	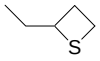	
1,2-dithiolanes				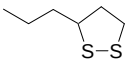	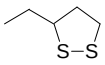

Table 4.6 Structures of thietanes and 1,2 dithiolanes sharing the same carbon backbone which have been detected in the anal gland excretions from small animals (18, 20).

The formation of thietanes in this reaction is postulated to result from a shunt pathway occurring after the formation of the C6 sulfur inserted protein bound intermediate **80**. As the formation of a protein bound intermediate is believed common for the formation of both products, stereochemistry is assumed identical to lipoic acid, the *R* enantiomer at C6 (10, 11). As in the case of lipoyl formation a subsequent hydrogen atom abstraction is required from C8, however the radical formed might first arrange itself into a conformation which favours cyclisation as opposed to a subsequent sulfur insertion. The nonanoyl substrate promotes thietane formation due to the formation of a more stable secondary radical and the substrate may result in a puckering of the alkyl chain forming a confirmation which favours quenching. The two distereomers might result from the radical species rotating along the C7-8 bond, the *cis*- thietane **83** from radical **86** and the *trans*-thietane from radical **87** (fig. 4.13). However, the predominance of the thermodynamically unfavoured cis thietane implies that the intermediate is confirmationally restricted in the active site.

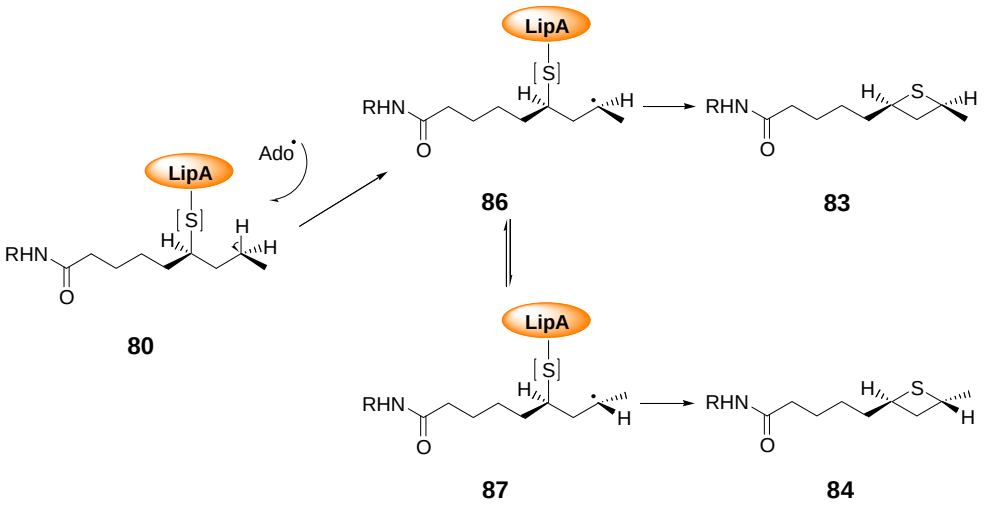

Figure 4.13 Proposed mechanism for the formation of the thietanes **83** and **84** from the bound intermediate **80**. The sulfur source (depicted as [S]) is unknown but is associated with the protein, presumably the second [4Fe-4S] cluster.

^{1}H Proton NMR characterisation of peak E: observed m/z = 527.2

The mass change from the substrate observed for this product (m/z = 527.2; M - 2.0 Da + H) is consistent with the loss of two hydrogen atoms from the substrate. Assuming this compound was derived from the common protein bound intermediate **80,** the following peptides could account for this observed mass change, the *cis*-alkenes **88** or **89**, the *trans*-alkenes **89** or **90** or the cyclopropyl peptides **92** or **93** (fig. 4.14) or by the formation of larger rings.

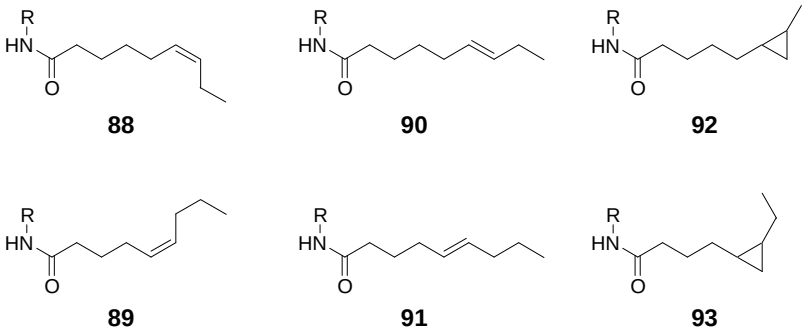

Figure 4.14 Possible structures of the peptide with the transformation M -2H formed in the reaction LipA with the nonanoyl peptide **75**.

An analogous reaction was observed for the octanoyl peptide **34** and formation of this unknown species was further enhanced in reactions where the 8,8,8- D_3 labeled peptide **39** was used as the substrate suggesting protons attached to the C8 position are not involved. The apparent loss of two hydrogen atoms from the starting substrate was further promoted in reactions using a heptanoyl substrate analogue. Analysis of this reaction at various time points showed an initial formation of a M + 32, or M + S species followed by complete conversion over time of that species to a M-2 species. These conditions enhancing the loss of two hydrogen atoms is consistent with the hypothesis that hydrogen atom abstraction from the C8 center is not required and eliminates the possible formation of the cyclopropyl product **92** but not any of the other reactions.

A COSY spectrum (fig. 4.15) coupled with a TOCSY (Appendix C) has shown the selective formation of the *trans*- alkene **90**.

In the COSY and TOCSY spectra correlations are observed between the terminal C9 methyl protons and the protons attached at the C8, C7 and C6 centres. The signals belonging to the C7 and C6 protons are found in the alkene region of the NMR (4 – 6 ppm) and have a coupling constant (15.6 Hz) which is more consistant with a *trans* geometry than the *cis* geometry and the product has therefore been characterised as the *trans*- alkene **90.**

Desaturation reactions with unreactive alkyl substrates have been reported for several families of oxidative enzymes including p450 systems (21, 22). These oxidative reactions are thought to proceed through carbon centered radical intermediates, similar to those which are formed in reactions which utilize radical SAM proteins. The formation of an alkene during lipoyl formation has demonstrated that a radical SAM protein is capable of acting as a desaturase type enzyme. An example of a known radical SAM protein with the role of a dehydrogenase is the protein BtrN, a product of the butirosin biosynthetic gene cluster (23). This protein is responsible for the oxidation of 2-deoxy-*scyllo*-inosamine to 3-amino-2,3-dideoxy-*scyllo*-inososе (fig. 4.16)

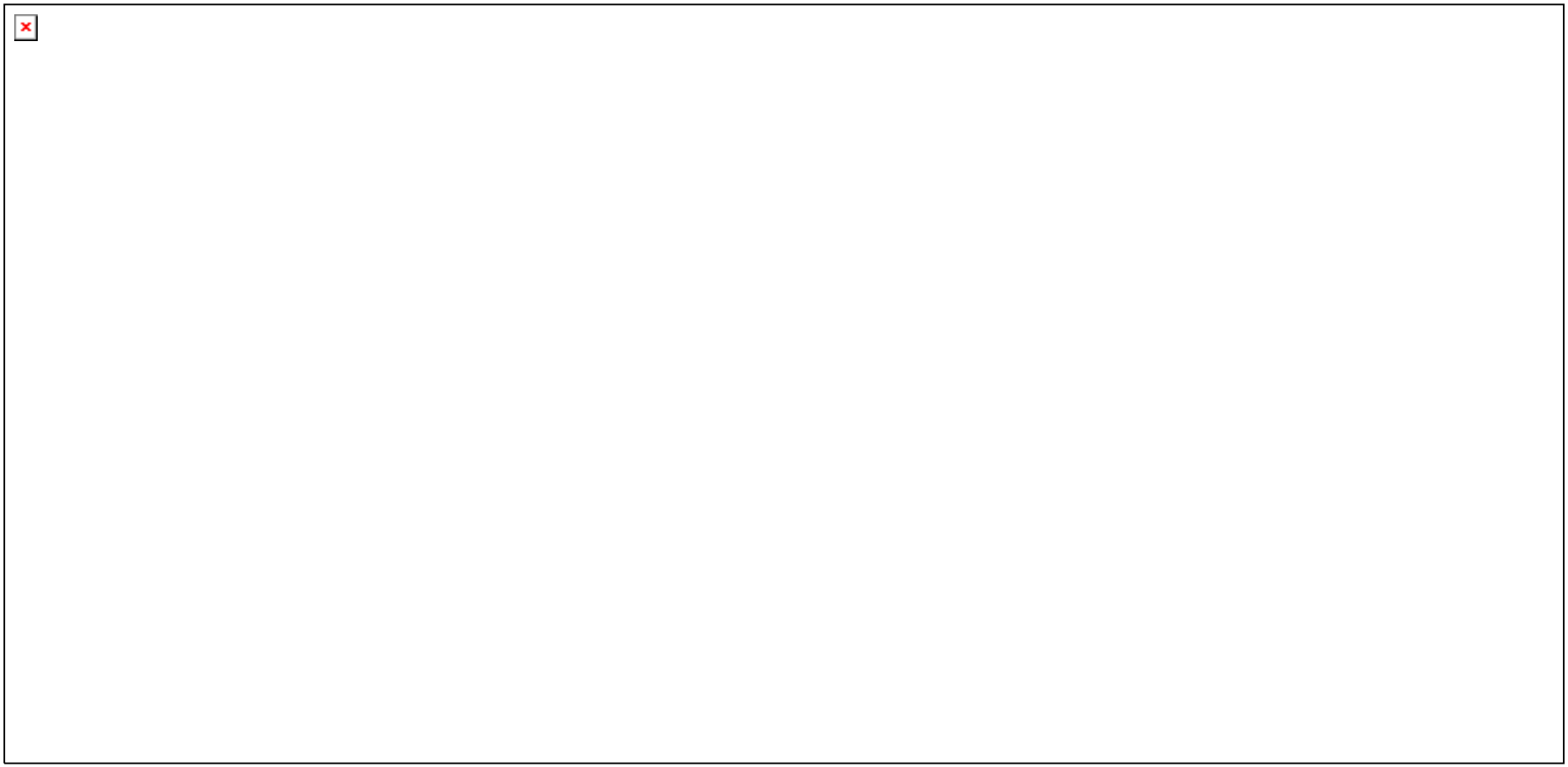

Figure 4.15 COSY NMR (600 MHz) of the isolated *trans*- alkene **90**. Correlations are marked between **C9-C8-C7-C6**. C7 and C6 can not be distinguished but two double triplets are clearly discernable, with a $J_{6\text{-}7}$ = 15.6 Hz, typical of a *trans*- alkene.

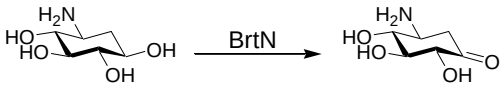

Figure 4.16 Conversion of 2-deoxy-*scyllo*-inosamine to 3-amino-2,3-dideoxy-*scyllo*-inosose.

The alkene product is assumed to originate from an alternate shunt pathway after formation of the C6 sulfur insertion intermediate **80.** Two likely mechanisms for alkene formation from this intermediate could exist: either a classical E2 elimination, which might be promoted by the iron atoms in one of the clusters acting as Lewis acids. This mode of action is observed for aconitase, in which the cluster acts a Lewis acid to catalyse the dehydration of citrate **94** forming *cis*- aconitate **95** (fig. 4.17).

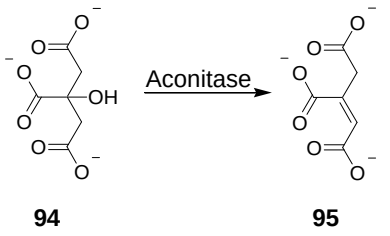

Figure 4.17 Conversion of citrate **94** to aconitate **95** by aconitase.

The second mechanism considered is radical mediated elimination of the sulfur source either in a concerted or stepwise manner. This would require a second Ado• to abstract a hydrogen atom from the adjacent C7 centre resulting in elimination of the sulfur source and could be further investigated in reactions using the heptanoyl peptide by monitoring the ratio of alkene to AdoH formed.

Isolation of the bound intermediate **80** demonstrated that fresh SAM and sodium dithionite was required for the occurrence of any further reactions and the stability of this intermediate complex suggests Ado• formation is required, consistant with the radical mediated pathway (fig. 4.18) as opposed to E2 elimination.

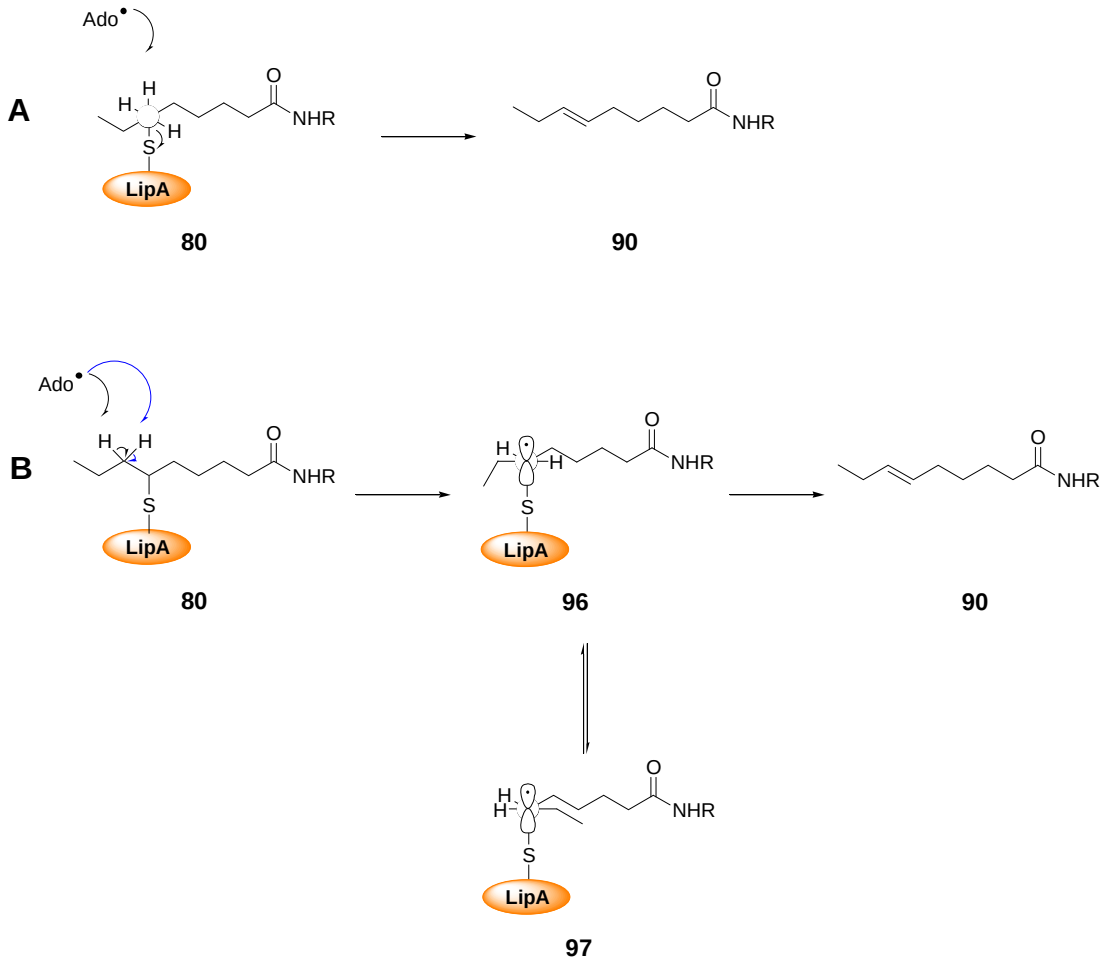

Figure 4.18 Proposed mechanism for the radical mediated formation of the *trans*- alkene **90** from the bound intermediate **8;** (**A**) concerted route using antiperiplaner geometry; (**B**) stepwise route showing confirmation of the two intermediate geometries which could result in the formation of either the *cis*-alkene **88** or the *trans*-alkene **90**.

If the pathway proceeded in a concerted manner, hydrogen atom abstraction would need to be stereoselective as only the *trans*-alkene is observed. However, if the process proceeds in a stepwise manner, abstraction of either hydrogen could result in *trans*-alkene formation as the radical intermediate could rotate into the desired conformation. The abstracted hydrogen, at the time of abstraction, would not need to be antiperiplaner to the leaving group. Rotation about the C6-C7 bond would result in the orbital overlap required for elimination. Two conformers of the radical intermediate could exist prior to elimination, either the conformer leading to *trans*- geometry **96** or to *cis*- geometry **97**. Conformer **97** has the ethyl group positioned in close proximity to the remaining alkyl chain. This sterically hindered conformation is not likely to be favored and would result in the

equilibrium favoring the *trans*- geometry conformer. To investigate whether the process proceeds via a stepwise or concerted pathway, stereospecifically labeled substrates would have to be prepared and their product distribution analyzed.

The observation that alkene formation is increased when hydrogen abstraction from C8 is hindered or removed suggests that the observed alkene formation is a product of a "shunt pathway," releasing compounds that have undergone a fast initial sulfur insertion reaction but undergo slow second sulfur insertion step.

^{1}H Proton NMR characterisation of peak B: observed m/z = 707.2.

Insufficient material was isolated to allow ^{1}H NMR characterization of this species. Ado• has been shown capable of abstracting hydrogen atoms from the C7 centre resulting in alkene formation and also from the C8 centre causing thietane formation. The proposed transformation which accounts for this observed mass ion is M + 2S + H^{+} and can be accounted for by formation of either 8-methyl dihydrolipoyl peptide **96** or 6,7-dithiooctanoyl peptide **97** (fig. 4.19).

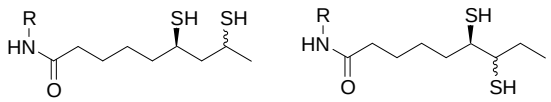

96 **97**

Figure 4.19 Possible structures of the peptide with the transformation M +2S formed in the reaction LipA with the nonanoyl peptide **75**.

Abstraction from C7 results in elimination of the first sulfur source and it is unlikely that the source of the second sulfur atom is position in a position favorable for insertion at either C7 or C8 making 6,7- dithiooctanoyl peptide **97** an unlikely product. It is proposed that the product formed is the 8-methyl dihydrolipoyl peptide **96** which more closely resembles the expected double sulfur inserted product from reactions using the octanoyl substrate **34**. The observation of two peaks in the unfunctionlised reaction mixture can be a result of partial separation of the two diastereomers of the 8-methyl dihydrolipoyl peptide **96** formed in a similar manner to that of the thietanes in a mechanism analgous to lipoyl formation (Section 2.5).

4.4 Conclusion

The protein LipA can form a range of products that are detected in reactions using the octanoyl substrate **34** but could not be isolated without using the nonanoyl substrate **75**. The products formed (fig. 4.20) using this nonanoyl substrate have been characterised by MS and NMR and the intermediate characterised using both systems.

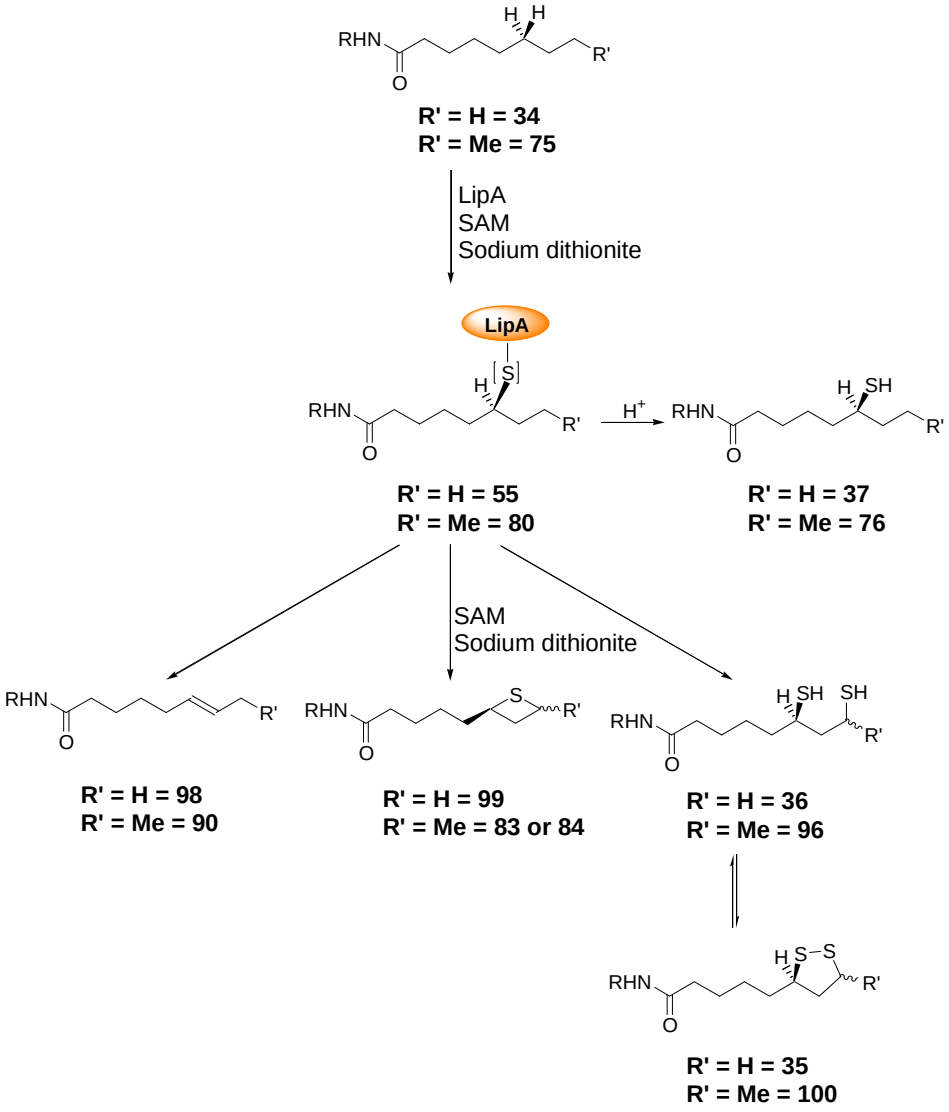

Figure 4.20 LipA can form a range of different products from a common intermediate **55** or **80**. Elimination chemistry results in the formation of an alkene species **98** or **90**, cyclisation results in thietane formation **99**, **83** or **84** and subsequent sulfur insertion results in the expected double sulfur insertion products **35/36** and **96/100**.

All the reactions appear to be formed after the formation of a common intermediate **55** or **80** which has been shown to remain bound to the protein. This intermediate can then

undergo further radical mediated elimination to form alkenes, cyclisation to form thietanes or further sulfur insertion results in the expected double sulfur inserted products.

4.5 References

1. Rétey, J., Enzymic Reaction Selectivity by Negative Catalysis or How Do Enzymes Deal with Highly Reactive Intermediates? *Angewandte Chemie International Edition*, 1990. **29**(4): p. 355-361.
2. Yocum, R.R., D.J. Waxman, J.R. Rasmussen, and J.L. Strominger, Mechanism of Penicillin Action: Penicillin and Substrate Bind Covalently to the Same Active Site Serine in Two Bacterial D-alanine Carboxypeptidases. *Proceedings of the National Academy of Sciences*, 1979. **76**(6): p. 2730-2734.
3. Baldwin, J.E. and M. Bradley, Isopenicillin N synthase: mechanistic studies. *Chemical Reviews* 1990. **90**(7): p. 1079-1088.
4. Howard-Jones, A.R., J.M. Elkins, I.J. Clifton, P.L. Roach, R.M. Adlington, J.E. Baldwin, and P.J. Rutledge, Interactions of isopenicillin N synthase with cyclopropyl-containing substrate analogues reveal new mechanistic insight. *Biochemistry*, 2007. **46**(16): p. 4755-62.
5. Long, A.J., I.J. Clifton, P.L. Roach, J.E. Baldwin, P.J. Rutledge, and C.J. Schofield, Structural studies on the reaction of isopenicillin N synthase with the truncated substrate analogues delta-(L-alpha-aminoadipoyl)-L-cysteinyl-glycine and delta-(L-alpha-aminoadipoyl)-L-cysteinyl-D-alanine. *Biochemistry*, 2005. **44**(17): p. 6619-28.
6. Hoshino, T. and T. Sato, Squalene-hopene cyclase: catalytic mechanism and substrate recognition. *Chemical communications (Cambridge, England)*, 2002(4): p. 291-301.
7. Baldwin, J.E., Lloyd, M.D,. Wha-Son, B., Schofield, C.J., Elson, S.W., Baggaley, K.H., Nicholson, N.H., A substrate analogue study on clavaminic acid synthase: Possible clues to the biosynthetic origin of proclavaminic acid. *Journal of the chemical society., Chemical communications*, 1993, p. 500-502.
8. Atkinson, J.K., Ingold, K.U., Cytochrom P450 hydroxylation of hydrocarbons: Variation in the rate of oxygen rebound using cyclopropyl radical clocks including two new ultrafast probes. *Biochemistry*. 1993, **32**, p. 9209-9214
9. Parry, R.J., Biosynthesis of lipoic acid. 1. Incorporation of specifically tritiated octanoic acid into lipoic acid. *Journal of the American Chemical Society*, 1977. **99**(19): p. 6464-6.

10. Parry, R.J. and D.A. Trainor, Biosynthesis of lipoic acid. 2. Stereochemistry of sulfur introduction at C-6 of octanoic acid. *Journal of the American Chemical Society*, 1978. **100**(16): p. 5243-4.
11. White, R.H., Stable isotope studies on the biosynthesis of lipoic acid in *Escherichia coli*. *Biochemistry*, 1980. **19**(1): p. 15-19.
12. White, R.H., Biosynthesis of lipoic acid - extent of incorporation of deuterated hydroxyoctanoic and thiooctanoic acids into lipoic acid. *Journal of the American Chemical Society*, 1980. **102**(21): p. 6605-6607.
13. Bryant, P., M. Kriek, R.J. Wood, and P.L. Roach, The activity of a thermostable lipoyl synthase from *Sulfolobus solfataricus* with a synthetic octanoyl substrate. *Analytical Biochemistry* 2006. **351**(1): p. 44-9.
14. Douglas, P., M. Kriek, P. Bryant, and P.L. Roach, Lipoyl synthase inserts sulfur atoms into an octanoyl substrate in a stepwise manner. *Angewandte Chemie International Edition* 2006. **45**(31): p. 5197-9.
15. Cicchillo, R.M. and S.J. Booker, Mechanistic investigations of lipoic acid biosynthesis in *Escherichia coli*: both sulfur atoms in lipoic acid are contributed by the same lipoyl synthase polypeptide. *Journal of the American Chemical Society*, 2005. **127**(9): p. 2860-1.
16. Trost, B.M., W.L. Schinski, F. Chen, and I.B. Mantz, Stereochemistry of desulfurization of thietane derivatives. *Journal of the American Chemical Society*, 1971. **93**(3): p. 676-684.
17. Wood, W.F., M.N. Terwilliger, and J.P. Copeland, Volatile compounds from anal glands of the wolverine, Gulo gulo. *Journal of Chemical Ecology*, 2005. **31**(9): p. 2111-7.
18. Zhang, J.X., H.A. Soini, K.E. Bruce, D. Wiesler, S.K. Woodley, M.J. Baum, and M.V. Novotny, Putative chemosignals of the ferret (Mustela furo) associated with individual and gender recognition. *Chemical Senses*, 2005. **30**(9): p. 727-37.
19. Zhang, J.X., L. Sun, Z.B. Zhang, Z.W. Wang, Y. Chen, and R. Wang, Volatile compounds in anal gland of Siberian weasels (Mustela sibirica) and steppe polecats (M. eversmanni). *Journal of Chemical Ecology*, 2002. **28**(6): p. 1287-97.
20. Schildknecht, H., Wilz, I., Enzmann, F., Grund, N., Ziegler, M., Mustelan, the Malodorous Substance from the Anal Gland of the Mink *(Mustela vison)* and the Polecat *(Mustela putorius)*, *Angewandte Chemie International Edition*, 1976, **15**(4): p 242-243.

21. Ortiz de Montellano, P.R., Cytochrome P-450 catalysis: radical intermediates and dehydrogenation reactions. *Trends in Pharmacological Sciences*, 1989. **10**(9): p. 354-359.
22. Rettie, A.E., A.W. Rettenmeier, W.N. Howald, and T.A. Baillie, Cytochrome P-450--catalyzed formation of delta 4-VPA, a toxic metabolite of valproic acid. *Science*, 1987. **235**(4791): p. 890-893.
23. Yokoyama, K., Numakura, M., Kudo, F., Ohmori, D., andEguchi, T, Characterization and mechanistic studies of a radical SAM dehydrogenase in the biosynthesis of butirosin.

Chapter 5. Conclusions

This thesis has described work carried out to investigate the transformations catalysed by the protein LipA. Early experiments aimed to validate a new *in vitro* assay (1, 2) by repeating feeding studies with single sulfur inserted peptides. However, LCMS analysis of this assay using an octanoyl substrate resulted in the detection of a monothiolated adduct formed within the reaction mixture. The potential of an intermediate that might be isolated shifted the aims to solving the order of sulfur insertion therefore; this initial validation was not progressed.

The initial plan for characterising this intermediate was to react a specifically labelled peptide, in this case the 8,8,8-trideutero peptide **39** and use the expected mass difference between the two possible monothiolated peptides to determine the order of sulfur insertion. Early experiments utilising this labelled peptide generated results strongly implying sulfur insertion occurred primarily at C6, contradicting the accepted model (3-6). This observed contradiction required further investigation. The monothiolated product appeared to form as the major product when the reaction temperature was reduced suggesting that this species could be isolated. The NMR from the initial isolated adduct was conclusive however, there was some contamination from the dihydrolipoyl peptide **36**. It was desired that this contamination was removed and so the alkylation method was developed. This resulted in the collection of a cleaner ^{1}H NMR spectrum and provided an opportunity for an improved kinetic analysis (2). The 6,6-dideutero peptide **40** also showed C6 sulfur insertion.

It was shown that AdoH alone inhibits LipA and that a strong synergistic inhibition occurred when methionine was also present. Although the addition of Pfs to the reaction mixture had the desired effect of removing this inhibition and increasing the quantity of lipoyl peptide formed by the protein, this was not sufficient to achieve catalytic activity *in vitro*. The source of sulfur in biotin biosynthesis by BioB is thought to be the second [Fe-S] cluster and cluster degradation has been observed during a single turnover of the protein (7). Similarly if cluster degradation is involved in the mechanism of LipA, catalytic activity could only be achieved if the cluster was regenerated *in situ*.

By challenging LipA with a larger nonanoyl substrate it was found that a range of previously unobserved products can be formed in the reaction. These products were isolated, characterised and found to be the C6 monothiolated, the *trans*-alkene, the *cis*- and *trans*-thietanes, and what is thought to be two diastereomers of the 8-methyl dihydrolipoyl peptides. Upon closer inspection of data collected from reactions using the standard octanoyl peptide, mass ions corresponding to analogous transformations were also present. These products were all shown to derive from a stable C6 monothiolated peptide which remains tightly bound to the protein as a common intermediate. It can be envisaged that apart from the C6 monothiolated peptide (a product of acid denaturing of the protein), all these species can be formed from this intermediate using hydrogen atom abstraction and/or sulfur insertion, two reactions that are carried out by LipA in order to achieve lipoyl formation. Mechanisms accounting for the formation of these products were proposed utilizing these steps.

In conclusion, the experiments described within this thesis have furthered our understanding of how LipA, a member of the rapidly emerging “radical SAM” superfamily of proteins, catalyses the insertion of two sulfur atoms into the unactivated C6 and C8 C-H bonds of specific octanoyl moieties.

5.1 References

1. Bryant, P., M. Kriek, R.J. Wood, and P.L. Roach, *The activity of a thermostable lipoyl synthase from Sulfolobus solfataricus with a synthetic octanoyl substrate.* Analytical Biochemistry 2006. **351**(1): p. 44-9.
2. Bryant, P., *Investigations into the Biosynthesis of Lipoic Acid*, in *School of Chemistry*. 2008, University of Southampton: Southampton.
3. Parry, R.J., *Biosynthesis of lipoic acid. 1. Incorporation of specifically tritiated octanoic acid into lipoic acid.* Journal of the American Chemical Society, 1977. **99**(19): p. 6464-6.
4. Cicchillo, R.M., K.H. Lee, C. Baleanu-Gogonea, N.M. Nesbitt, C. Krebs, and S.J. Booker, *Escherichia coli lipoyl synthase binds two distinct [4Fe-4S] clusters per polypeptide.* Biochemistry, 2004. **43**(37): p. 11770-81.
5. Cicchillo, R.M. and S.J. Booker, *Mechanistic investigations of lipoic acid biosynthesis in Escherichia coli: both sulfur atoms in lipoic acid are contributed by the same lipoyl synthase polypeptide.* Journal of the American Chemical Society, 2005. **127**(9): p. 2860-1.
6. White, R.H., *Biosynthesis of lipoic acid - extent of incorporation of deuterated hydroxyoctanoic and thiooctanoic acids into lipoic acid.* Journal of the American Chemical Society, 1980. **102**(21): p. 6605-6607.
7. Ugulava, N.B., C.J. Sacanell, and J.T. Jarrett, *Spectroscopic changes during a single turnover of biotin synthase: destruction of a [2Fe-2S] cluster accompanies sulfur insertion.* Biochemistry, 2001. **40**(28): p. 8352-8.

Chapter 6. Experimental

6.1 Materials

Yeast extract and tryptone were purchased from Oxoid (Basingstoke, UK). *E.* coli strain TOP-10 competent cells were purchased from Invitrogen and strains BL-21 (DE3) and LMG-194 competent cells were prepared in house using the rubidium chloride method (NEB). Fluorenylmethoxycarbonyl (Fmoc) amino acids, coupling reagents diisopropylcarbodiimide (DIC), dicyclohexylcarbodiimide (DCC), benzotriazolyloxy-tris[pyrrolidino]-phosphonium hexafluorophosphate (PyBOP), hydroxybenzotriazole (HOBt) and Wang resin were purchased from Novabiochem (Nottingham, UK). (*DL*)-Lipoic acid, TFA, iodoacetamide, TCEP, AdoH, *L*-methionine, 1-morpholinocyclopentene, propionyl chloride, *p*-toluenesulfonyl chloride, sodium borodeuteride, lithium aluminum deuteride, and N,N,N',N'-tetramethylethylenediamine (TEMED) were purchased from Sigma-Aldrich (Poole, UK). *S*-adenosylmethionine tosylate salt was a generous gift from H. Schroeder (BASF, Ludwigshafen, Germany). *N*,*N*-dimethylformamide (DMF) and *N*-methylpyrrolidone (NMP) were purchased from Rathburn Chemicals (Walkerburn, UK). HEPES and dithiothreitol (DTT) were purchased from Melford Laboratories (Ipswich, UK). Deuterium oxide, D_4- methanol and deuterated chloroform were purchased from Goss Scientific Instruments (Great Baddow, Essex). 8,8,8- D_3- octanoic acid was purchased from QMX Laboratories Limited (Thaxted, Essex). Octanoic acid, HPLC-grade acetonitrile, trishydroxymethylaminomethane, THF, formic acid, hydrochloric acid, sulphuric acid, DCM, MeOH, acetone, sodium hydroxide, methanol, ammonium bicarbonate and all other reagents were purchased from Fisher Scientific (Loughborough, UK). Normal and reverse phase TLC plates were aluminium backed and purchased from Merck (Nottingham, UK).

NAP-10 and PD-10 columns were purchased from Amersham Biosciences (Buckinghamshire, UK). Supelclean™ LC-18 solid phase extraction columns from Supelco were purchased through Sigma-Aldrich (Poole, UK).

HPLC columns were purchased from Phenomenex (Cheshire, UK).

6.2 Instrumentation

HPLC

Preparative reversed-phase HPLC was carried out on a Gilson workcenter equipped with a dual wavelength UV-visible detector.

Mass spectrometry

Electrospray mass spectra were recorded on a Waters ZMD single quadrupole mass spectrometer or a ThermoFinnigan Surveyor MSQ electrospray mass spectrometer. High resolution electrospray mass spectra were recorded on a Bruker Apex IIIFT-ICR mass spectrometer.

LCMS

Reversed-phase HPLC analysis was carried out on a Gilson system workcenter. Analytical or preparative LCMS experiments coupled this HPLC via a 1:4 or 1:20 split respectively with a ThermoFinnigan Surveyor MSQ electrospray mass spectrometer. Data was collected and processed using the XCalibur software system.

Freeze drying

Samples were freeze dried using a Heto PowerDry LL3000.

NMR

^{1}H NMR and ^{13}C NMR spectra were recorded using either a Bruker AC300 FT-NMR spectrometer (^{1}H, 300 MHz), a Bruker DPX 400 spectrometer (^{1}H, 400 MHz) or a Varian Innova 600 spectrometer (^{1}H, 600 MHz). COSY and TOCSY spectra facilitated the assignment of peptide ^{1}H NMR signals.

Sterilisation

Media was sterilised using a Priorcalve: Tactrol PL/LAC/EV100 autoclave or by filtration through a 2 μm Millex sterile syringe driven filter unit.

Fermentation

Fermentation experiments were carried out in a BioFlo 110 fermentor (New Brunswick Scientific).

Centrifugation

Samples were centrifuged using a Beckmann Avanti J-25 cenrtifuge with appropriate rotor (eg. JA14), a Sorvall Evolution RC centrifuge with SLC-6000 rotor, or an Eppendorf 5418-C microcentrifuge.

Anaerobic Experiments

All experiments using LipA were carried out in an anaerobic glovebox (Belle Technology, Portesham, UK) maintained under nitrogen (BOC gasses, Manchester) at less than 0.2 ppm O_2.

Sonication

Cells were lysed using a sonic probe attached to a Sonics: Vibra-cell untrasonic processor.

FPLC

Nickel affinity and size exclusion chromatography were carried out on an AKTAprime^{TM} liquid chromatography system. UV absorbance at 280 nm was recorded on a Pharmacia LKB-REC102 chart recorder.

UV absorbance

UV absorbances were recorded using a Varian: Cary 1 Bio UV-visible spectrophotometer.

Gel imager

Gel images were recorded using a Syngene: Gene genius+ bio imaging system.

6.2 General experimental methods

6.3.1 Expression and purification of His tagged proteins

Media

SOC (100 ml)

To sterile (autoclaved) 2YT (100 mL) was added the following:

1mL filter sterilised $MgSO_4$ (1 M)

1mL filter sterilised $MgCl_2$ (1M)

1mL filter sterilised glucose (2M).

2YT (1 L)

The following were dissolved in water (1 L) and sterilized by autoclaving:

Yeast extract	10 g
Bacto-tryptone	16 g
NaCl	5 g.

Buffers

Buffers for the purification and manipulation of proteins are described in table 6.1 and were adjusted to pH 7.5 and degassed under nitrogen prior to use.

Component	Buffer A[a]	Buffer B[a]	Buffer C[a]	Buffer D[b]
HEPES	25 mM	25 mM	25 mM	0 mM
Imidazole	50 mM	250 mM	0 mM	0 mM
NaCl	500 mM	500 mM	100 mM	0 mM
Glycerol	10% (w/v)	10% (w/v)	10% (w/v)	0 mM
Ammonium bicarbonate	0 mM	0 mM	0 mM	10 mM

Table 6.1 Buffers for the purification of His_6- tagged proteins and their subsequent manipulations. a) buffers were adjusted to pH 7.5 using 5 M NaOH and 5 M HCl; b) buffer was adjusted to pH 7.5 using $NH_{3(aq)}$ and formic acid.

General method 1- Transformations

Expression plasmids were transformed into *E. coli* expression strain BL-21(DE3) or LMG-194 cells. The plasmid and cells were incubated on ice, after 10 min plasmid mixtures (1.0 μL) were added to cells (50 μL). The resulting mixtures were incubated on ice for a further 30 min and then heat shocked for 40 s at 42 ^{o}C. Mixtures were returned to ice for 3 min, SOC medium (250 μL) was added followed by further incubation at 37 ^{o}C for 1 h. Cell mixtures (50 μL aliquots) were spread onto agar plates containing ampicillin (100 mg/L), which were incubated at 37 ^{o}C overnight.

General method 2- Cell growth and protein expression

2YT medium (50 mL) containing ampicillin (100 mg/L) was inoculated with single colonies from a plate or cells from a glycerol stock (prepared previously from overnight

culture, General method 3), which were grown overnight at 37 °C and 180 rpm. The overnight culture was used to inoculate fresh sterile 2YT medium (5 L) containing ampicillin (100 mg/L) and antifoam (0.1 mL/L). Bacterial cultures were incubated at 37 °C and 40% dissolved oxygen (DO) maintained by varying agitation (50 - 250 rpm) until OD_{600} reached 0.8 - 1.0, at which point expression was induced by addition of a filter sterilised arabinose solution (20% w/v, 50 mL/L). Growth was continued at 27 °C, 40% DO controlled with varying agitation for 4 h before harvesting by centrifugation (Sorvall SLC 6000 rotor; 6 000 rpm; 4 °C, 15 min). Cell pellets were stored at −80 °C until required.

General method 3- Preparation of Glycerol stocks for cell growth.

Glycerol stocks of cells were prepared by mixing an overnight culture (0.5 mL) with sterile 75% glycerol (0.5 mL). Mixtures were stored at −80 °C until required.

General method 4- Anaerobic purification of His_6- tagged proteins.

Purification was carried out in an anaerobic glovebox and all buffers were first degassed in the glovebox for 24 hours. Cell paste (30-50 g) was resuspended in anaerobic buffer A (3 mL/g of cells). Lysozyme (10 mg) and benzonase (4 μL, 25 U/μL) were added and the suspension stirred for 1 h. Cells were lysed by sonication (2 × 10 min, 1 s pulse, 20 W) and the lysate was cleared by centrifugation (Beckmann JA-14 rotor, 12 000 rpm, 4 °C, 30 min). The supernatant was applied to a nickel-charged affinity column (Chelating Sepharose FF) previously equilibrated in buffer A. The column was washed with buffer A (5 column volumes) before stepping to buffer B to elute the protein. LipA containing fractions were pooled and concentrated to 10 mL (~25 mg/mL) then either applied to a S-75 gel filtration column (33 × 750 mm) or a a S-75 desalting column (25 × 250 mm) equilibrated with anaerobic buffer C. The protein was eluted with buffer C and the purest fractions, as judged by SDS-PAGE, were concentrated (18 mg/mL) and stored at −80 °C (1 mL aliquots).

Determination of protein concentration

Protein concentrations were determined using the method of Bradford (1).

SDS-PAGE denaturing gel

A 15% resolving gel (10 mL, 5 mL per plate) was prepared by mixing the following components in the order shown below in table 6.2:

Component	Volume
H_2O	4.0 mL
30% Acrylamide / bis acrylamide mix	3.3 mL
1.5 M Tris (pH 8.8) buffer solution	2.5 mL
10% SDS	0.1 mL
10% Ammonium persulfate	0.1 mL
TEMED	4 μL

Table 6.2 Components for a 15% SDS-PAGE resolving gel.

This solution (5 mL) was then applied into each plate (Bio-Rad Mini Protean II system) and the surface of the gel covered with a thin layer of isopropanol (50%) whilst the gel was allowed to set for 45 min. The thin layer of isopropanol was then removed carefully and a stacking gel was then prepared by mixing the following components in the order shown below in table 6.3:

Component	Volume
H_2O	3.4 mL
30% Acrylamide / bis acrylamide mix	0.83 mL
1.5 M Tris (pH 8.8) buffer solution	0.63 mL
10% SDS	0.05 mL
10% Ammonium persulfate	0.05 mL
TEMED	2 μL

Table 6.3 Components for a SDS-PAGE stacking gel.

This mixture was then applied directly onto the top of the resolving gel and a Teflon comb inserted into the gel solution. The stacking gel was left to set for 1 h, after which time the Teflon comb was removed and the wells washed with distilled water.

Samples for analysis by SDS-PAGE were prepared by mixing the required protein solution (20 μL, ~ 2 mg/mL) with sample loading buffer (20 μL, table 6.4). Each sample was then heated to 90 °C for 5 min and then applied onto the gel. Electrophoretic separation was at 180 V for 45 min in SDS-PAGE running buffer (table 6.5). Gels were visualized using Coomaissie brilliant blue stain (table 6.6) followed by destaining overnight in destain (table 6.7).

Component	Quantity
0.2 M Tris-HCl (pH 6.8)	2.5 mL
DTT	154 mg
SDS	200 mg
Bromophenol blue	10 mg
Glycerol	1 mL
Deionised water	Adjust volume to 10 mL

Table 6.4 Sample loading buffer (×1 stock solution).

Component	Quantity
Tris Base	15.1 g
Glycine	94 g
10% SDS solution	50 mL
Deionised water	Adjust volume to 10 mL

Table 6.5 SDS-PAGE running buffer (×5 stock solution).

Component	Quantity
Coomaissie brilliant blue	2.5 g
Methanol:water (1:1)	90 mL
Glacial acetic acid	10 mL

Table 6.6 Coomaissie brilliant blue protein stain.

Component	Quantity
Deionised water	4375 mL
Methanol	375 mL
Glacial acetic acid	250 mL

Table 6.7 Destain solution.

Iron analysis

Iron analysis was carried out according to the method of Fish (2).

General method 5- Reconstitution of LipA Fe-S clusters (3, 4).

LipA (1 mL, ~10 mg/mL) was applied to a NAP-10 column freshly equilibrated with buffer D (10 mM NH_4HCO_3, pH 7.5) and then eluted in the same buffer. Stock solutions of $FeCl_3$ (100 mM), $Na_2S.9H_2O$ (30 mM) and DTT (200 mM) in buffer D were prepared. DTT was added (5 mM final concentration) to LipA and the resulting mixture incubated at room temperature for 90 min. Iron chloride (5 mole equiv wrt LipA) was added dropwise followed by sodium sulfide (10 mole equiv). The resultant assay mixtures were incubated at RT for 90 min after which time the protein samples were a dark brown colour. Precipitated iron sulfide was removed by centrifugation (7 000 rpm, Eppendorf 5415-C microcentrifuge, 10 min). The protein solution was then concentrated using a Millipore microcentrifugal filter (~20 mg/mL).

General method 6- Test *in vitro* assays of *S. solfataricus* LipA with peptide substrates (3).

Reactions were carried out in buffer D (final volume of 500 µL) and contained reconstituted LipA (300 µM), sodium dithionite (1 mM), SAM tosylate salt (1 mM), and the substrate peptide (150 µM) which were added in the order stated. Assays were incubated at 37 °C for 120 min. Proteins were then precipitated by the addition of TFA (25 µL). Precipitated protein was removed by centrifugation (12 000 rpm, Eppendorf 5415-C microcentrifuge, 20 min) and the supernatants (100 µL) analyzed by LCMS (General method 7).

General method 7- LCMS analysis of assay mixtures.

Supernatants (100 μL) were analysed by LCMS using a Hypersil C18 column (5 μm, 150 × 4.6 mm) column with UV detection at 230 nm and a 1:4 split for MS analysis. The mobile phase was a mixture of 0.1% TFA in water (Pump A) and 0.1% TFA in acetonitrile (Pump B), typically beginning with 10% organic and 90% aqueous for 2 min at 0.8 mL/min followed by a 23 min linear gradient to 50% organic followed by a 5 min linear gradient to 100% organic. This was maintained for 5.6 min followed by a return to initial conditions over 0.1 min. Each injection was complete in 45 min. Mass spectra were recorded using an ES^+ ionisation mode. Quantification was achieved using Thermo Finnigan Excalibur software with smoothing (Boxcar ×15) and SIM (500 - 600).

General methods 8a and 8b- *In vitro* assays for the identification of a protein bound intermediate.

General method 8a- Spin filtration protein removal.

Reactions were carried out in buffer D (final volume of 500 μL) and contained reconstituted LipA (300 μM), sodium dithionite (1 mM), SAM tosylate salt (1 mM), and substrate peptide (150 μM) which were added in the order stated. Assays were incubated at 37 °C for 120 min. Protein was removed by filtration through a 5 kDa molecular weight cut off spin filter (13 000 rpm, Eppendorf 5415-C microcentrifuge, 3 × 20 min) and the filtrate (100 μL) analyzed by LCMS (General method 8).

General method 8b-PD10 separation of the protein

Reactions were carried out in buffer D (final volume of 500 μL) and contained reconstituted LipA (300 μM), sodium dithionite (1 mM), SAM tosylate salt (1 mM), and substrate peptide **34**, **39** or **40** (150 μM) which were added in the order stated. Assays were incubated at 23 °C for 30 min before being filtered through a PD10 column pre equilibrated with buffer D. The protein containing filtrate was treated in one of 5 ways:

1) Protein was precipitated by the addition of TFA (25 μL). Precipitated protein was removed by centrifugation (12 000 rpm, Eppendorf 5415-C microcentrifuge, 20 min), and the supernatant (100 μL) analyzed by LCMS (General method 7).

2) The sample was incubated at 60 °C for 120 min before the protein was precipitation by TFA. Precipitated protein was removed by centrifugation and the supernatants (100 μL) were analyzed by LCMS (General method 7).

3) Fresh SAM (1 mM end concentration) was added prior to incubation at 60 °C for 120 min followed by TFA precipitation. Precipitated protein was removed by centrifugation and the supernatant (100 μL) analyzed by LCMS (General method 7).

4) Fresh sodium dithionite (1 mM final concentration) was added prior to incubation at 60 °C for 120 min followed by TFA precipitation of the protein. Precipitated protein was removed by centrifugation and the supernatant (100 μL) analyzed by LCMS (General method 7).

5) Fresh SAM (1 mM final concentration) and sodium dithionite (1 mM final concentration) was added prior to incubation at 60 °C for 120 min followed by TFA precipitation of the protein. Precipitated protein was removed by centrifugation and the supernatant (100 μL) analyzed by LCMS (General method 7).

General methods 9- HPLC purification of reaction mixtures

Reactions were purified using HPLC using a Hypersil C18 column (5 μm, 150 × 4.6mm) column with UV detection at 230 nm and a 1:20 split for MS analysis. The mobile phase was a mixture of 0.1% TFA in water (Pump A) and 0.1% TFA in acetonitrile (Pump B), typically beginning with a 10% organic and 90% aqueous isocratic phase for 2 min at 0.8 mL/min followed by a 23 min linear gradient to 50% organic followed by a 5 min linear gradient to 100% organic. This was maintained for 5.6 min followed by a return to initial isocratic conditions over 0.1 min. Each injection (100 μL) was complete after 45 min. Fractions containing the monothiolated species were pooled and lyophilized yielding a white powder.

6.4 Experimental for Chapter 2

6.4.1 Expression and purification of His tagged LipA

Plasmid

pMK024 – pBADHis(lipAHis, iscSUA, hscBA, fdx)(See appendix D)(5)

This plasmid was constructed by Dr Marco Kriek. It is a pBADHis derived plasmid which encodes the His tagged lipA gene from *S. solfotaricus* (ORF no. SSO3158) and also isc, hsc and fdx genes. The plasmid possesses an ampicillin resistance marker.

Expression and purification of His tagged LipA

LMG-194 competent cells were transformed with pMK024 – pBADHis(lipAHis, iscSUA, hscBA, fdx) according to **general method 1**. Cells were grown and LipA expressed (**general method 2**) and the protein purified according to **general method 4**.

6.4.2 Preparation of peptide substrates

Preparation of 6,6-D_2-octanoic acid 52 (6)

Preparation of 6-oxo-octanoic acid 47 **(7)**

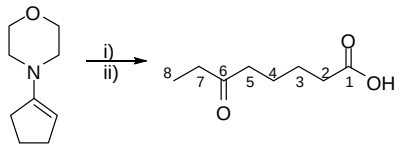

Scheme 6.1 Preparation of 6-oxo-octanoic acid. *Reagents and conditions*: i) EtCOCl, Et_3N, DCM, RT, 16 h. ii) 20% $HCl_{(aq)}$, 50 °C, 16 h, 49%.

6-oxo-octanoic acid was prepared according to the method of White (7). To a stirred solution of 1-morpholino-1-cyclopentene (10 g, 65.4 mmol) and Et_3N (6.6 g, 63.4 mmol) in DCM (50 mL) at 0 °C was added dropwise a solution of propionyl chloride (6.05 g, 63.4 mmol) in DCM (25 mL) over 30 min. The resulting solution was stirred at RT for 15 h after which 20% $HCl_{(aq)}$ (50 mL) was added and the mixture was warmed to reflux for 5 days. DCM (50 mL) was added and the mixture was washed with water (6 × 100 mL) followed by brine (2 × 100 mL). The organic phase was dried over $MgSO_4$ and the solvent removed under reduced pressure to give a brown solid (4.9 g, 30.82 mmol, 49%); **ES-MS (ES^-)**: *m/z* 157.1 ($[M-H]^-$, 100%); $\mathbf{R_f}$ 0.05 (ethyl acetate/hexane, 1:1); **ES-MS (ES^+)**: *m/z* 181.2 ($[M+Na]^+$, 100%); **HRES-MS** calculated for $C_8H_{14}NaO_3^+$: 181.0835, found: 181.0838; **^{1}H NMR** (400 MHz; $CDCl_3$): δ 2.49-2.44 (4H, m, H-7, H-5), 2.44-2.38 (2H, m,

H-2), 1.67 (4H, t, *J* = 3.51 Hz, H-3, H-4), 1.09 (3H, t, *J* = 7.3 Hz, H-8); **^{13}C NMR** (100 MHz, $CDCl_3$) δ 211.7 (C-6), 179.8 (C-1), 42.2 (C-5), 36.3 (C-7), 34.2 (C-2), 24.6 (C-3 or C-4), 23.6 (C-3 or C-4), 8.2 (C-8).

***Preparation of methyl 6-oxo-octanoate 48* (8)**

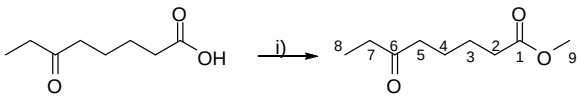

Scheme 6.2 Preparation of methyl 6-oxo-octanoate. *Reagents and conditions*: i) MeOH, H_2SO_4, DCM, 50 °C, 16 h, 99%.

Esterification was achieved using the method of Coleman *et al.* (9). To a stirred solution of 6-oxo-octanoic acid (2.0 g, 12.7 mmol) in DCM (10 mL) was added MeOH (4 mL) and H_2SO_4 (3 drops) and the mixture was refluxed for 16 h. The reaction mixture was washed with conc. $NaHCO_3$ (2 × 5 mL) followed by brine (2 × 5 mL). The organics were combined and dried over $MgSO_4$ and the solvent removed under reduced pressure yielding a clear oil (2.17 g, 12.6 mmol, 99%); **R_f** 0.60 (ethyl acetate/hexane, 1:1); **ES-MS (ES^+)**: *m/z* 195.2 ($[M+Na]^+$, 100%), *m/z* 173.2 ($[M+H]^+$, 15%); **HRES-MS** calculated for $C_9H_{16}NaO_3^+$: 195.0992, found: 195.0993; **^{1}H NMR** (400 MHz; $CDCl_3$): δ 3.65 (3H, s, C-9), 2.43-2.37 (4H, m, H-7, H-5), 2.32-2.29 (2H, m, H-2), 1.60 (4H, qi, *J* = 3.5 Hz, H-3, H-4), 1.04 (3H, t, *J* = 7.6 Hz, H-8); **^{13}C NMR** (100 MHz, $CDCl_3$) δ 211.5 (C-6), 174.2 (C-1), 51.9 (C-9), 42.3 (C-5), 36.3 (C-7), 34.2 (C-2), 24.9 (C-3 or C-4), 23.7 (C-3 or C-4), 8.2 (C-8).

Preparation of methyl 6-hydroxy-6-D-octanoate 49

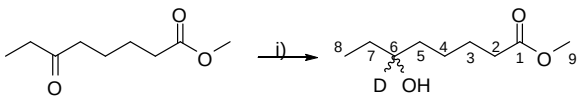

Scheme 6.3 Preparation of methyl 6-hydroxy-6-D-octanoate. *Reagents and conditions*: i) $NaBD_4$, THF, D_2O, 0 °C, 1 h, 91%.

To a stirred solution of methyl 6-oxo-octanoate (1 g, 5.8 mmol) in THF (5 mL) and D_2O (10 mL) at 0 °C under nitrogen was added $NaBD_4$ (256 mg, 6.1 mmol). After 1 h the mixture was washed with saturated $NH_4Cl_{(aq)}$ (5 mL) and extracted into DCM. The organics were combined, washed with brine (2 × 10 mL), dried over $MgSO_4$ and the solvent removed under reduced pressure yielding a yellow oil (1.05 g, 6 mmol). The oil was purified using flash chromatography (SiO_2, 30% EtOAc in hexane) yielding a clear oil (925 mg, 5.3 mmol, 91%); **R_f** 0.38 (ethyl acetate/hexane, 1:1); **ES-MS (ES^+)**: *m/z* 198.2 ($[M+Na]^+$, 100%); **HRES-MS** calculated for $C_9H_{17}DNaO_3^+$: 198.1211, found: 198.1212; **^{1}H NMR** (400 MHz; $CDCl_3$): δ 3.66 (3H, s, C-9), 2.32 (2H, t, *J* = 7.3 Hz, H-2), 1.67-1.60 2H, m, H-3), 1.52-1.35 (6H, m, H-4, H-5 and H-7), 0.93 (3H, t, *J* = 7.3 Hz, H-8); **^{13}C NMR** (100 MHz, $CDCl_3$) δ 172.8 (C-1), 70.9 (t, *J* = 21.4 Hz, C-6), 49.9 (C-9), 34.8 (C-2), 32.4 (C-3, C-4, C-5 or C-7), 28.5 (C-3, C-4, C-5 or C-7), 23.6 (C-3, C-4, C-5 or C-7), 23.3 (C-3, C-4, C-5 or C-7), 8.2 (C-8).

Preparation of methyl 6-tosyl-6-D-octanoate 50

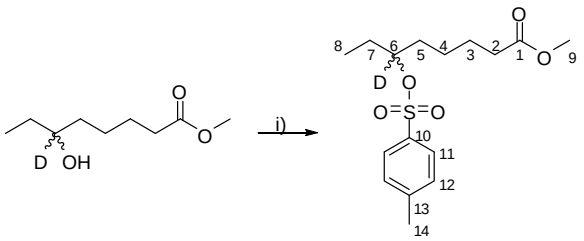

Scheme 6.4 Preparation of methyl 6-tosyl-6-D-octanoate. *Reagents and conditions*: i) TsCl, pyridine, RT, 16 h, 49%.

To a stirred solution of methyl 6-hydroxy-6-D-octanoate (1.3 g, 7.47 mmol) in pyridine (20 mL) at 0 °C under nitrogen was added dropwise a solution of *p*-toluenesulfonyl chloride (1.57 g, 8.22 mmol) in pyridine (8 mL) over 10 min. After 16 h, water (50 mL) was added and the mixture extracted with DCM. The DCM layer was washed with 5N H_2SO_4 (2 × 50 mL) followed by water (2 × 50 mL), conc. sodium bicarbonate (2 × 50 mL) and brine (2 × 50 mL). The organic phases were combined, dried over $MgSO_4$ and the solvent removed under reduced pressure. The compound was purified using flash chromatography (SiO_2, 25% Et_2O in hexane) to give the target compound (1.2 g, 3.65 mmol, 49%); **R_f** 0.68 (ethyl acetate/hexane, 1:1); **ES-MS (ES^+)**: *m/z* 352.1 ($[M+Na]^+$, 100%), 681.4 ($[2M+Na]^+$, 65%);

HRES-MS calculated for $C_{16}H_{23}DNaO_5S^+$: 352.1229, found: 352.1310; **^{1}H NMR** (400 MHz; $CDCl_3$): δ 7.82 (2H, d, *J* = 8.0 Hz, H-11), 7.36 (2H, d, *J* = 8.0 Hz, H-12), 3.70 (3H, s, C-9), 2.48 (3H, s, C-14[4]), 2.26 (2H, t, *J* = 7.3 Hz, H-2), 1.67-1.58 (4H, m, H-3 and H-5), 1.58-1.53 (2H, q, *J* = 7.5, H-7) 1.35-1.23 (2H, m, H-4) 0.93 (3H, t, *J* = 7.3 Hz, H-8); **^{13}C NMR** (100 MHz, $CDCl_3$) δ 174.2 (C-1), 144.8 (C-10), 135.1 (C-13), 130.1 (C-12), 128.1 (C-11), 85.0 (t, *J* = 22.5 Hz, C-6), 51.9 (C-9), 34.1 (C-2 or C-5), 33.5 (C-2 or C-5), 27.4 (C-3, C-4, or C-7), 24.9 (C-3, C-4, or C-7), 24.6 (C-14), 22.0 (C-3, C-4, or C-7), 9.4 (C-8).

Preparation of 1,1,6,6-D$_4$-octanol 51

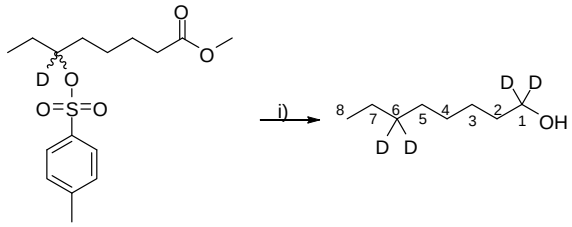

Scheme 6.5 Preparation of 1,1,6,6-D_4-octanol. *Reagents and conditions*: i) $LiAlD_4$, THF, 0 °C, 5 h, 69%.

A solution of methyl 6-tosyl-6-D-octanoate (1.1 g, 3.3 mmol) in THF (10 mL) was cooled to -78 °C. $LiAlD_4$ (436 mg, 10.4 mmol) was added and the mixture stirred for 3 h. The mixture was warmed to RT and conc. $NH_4Cl_{(aq)}$ (5 mL) was added followed by conc. $HCl_{(aq)}$ (10 mL). The mixture was extracted with DCM (3 × 10 mL) and the organics washed with conc. sodium bicarbonate (2 × 15 mL) and brine (2 × 15 mL). The organic phases were combined, dried over $MgSO_4$ and the solvent removed under reduced pressure. The compound was purified using flash chromatography (SiO_2, 35% Et_2O in hexane) to give a clear oil (310 mg, 2.3 mmol, 69%); **R_f** 0.80 (ethyl acetate/hexane, 1:1); **^{1}H NMR** (400 MHz; $CDCl_3$): δ 1.53 (2H, t, *J* = 7.3 Hz, H-2), 1.40-1.20 (8H, m, H-3, H-4, H-5 and H-7), 0.87 (3H, t, *J* = 7.5, H-8); **^{13}C NMR** (100 MHz, $CDCl_3$) δ 62.7 (qi, *J* = 21.3 Hz, C-1), 33.0 (C-2, C-3, C-4, C-5 or C-7), 31.3 (qi, *J* = 19.0 Hz, C-6), 29.8 (C-2, C-3, C-4, C-5 or C-7), 29.5 (C-2, C-3, C-4, C-5 or C-7), 26.1 (C-2, C-3, C-4, C-5 or C-7), 22.8 (C-2, C-3, C-4, C-5 or C-7), 14.4 (C[8]).

Preparation of 6,6-D_2-octanoic acid 52

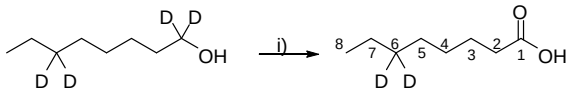

Scheme 6.6 Preparation of 6,6-D_2-octanoic acid. *Reagents and conditions*: i) CrO_3, H_2SO_4, H_2O, acetone, RT, 5 h, 28%.

To a solution of 1,1,6,6-D_4-octanol (300 mg, 2.24 mmol) in acetone (10 mL) was added 2.66 M Jones reagent (0.87 mL, 2.46 mmol) (formed by dissolving CrO_3 (1 g,) in H_2SO_4 (0.89 mL) and water (2.9 mL) and the reaction stirred for 5 h. Ether (25 mL) and water (50 mL) were added, the organics were extracted with ether (3 × 50 mL) and washed with brine (3 × 50 mL). DCM (50 mL) was added and the mixture washed with brine (2 × 25 mL), the organic phases combined, dried over $MgSO_4$ and evaporated to dryness to give a clear oil (280 mg, 1.92 mmol, 86%). 5 M NaOH (1 mL) was added followed by acetone (10 mL) forming a white precipitate which was collected by filtration which and treated with 5 M HCl (2 mL). The organics were extracted with DCM (3 × 10 mL), washed with brine (2 × 5 mL), dried over $MgSO_4$ and evaporated to dryness to give a clear oil (90 mg, 0.62 mmol, 28%); $\mathbf{R_f}$ 0.16 (ethyl acetate/hexane, 1:1); **ES-MS (EI)**: *m/z* 147 ($[M+H]^+$, 100%), 129, 101, 86, 72, 58, 43; $^{\mathbf{1}}$**H NMR** (400 MHz; $CDCl_3$): δ 2.28 (2H, t, *J* = 7.5 Hz, H-7), 1.6 (2H, qi, *J* = 7.4 Hz, H-3), 1.29-1.17 (6H, m, C-4, C-5 or C-7), 0.81 (3H, t, *J* = 7.4 Hz, C-8); $^{\mathbf{13}}$**C NMR** (100 MHz, $CDCl_3$) δ 180.4 (C-1), 34.4 (C-2), 31.2 (qi, *J* = 19.2 Hz, C-6), 29.4 (C-3, C-4, C-5 or C-7), 29.1 (C-3, C-4, C-5 or C-7), 25.1 (C-3, C-4, C-5 or C-7), 22.8 (C-3, C-4, C-5 or C-7), 14.4 (C-8).

Preparation of reagents for peptide chemistry

Preparation of 2-acetyldimedone (Dde) **(10)**

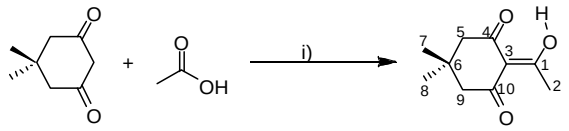

Scheme 6.7 Preparation of 2-acetyldimedone (Dde). *Reagents and Conditions*: i) DMAP, DCC, DMF, RT, 72 h, 34%.

To a stirred solution of acetic acid (6.75 mL, 95 mmol) in DMF (200 mL) were added dimedone (20 g, 143 mmol), DCC (29.43 g, 143 mmol) and DMAP (1.74 g, 0.0143 mmol). After 72 h at RT the reaction mixture was filtered and the filtrate evaporated to dryness. The residue was redissolved in ethyl acetate and washed with 1M $KHSO_4$ (3 × 200 mL) then sat. $NaHCO_3$ (3 × 200 mL). The aqueous solution was acidified and the product extracted into DCM. The organic layer was dried over $MgSO_4$ and the solvent removed under reduced pressure. The oil was purified using flash chromatography (SiO_2, 10 - 25% EtOAc in hexane) yielding a yellow oil (23.8 g, 130 mmol, 91%) which was recrystallised from MeOH/H_2O (1:1) to afford a white crystalline solid (8.43 g, 34 %); $\mathbf{R_f}$ 0.27 (ethyl acetate/hexane, 4:1), **ES-MS**: *m/z* 183.2 ($[M+H]^+$, 100%) **^{1}H NMR** (300 MHz; $CDCl_3$): δ 1.01 (6H, s, H-7, H-8), 2.31 (2H, s, H-5a[a], H-9a), 2.50 (2H, s, H-5b, H-9b), 2.53 (3H, s, H-2); **^{13}C NMR** (75 MHz, $CDCl_3$) δ 28.2 (C-7, C-8), 28.5 (C-2), 30.6 (C-6), 46.91 (C-5 or C-9), 52.5 (C-5 or C-9), 112.4 (C-3), 195.2 (C-4 or C-10), 197.9 (C-4 or C-10), 202.4 (C-1).

***Preparation of Fmoc-(L)-Lys(Dde)-OH* (10)**

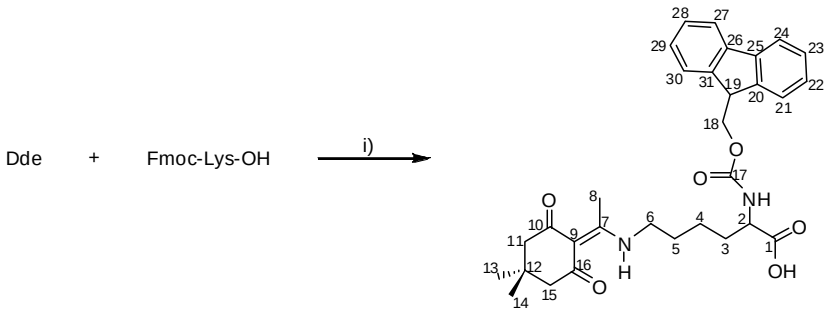

Scheme 6.8 Preparation of Fmoc-(L)-Lys(Dde)-OH. *Reagents and Conditions*: i) 0.1% TFA in EtOH, reflux, 96 h, 72%.

Fmoc-(*L*)-Lys(Dde)-OH was prepared according to the method of Bycroft *et al.* (10). To a stirred suspension of Fmoc-(*L*)Lys-OH (7.35 g, 20 mmol) and Dde (4.0 g, 20 mmol) in ethanol (200 mL) was added TFA (0.15 mL, 20 mmol). The resulting mixture was heated under reflux for 96 h. The solvent was removed by evaporation and the resulting orange residue redissolved in ethyl acetate (200 mL). The solution was washed with 1 M $KHSO_4$ (3 × 50 mL) then dried over $MgSO_4$. The solvent was removed under reduced pressure affording yellow foam which was dissolved in DCM (250 mL). Dropwise addition of the resulting solution to ice cold hexane led to precipitation of a solid, which was collected by filtration, washed with ice cold hexane and dried *in vacuo* leaving a white solid (7.63 g, 72%); **Rf** 0.10 (chloroform, methanol, acetic acid, 15:4:1); **ES-MS**: *m/z* 532.6 ($[M+Na]^+$, 100%); **^{1}H NMR** (300 MHz; $CDCl_3$): δ 1.01 (6H, s, H-13, H-14), 1.48-1.61 (2H, m, H-4), 1.65-1.89 (3H, m, H-3a, H-5), 1.90-2.04 (1H, m, H-3b), 2.36 (4H, s, H-11, H-15), 2.53 (3H, s, H-8), 3.40 (2H, d, *J = 6.0* Hz, H-6), 4.19 (1H, t, *J = 6.9* Hz, H-19), 4.36 (2H, d, *J* = 6.9 Hz, H-18), 4.46 (1H, t *J = 3.0* Hz, H-2), 7.29 (2H, dd, *J = 1.2*, 7.5 Hz, Fmoc), 7.34 (2H, t, *J = 7.5* Hz, Fmoc), 7.57 (2H, t, *J* = 6.7 Hz, Fmoc), 7.73 (2H, d, *J* = 7.5 Hz, Fmoc); **^{13}C NMR** (75 MHz, $CDCl_3$) δ 14.2 (C-12), 18.1 (C-8), 22.4 (C-4), 28.2 (C-13 or C-14), 28.4 (C-13 or C-14), 30.1 (C-3), 32.0 (C-5), 43.3 (C-19), 47.2 (C-6), 52.5 (C-11, C-15), 53.4 (C-18,), 67.1 (C-2), 107.9 (C-9), 119.9 (C-23, C-28), 125.1 (C-24, C-27), 127.1 (C-22, C-29), 127.7 (C-21, C-30), 141.3 (C-23, C-26), 143.8 (C-20, C-31), 156.1 (C-17), 173.9 (C-7), 174.4 (C-1), 198.2 (C-10, C-16).

Solid phase peptide synthesis

Peptides were prepared manually, according to standard solid phase protocols (11). Reactions were carried out in a sintered glass bubbler device (11) unless stated otherwise.

Analysis- Qualitative Kaiser (ninhydrin) test

KCN (32 mg) was dissolved in water (50 mL) then 1 mL of this solution diluted to 50 mL with pyridine. Solution A was then prepared by adding this resulting mixture to a solution of phenol (20 g) in ethanol (5 mL). Solution B was prepared by dissolving ninhydrin (1.25 g) in ethanol (25 mL). A small resin sample was and rinsed with ethanol then solution A (100 μL) and solution B (25 μL) were added and the mixture heated to 100 ^{o}C for 5 min. If positive for free amino groups a strong blue colour was seen and if negative a straw colour.

Loading of Fmoc (L)-Ile-OH onto Wang resin

DIC (0.48 mL) was added to a stirred solution of Fmoc-(L)-Ile-OH (2.12 g, 6.0 mmol) in DMF (10 mL) for 10 min before being added to Wang resin (12) (1.68 g, 0.89 mmol/g). To this was added DMAP (37 mg, 0.3 mmol) and the mixture agitated in an ultrasonic bath at RT for 3 h. The resin was then filtered, washed with DMF (3 × 30 mL) followed by alternating DCM (3 × 30 mL) and diethyl ether (3 × 30 ml) before being dried *in vacuo*.

Quantitative Fmoc test

To a known mass (<5 mg) of loaded resin was added a solution of 20% (v/v) piperidine in DMF (1.5 mL) in a 25 mL volumetric flask. The resin was allowed to stand for 15 min, then filtered through a pipette with a glass wool plug and the filtrate diluted to 25 mL with 20% (v/v) piperidine in DMF. The absorbance at 302 nm was recorded against a blank (20% (v/v) piperidine in DMF) and the loading yield calculated from the following equation:

$$\text{Loading (mmol/g)} = [(A_{302} \times V)/(\varepsilon_{302} \text{ x } W)] \times 1000$$

A_{302} = absorbance of the piperidyl-fulvene adduct

V = final volume (25 mL)

W = mass of the resin sample (mg)

ε_{302} = molar extinction co-efficient of the adduct at 302 nm (7800 $M^{-1}cm^{-1}$)

Capping of unreacted groups on resin

After loading the unreacted groups were capped by adding the resin (1.0 g) to a solution of benzoyl chloride (0.5 mL) and pyridine (0.5 mL) in DCM (20 mL) which had been cooled to 0 ^{o}C. The resulting suspension was agitated gently for 30 min at RT before being filtered and washed with alternating DCM (3 × 30 mL) and diethyl ether (3 × 30 mL). The resin was then dried *in vacuo*.

Removal of the N^{ε}-Fmoc protecting group

20% (v/v) piperidine in DMF (10 mL) was added to Fmoc protected peptidyl resins in reaction vessel. The suspended resin was then agitated for 30 min then washed with DMF (5 × 10 mL, 1 min agitation). This process was repeated once and the resin was washed with alternating DCM (3 × 30 mL) and diethyl ether (3 × 30 mL). The removal of the Fmoc group was confirmed by qualitative Ninhydrin test.

Coupling of Fmoc (L)-amino acids to peptide

Fmoc amino acid (3 eq wrt resin loading) and HOBt (3 eq) were dissolved in DMF, DIC (3 eq) was added and the resulting solution stirred at RT for 10 min. The activated amino acid solution was transfered to the peptidyl resin in the reaction vessel and the mixture was agitated for 1 h. The resin was then filtered and washed with DMF (5 × 10 mL, 1 min agitation) followed by alternating DCM (3 × 30 mL, 1 min agitation) and diethyl ether (3 × 30 mL, 1 min agitation). Completion of the coupling reaction was confirmed by qualitative Kaiser test.

Dde deprotection

The Dde group was selectively removed with hydroxylamine hydrochloride and imidazole in NMP/DMF according to the method of Diaz-Mochon *et al*. (13). Hydroxylamine hydrochloride (1.25 g, 1.80 mmol) and imidazole (0.92 g, 1.35 mmol) were suspended in NMP (5 mL) and the mixture was agitated in an ultrasonic bath until complete dissolution. The solution was diluted in DMF (1 mL) and the mixture was then transferred to the peptidyl resin in the reaction vessel. The mixture was then agitated in the reaction vessel for 3 h. The liquid was then drained and the resin washed with DMF (5 × 10 mL, 1 min agitation) followed by alternating DCM (3 × 30 mL) and diethyl ether (3 × 30 mL). Removal of the Dde protecting group was confirmed by the qualitative Kaiser test.

Coupling of carboxylic acids to the lysine N^{ϵ} amine

The carboxylic acid (5 molar equivalents with respect to resin loading) was dissolved in DMF (10 mL), PyBOP (14) (4.75 equiv) and N,N'-diisopropylethylamine (DIPEA) (0.50 mL) were added and the solution was then transferred to the resin. The suspended resin was agitated for 1 h then filtered and washed with DMF (5 × 10 mL, 1 min agitation) followed by alternating DCM (3 × 30 mL) and diethyl ether (3 × 30 mL). Completion of the coupling reaction was confirmed by qualitative Kaiser test.

Cleavage of peptides from resin

Peptidyl resins were transferred to a round bottomed flask and a mixture of TFA, anisole and water (10:1:1, 12 mL) was added. The suspended resin was stirred for 2 h then the liquid was drained and the resin washed with TFA (3 × 5 mL). The combined TFA washings were concentrated *in vacuo* and the crude peptide precipitated by the addition of diethyl ether.

Preparation of Glutamyl-(N6-octanoyl)-lysyl isoleucine 34 (15)

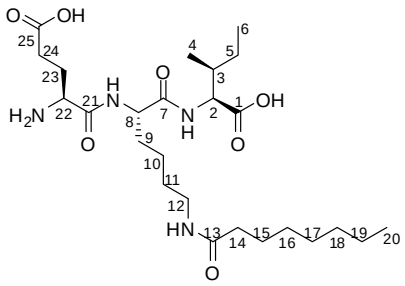

The crude yield of peptide upon cleavage from the resin was 85 mg (66%). An aliquot (50 mg) was purified by reverse phase chromatography to yield 30 mg of a white solid (40% yield overall): **TLC reverse phase Rf** 0.23 (MeCN: water (1:10), 0.1%TFA); **ES-MS**: *m/z* 515.3 ($[M+H]^+$, 100%); **HRES-MS** calculated for $C_{25}H_{47}N_4O_7^+$: 515.3439, found: 515.3438; **^{1}H NMR** (400 MHz, D_2O): δ 4.41 (1H, t, *J* = 7.3 Hz, H-8), 4.17 (1H, d, *J* = 5.8 Hz, H-2), 3.81 (1H, t, *J* = 6.4 Hz, H-22), 3.23 (2H, t, *J* = 6.8 Hz, H-12), 2.32-2.39 (2H, m, H-24), 2.27 (2H, t, *J* = 7.3 Hz, H-14), 2.15-1.95 (2H, m, H-23), 1.93-1.75 (3H, m, H-3 and H-9), 1.66-1.55 (4H, m, H-15 and H-11), 1.52-1.40 (3H, m, H-10 and H-5a or 5b), 1.36-1.30 (8H, m, H-16, H-17, H-18 and H-19), 1.24-1.14 (1H, m, H-5a or 5b) 0.96-0.89 (9H, m, H-4, H-6 & H-20); **^{13}C NMR** (100 MHz, D_2O): δ 60.4 (C-2), 54.4 (C-8), 53.9 (C-22), 39.4 (C-12), 37.6 (C-3), 36.2 (C-14), 33.8 (C-24), 31.3 (C-16, C-17, C-18 or C-19), 30.8 (C-16, C-17, C-18 or C-19), 29.8 (C-23), 28.5 (C-5, C-9, C-16, C-17, C-18 or C-19), 28.4 (C-5, C-9, C-16, C-17, C-18 or C-19), 28.3 (C-5, C-9, C-16, C-17, C-18 or C-19), 25.8 (C-15), 25.0 (C-11), 22.8 (C-10), 22.3 (C-16, C-17, C-18 or C-19), 15.7 (C-20), 13.8 (C-4 or C-6), 11.2 (C-4 or C-6).

Preparation of Glutamyl-(N6- (8,8,8-D_3-octanoyl)-lysyl isoleucine 39 (15)

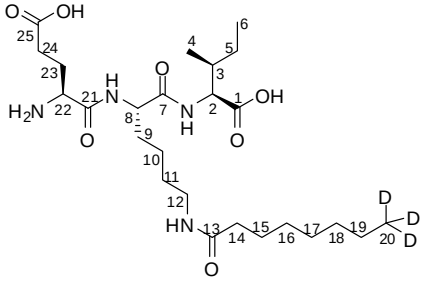

The crude yield of peptide upon cleavage from the resin was 120 mg (93%). An aliquot (40 mg) was purified by reverse phase chromatography to yield 29.6 mg of a white solid (69% yield overall): **TLC reverse phase Rf** 0.23 (MeCN: water (1:10), 0.1%TFA), **ES-MS**: *m/z* 518.4 ($[M+H]^+$, 100%)**; HRES-MS** calculated for $C_{25}H_{44}D_3N_4O_7^+$: 518.3628, found: 518.3621; **^{1}H NMR** (400 MHz; D_2O) δ 4.42 (1H, t, *J* = 7.2 Hz, H-8), 4.19 (1H, d, *J* = 6.4 Hz, H-2), 4.11 (1H, t, *J* = 6.4 Hz, H-22), 3.21 (2H, t, *J* = 6.8 Hz, H-12), 2.50-2.43 (2H, m, H-24), 2.25 (2H, t, *J* = 7.2, H-14), 2.2-2.12 (2H, m, H-23), 1.93-1.73 (3H, m, H-3 and H-9), 1.65-1.52 (4H, m, H-15 and H-11), 1.52-1.36 (3H, m, H-10 and H-5a or 5b), 1.35-1.25 (8H, m, (1.64-1.15, m, H-16, H-17, H-18 and H-19), 1.25-1.14 (1H, m, H-5a or 5b), 0.96-0.87 (6H, m, H-4 and H-6); **^{13}C NMR** (100 MHz, D_2O): δ 59.9 (C-2), 54.5 (C-8), 52.9 (C-22), 39.3 (C-12), 37.4 (C-3), 36.2 (C-14), 32.0 (C-24), 30.8 (C-16, C-17, C-18 or C-19), 28.4 (C-5, C-9, C-16, C-17, C-18 or C-19), 28.4 (C-5, C-9, C-16, C-17, C-18 or C-19), 28.3 (C-5, C-9, C-16, C-17, C-18 or C-19), 27.4 (C-23), 25.8 (C-11), 25.0 (C-5), 22.7 (C-10), 22.0 (C-16, C-17, C-18 or C-19), 16.6 (C-20), 15.5 (C-4), 11.1 (C-6).

Preparation of Glutamyl-(N6- (6,6-D_2-octanoyl)-lysyl isoleucine 40

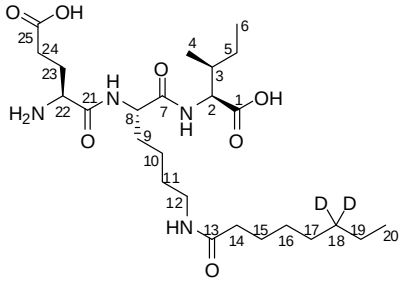

The crude yield of peptide upon cleavage from the resin was 41.3 mg (98%). An aliquot (5 mg) was purified by reverse phase chromatography to yield 1.2 mg of a white solid (24% yield overall): **TLC reverse phase Rf** 0.25 (MeCN: water (1:10), 0.1%TFA), **ES-MS**: *m/z* 517.4 ($[M+H]^+$, 100%)**; HRES-MS** calculated for $C_{25}H_{45}D_2N_4O_7^+$: 517.3565, found: 517.3565; **^{1}H NMR** (400 MHz; D_2O) δ 4.24 (1H, t, *J* = 7.0 Hz, H-8), 4.15 (1H, d, *J* = 6.0 Hz, H-2), 3.95 (1H, t, *J* = 6.5 Hz, H-22), 3.02 (2H, t, *J* = 6.8 Hz, H-12), 2.38 (2H, t, *J* = 7.5 Hz, H-24), 2.06 (2H, t, *J* = 7.5, H-14), 1.98-2.05 (2H, m, H-23), 1.84-1.75 (1H, m, H-3), 1.69-1.57 (2H, m, H-9), 1.45-1.20 (7H, m, H-15, H-11, H-10 & H-5a or H-5b), 1.18-

1.05 (7H, m, H-19, H-17, H-16 & H-5a or H-5b), 0.79 (3H, d, *J* = 7.0 Hz, H-4), 0.74 (3H, t, *J* = 7.5, H-20 or H-4), 0.70 (3H, t, *J* = 7.5, H-20 or H-4).

6.4.3 Test *in vitro* assays of *S. solfataricus* LipA with peptide substrates 34, 39 or 40.

LipA activity was tested in reactions using peptides **34**, **39** or **40** according to **general method 6**.

6.4.4 In vitro assays identifying a protein bound intermediate.

A protein bound intermediate was identified in reactions with using peptide **34** following **general methods 8a** and **8b.**

6.4.5 Assays for C8 KIE calculation

Reactions were carried out in buffer D (final volume of 500 μL) maintained at 37 °C and contained reconstituted LipA (300 μM), sodium dithionite (1 mM), SAM tosylate salt (1 mM) and were initiated by the addition of substrate peptide **34** or **39** (150 μM). Reactions were quenched after 20 or 120 min by the addition of TFA (50 μL). Precipitated protein was removed by centrifugation (12 000 rpm, Eppendorf 5415-C microcentrifuge, 20 min), and the supernatants (100 μL) were analyzed by LCMS according to **general method 7**. Integrals for C8 KIE calculation are shown in table 6.8.

Time/ min	**Total Peak Area for double sulphur inserted products (× 10^6)**		**KIE**
	Substrate **34**	Substrate **39**	
20	17.7	1.17	15.0
120	35.2	2.35	15.0

Table 6.8 Areas used to calculate the KIE for hydrogen atom abstraction from C8.

6.4.6 Assays for a time course to calculate C6 KIE

Reactions were carried out in buffer D (final volume of 2500 μL) maintained at 23 °C and contained reconstituted LipA (300 μM), sodium dithionite (1 mM), SAM tosylate salt (1 mM) and were initiated by the addition of substrate peptide **34** or **40** (150 μM). Aliquots

(250 μL) were quenched after 0, 10, 20, 30, 40, 50 and 60 min by TFA (25 μL) addition. Precipitated protein was removed by centrifugation (12 000 rpm, Eppendorf 5415-C microcentrifuge, 20 min), and the supernatants (100 μL) were analyzed by LCMS according to **general method 7**. Integrals for C6 KIE calculation are shown in table 6.9, data for the C6 compound was fitted to a pseudo first order process and the rate constant was calculated from the data shown in table 6.10.

Time/ s	**Substrate 34**		**Substrate 40**	
	Peak area ($\times 10^6$)	Concentration / μM	Peak area ($\times 10^6$)	Concentration / μM
0	14.8	150	50.2	150
600	9.09	92.2	34.5	103
1200	3.04	30.9	24.0	71.7
1800	1.52	15.5	19.0	56.8
2400	0.880	8.92	12.7	37.8
3000	0.543	5.50	8.78	26.2
3600	0.211	2.14	5.86	17.5

Table 6.9 Areas used to calculate the exhaustion of peptide starting material. Peak area for starting concentration was defined as 150 μM for the two substrates.

Time/ s	**Substrate 34**		**Substrate 40**	
	$\frac{Concentration}{Concentration_0}$	$Ln\left(\frac{Concentration}{Concentration_0}\right)$	$\frac{Concentration}{Concentration_0}$	$Ln\left(\frac{Concentration}{Concentration_0}\right)$
0	1	0	1	0
600	0.615	-0.487	0.687	-0.376
1200	0.206	-1.58	0.478	-0.738
1800	0.103	-2.27	0.387	-0.971
2400	0.0595	-2.82	0.252	-1.38
3000	0.0367	-3.31	0.175	-1.74
3600	0.0143	-4.25	0.117	-2.15

Table 6.10 Data used to calculate rate constants for substrates **34** and **40**. The rate constant for **34** was found to be 11.7×10^{-4} s^{-1}, whilst the rate constant for substrate **40** was found to be 5.84×10^{-4} s^{-1}. The KIE calculated for C6 hydrogen abstraction using these rate constants was 2.00.

6.4.7 Reactions for the isolation of the monothiolated species

Fourteen reactions were carried out in buffer D (final volume of 500 µL) maintained at 37 °C and contained reconstituted LipA (300 µM), sodium dithionite (1 mM), SAM tosylate salt (1 mM) and were initiated by the addition of substrate peptide **34** (150 µM). Reactions were quenched after 20 min by the addition of TFA (50 µL). Precipitated protein was removed by centrifugation (12 000 rpm, Eppendorf 5415-C microcentrifuge, 20 min). The supernatants were combined and lyophilized yielding a yellow powder, which was dissolved in water (250 µL) and purified by HPLC with MS detection.

6.4.8 HPLC isolation of the monothiolated species

Reactions were purified according to **general method 9**.

Characterisation of Glutamyl-[N6-(6-thiol-octanoyl)-lysyl] isoleucine 37

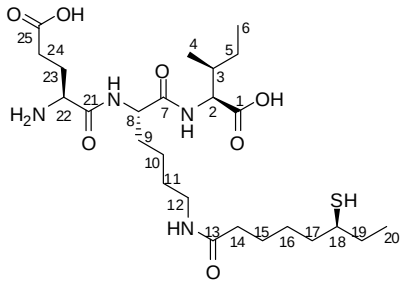

ES-MS: *m/z* 547.3 ($[M+H]^+$, 100%); **HRES-MS** calculated for $C_{25}H_{47}N_4O_7S^+$: 547.3087; found: 547.3156; **HPLC** Rt 19.94 min; **^{1}H NMR** (400 MHz, D_2O): δ 4.33 (1H, t, *J* = 7.1 Hz, H-8), 4.06 (1H, d, *J* = 5.9 Hz, H-2), 3.99 (1H, t, *J* = 6.2 Hz, H-22), 3.13 (2H, t, *J* = 6.6 Hz, H-12), 2.85-2.75, (1H, m, H-18), 2.38-2.25(2H, m, H-24), 2.25-2.16 (2H, t, *J* = 7.0 Hz, H-14), 2.16-1.95 (1H, m, H-23[a] or H-23b), 1.85-1.23 (17H, m, H-3, H-9, H-10, H-11, H-15, H-16, H-19 and H-5[a] or H-5b), 1.15 (1H, m, H-5[a] or H-5b), 0.90 (3H, t, *J* = 7.3 Hz, H-20), 0.89-0.79 (6H, m, H-4 & H-6).

6.4.9 Modified procedure for isolation of the monothiolated species

Fourteen reactions were carried out in buffer D (final volume of 500 µL) maintained at 37 °C and contained reconstituted LipA (300 µM), sodium dithionite (1 mM), SAM tosylate

salt (1 mM) and were initiated by the addition of substrate peptide **34** or **39** (150 μM). Reactions were quenched at 20 min by the addition of TFA (50 μL). Precipitated protein was removed by centrifugation (12,000 rpm, Eppendorf 5415-C microcentrifuge, 20 min). The supernatants were combined and lyophilized to give a yellow powder, which was anaerobically dissolved in Buffer D (250 μL). TCEP (10 eq wrt substrate) in buffer D was added and the mixture stood for 3 h before the addition of iodoacetamide (20 eq wrt substrate) and the mixture stood for 2 h. The mixture was lyophilized and purified by HPLC with MS detection according to **general method 9**.

Characterisation of Glutamyl-[N6-(6-carbamoylmethylsulfanyl-octanoyl)-lysyl] isoleucine 54

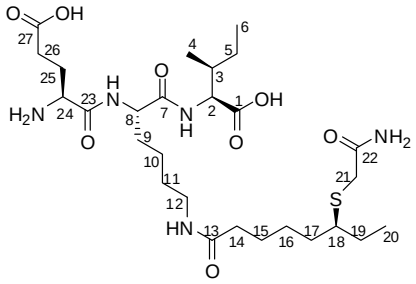

ES-MS: *m/z* 604.7 ($[M+H]^+$, 100%); **HRES-MS** calculated for $C_{27}H_{50}N_5O_8S^+$: 604.3375; found: 604.3372; **HPLC** Rt 19.94 min; **^{1}H NMR** (600 MHz, D_2O): δ 4.36 (1H, dd, *J* = 6.6 & 8.4 Hz, H-8), 4.12 (1H, d, *J* = 6.0 Hz, H-2), 3.71 (1H, m, H-24), 3.28 (2H, s, H-21), 3.19 (2H, dt, *J* = 2.4 & 6.6 Hz, H-12), 2.72, (1H, m, H-18), 2.29 (2H, m, H-26), 2.25 (2H, t, *J* = 7.2 Hz, H-14), 2.01 (1H. m, H-25^a or H-25b), 1.93 (1H. m, H-25^a or H-25b), 1.83 (2H, m, H-3 & H-9^a or H-9b), 1.74 (1H, m, H-9^a or H-9b), 1.58 (8H, m, H-11, H-19, H-15 and H-16 or H-17), 1.40 (5H, m, H-15, H-16 or H-17, H-10, H-5^a or H-5b), 1.15 (1H, m, H-5^a or H-5b), 0.95 (3H, t, *J* = 7.5 Hz, H-20), 0.89 (3H, d, *J* = 6.6 Hz, H-4), 0.87 (3H, t, *J* = 7.2 Hz, H-6).

6.5 Experimental for Chapter 3

6.5.1 Expression and purification of Pfs

Plasmid

pProExHTApfs (See appendix D)

This plasmid was a generous gift from Prof. K. Conell (OHSU, Portland, USA). It is a pBADHis derived plasmid which encodes the His tagged *pfs* gene from *E. coli* (ORF no. NP752145). The plasmid possesses an ampicillin resistance marker.

Expression and purification of His tagged Pfs

BL21 (DE3) competent cells were transformed with pProExHTApfs according to **general method 1**. Cells were grown, Pfs expressed (**general method 2**) and the protein purified according to **general method 4**.

Inhibitors

Stock solutions of AdoH (4.0 mM) and methionine (6.7 mM) in buffer D were prepared for use in inhibition studies

6.5.2 Concentration calibration curves for peptides 34 and 39

Substrate tripeptides **34** and **39** (1 mg) were dissolved in 10 mM ammonium bicarbonate (1 mL) and then standard solutions were prepared by dilution of this stock solution (table 5.7). These solutions were then analysed by LCMS using the method for analysis of assays with a 1:4 split. Peak areas were determined by integration using Excalibur software with smoothing (Boxcar ×15) and SIM (500 - 600). Peak areas were then plotted against concentration of peptide to generate standard curves (table 6.11).

Concentration / μM	Peptide 34	Peptide 39	
	Peak area I ($\times 10^6$)	Peak area I ($\times 10^6$)	Peak area II ($\times 10^6$)
156	31.8	218	168
117	24.8	145	102
77.8	15.9	103	68.4
58.4	12.6		
38.9	9.10	47.7	33.4
29.2	7.40		
19.5	3.77	38.0	26.4
9.73	1.81	19.8	14.1

Table 6.11 Peak **a**reas determined by LCMS analysis of standard solutions of octanoyl tripeptides **34** and **39**.

6.5.3 Investigating the product inhibition of LipA by AdoH and methionine

To test for inhibition of LipA, the reaction protocol (**general method 6**) was modified so that it also contained a known quantity of the potential inhibitors AdoH (table 6.12), (*L*)- methionine (table 6.13) or an equimolar mixture of both AdoH and (*L*)- methionine (table 6.14) prior to initiation by the addition of substrate peptide **34**. The final reaction volume was 200 μL.

AdoH concentration / µM	TIC areas for double sulphur inserted peptides (SIM 570 - 580) (×10^6)	
	Peak area I	Peak area II
0	94.9	76.8
50	84.7	66.7
100	75.1	69.5
250	78.9	64.9
500	65.9	49.8
750	48.3	46.8
1000	42.7	43.1

Table 6.12 Peak **a**reas of double sulphur inserted products from LipA reactions containing a known quantity of AdoH after incubation at 37 °C for 120 min determined by LCMS analysis using SIM 570 - 580.

(*L*)- Methionine concentration / µM	TIC areas for double sulphur inserted peptides (SIM 570 - 580) (×10^6)	
	Peak area I	Peak area II
0	88.5	88.5
50	68.8	69.0
100	74.5	79.3
250	68.8	66.7
500	63.3	54.7
750	75.8	74.9
1000	61.7	62.0

Table 6.13 Peak **a**reas of double sulphur inserted products from LipA reactions containing a known quantity of (*L*)- methionine after incubation at 37 °C for 120 min determined by LCMS analysis using SIM 570 - 580.

AdoH + (*L*)- methionine concentration / µM	TIC areas for double sulphur inserted peptides (SIM 570 - 580) ($\times 10^6$)	
	Peak area I	Peak area II
0	130.0	92.0
50	109.0	87.7
100	81.8	73.1
250	56.5	50.0
500	41.0	36.7
750	21.7	20.5
1000	24.3	20.4

Table 6.14 Peak **a**reas of double sulphur inserted products from LipA reactions containing a known quantity of AdoH and (*L)*- methionine after incubation at 37 °C for 120 min determined by LCMS analysis using SIM 570 - 580.

6.5.4 Removal of synergistic inhibition by the addition of Pfs

To test for reversal of synergistic inhibition of LipA by AdoH and (*L)*- methionine the reaction protocol (**general method 6**) was modified so that it also contained an equimolar mixture of both AdoH and methionine (table 6.15) with and without Pfs (1 µM) (table 5.10) prior to initiation by the addition of substrate peptide **34** and had an end volume of 200 µL.

AdoH + methionine concentration / µM	TIC areas for double sulphur inserted peptides (SIM 570 - 580) (×10^6)	
	Without Pfs	With Pfs
0		
50	29.3	45.3
100	26.3	42.9
250	22.0	43.7
500	14.6	39.8
750	10.6	40.8
1000	5.93	39.3

Table 6.15 Peak **a**reas of double sulphur inserted products from LipA reactions containing a known quantity of AdoH and (*L*)- methionine with and without Pfs after incubation at 37 °C for 120 min determined by LCMS analysis using SIM 570 - 580. Samples at 0 µM inhibitor concentration failed to inject properly and are not included.

6.6 Experimental for Chapter 4

6.6.1 Test *in vitro* assays of *S. solfataricus* LipA with a nonanoyl substrate

Reactions were carried out according to **general method 6** utilizing the substrate peptide **73**.

6.6.2 LCMS analysis of a reaction using a nonanoyl substrate

Reactions were analysed using **general method 7**.

6.6.3 Identification of a nonanoyl protein bound intermediate

A protein bound intermediate was identified in reactions with using peptide **73** following **general method 8b.**

6.6.4 Reactions for the isolation of products formed in a LipA reaction using a nonanoyl substrate

Fifty four reactions were carried out according to **general method 6** using substrate peptide **73**. The supernatants were combined and lyophilized leaving a yellow powder. The powder was anaerobically dissolved in Buffer D (3 mL) and TCEP (10 eq wrt substrate) in buffer D was added. The mixture was allowed to stand for 3 h prior to the addition of iodoacetamide (20 eq wrt substarte) and the mixture left standing for a further 2 h. The mixture was lyophilized, dissolved in water (1.6 mL) and purified by HPLC.

6.6.5 HPLC purification of products formed in a LipA reaction using a nonanoyl substrate

Reactions were purified using HPLC using a Phenomenex Gemini C18 column (5 µm, 150 × 10.0 mm) column with UV detection at 230 nm. The mobile phase was a mixture of 0.1% TFA in water (Pump A) and 0.1% TFA in acetonitrile (Pump B), beginning with 15% organic and 85% aqueous for 10 min at 2.5 mL/min followed by a 43 min linear gradient to 40% organic followed by a 5 min linear gradient to 100% organic. This was maintained for 5.6 min followed by a return to initial conditions over 0.1 min. Each injection (500 µL) was complete after 72 min. Fractions of interest were confirmed using MS, identical species were pooled and lyophilized yielding white powders.

Characterisation of Glutamyl-[N6-(6-carbamoylmethylsulfanyl-nonanoyl)-lysyl]-isoleucine 74.

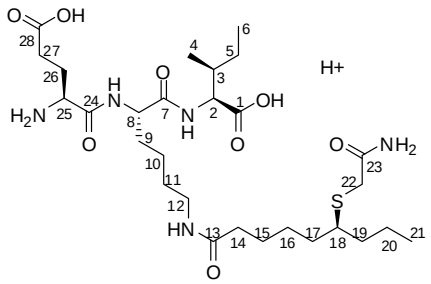

ES-MS: *m/z* 618.3 ($[M+H]^+$, 100%); **HRES-MS** calculated for $C_{28}H_{53}N_5O_8S^+$: 618.3531; found: 618.3539; **HPLC** Rt 20.85 min; **^{1}H NMR** (600 MHz, D_2O): δ 4.38 (1H, t, *J* = 7.5 Hz, H-8), 4.11 (1H, d, *J* = 6.0 Hz, H-2), 4.05 (1H, t, *J* = 6.3 Hz, H-25), 3.27 (2H, s, H-22),

3.18 (2H, t, *J* = 7.2 Hz, H-12), 2.81-2.70 (1H, m, H-18), 2.44-2.32 (2H, m, H-28), 2.24 (2H, t, *J* = 7.8 Hz, H-14), 2.18-2.02 (2H, m, H-26), 1.88-1.80 (1H, m, H-3), 1.88-1.70 (2H, m, H-9), 1.66-1.48 (8H, m, H-15, H-16, H-17 and H-19), 1.64-1.50 (2H, m, H-11), 1.50-1.32 (1H, m, H-5[a] or H-5b), 1.46-1.34 (2H, m, H-10), 1.46-1.43 (2H, m, H-20), 1.20-1.10 (1H, m, H-5[a] or H-5b), 0.89 (3H, d, *J* = 7.8 Hz, H-4), 0.88 (3H, t, *J* = 7.2 Hz, H-6), 0.88 (3H, t, *J* = 7.2 Hz, H-21).

Characterisation of Glutamyl-[N6-(5-(4-methylthietan-2-yl)pentanoyl)-lysyl] isoleucine 81 and 82.

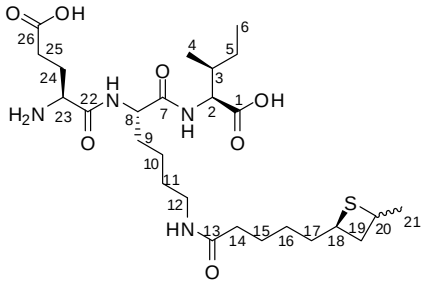

ES-MS: *m/z* 559.2 ($[M+H]^+$, 100%); **HRES-MS** calculated for $C_{26}H_{47}N_4O_7S^+$: 559.3160; found: 559.3145; **HPLC** Rt 23.35 min; **^{1}H NMR** (600 MHz, D_2O): δ 4.40 (1H, t, *J* = 7.2 Hz, H-8), 4.14 (1H, d, *J* = 6.0 Hz, H-2), 4.07 (1H, t, *J* = 6.6 Hz, H-23), 3.87-3.74 (1H, m, H-20_{cis} and H-20_{trans}), 3.18 (2H, t, *J* = 6.0 Hz, H-12), 3.03-2.99 (0.6H, m, H-$19a_{cis}$ or H-$19b_{cis}$) 2.67-2.60 (0.8H, m, H-$19a_{trans}$ & H-$19b_{trans}$), 2.46-2.37 (2H, m, H-25), 2.29-2.20 (0.6H, m, H-$19a_{cis}$ or H-$19b_{cis}$), 2.25-2.20 (1H, m, H-18) 2.18-2.09 (2H, m, H-24), 1.88-1.80 (2H, m, H-14), 1.88-1.70 (3H, m, H-3 and H-9), 1.80-1.72 (2H, m, H-15), 1.62-1.51 (4H, m, H-11 and H-17), 1.49 (1.2H, d, *J* = 6.9 Hz, H-21_{trans}) 1.47-1.36 (5H, m, H-5[a] or H-5b, H-10 and H-16), 1.34 (1.8H, d, *J* = 6.9 Hz, H-21_{cis}), 1.21-1.12 (1H, m, H-5[a] or H-5b), 0.91-0.85 (6H, m, H-4 and H-6).

Characterisation of Glutamyl-[N6-(*(E)*-non-6-enoyl)-lysyl] isoleucine 73.

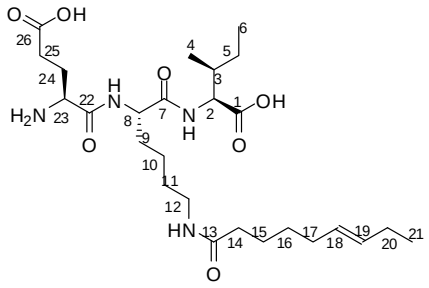

ES-MS: *m/z* 527.2 ($[M+H]^+$, 100%); **HRES-MS** calculated for $C_{26}H_{47}N_4O_7^+$: 527.3439; found: 527.3449; **HPLC** Rt 25.41 min; **^{1}H NMR** (600 MHz, D_2O): δ 5.58 (1H, dt, *J* = 15.6, 6.0 Hz, H-18 or H-19), 5.50 (1H, dt, *J* = 15.6, 6.3 Hz, H-18 or H-19), 4.39 (1H, t, *J* = 7.5 Hz, H-8), 4.15 (1H, d, *J* = 6.0 Hz, H-2), 4.07 (1H, t, *J* = 6.3 Hz, H-23), 3.25-3.16 (2H, m, H-12), 2.46-2.40 (2H, m, H-25), 2.23 (2H, t, *J* = 7.2 Hz, H-14), 2.18-2.09 (2H, m, H-24), 2.04-1.96 (4H, m, H-17 and H-20), 1.88-1.80 (1H, m, H-3), 1.88-1.70 (2H, m, H-9), 1.64-1.50 (4H, m, H-12 and H-14), 1.64-1.50 (2H, m, H-11), 1.50-1.32 (3H, m, H-5^a or H-5b and H-10), 1.40-1.32 (2H, m, H-16), 1.20-1.12 (1H, m, H-5^a or H-5b), 0.95 (3H, t, *J* = 7.5 Hz, H-21), 0.91 (3H, d, *J* = 7.2 Hz, H-4), 0.88 (3H, t, *J* = 7.5 Hz, H-6).

6.7 References

1. Bradford, M.M., *A rapid and sensitive method for the quantitation of microgram quantities of protein utilizing the principle of protein-dye binding.* Analytical Biochemistry 1976. **72**: p. 248-54.
2. Fish, W.W., *Rapid colorimetric micromethod for the quantitation of complexed iron in biological samples.* Methods in Enzymology, 1988. **158**: p. 357-64.
3. Bryant, P., M. Kriek, R.J. Wood, and P.L. Roach, *The activity of a thermostable lipoyl synthase from Sulfolobus solfataricus with a synthetic octanoyl substrate.* Analytical Biochemistry 2006. **351**(1): p. 44-9.
4. Bryant, P., *Investigations into the Biosynthesis of Lipoic Acid*, in *School of Chemistry*. 2008, University of Southampton: Southampton.
5. Kriek, M., L. Peters, Y. Takahashi, and P.L. Roach, *Effect of iron-sulfur cluster assembly proteins on the expression of E. coli lipoic acid synthase.* Protein Expression and Purification, 2003. **28**: p. 241-245.
6. Boden, N., R.J. Bushby, and L.D. Clark, *Assignment of the Deuterium Quadrupolar Splittings for the End-chain of 4-cyano-4'-octylbiphenyl in the Nematic Phase: A Test Between Theoretical Models for End-chain Conformational Motion and Orientational Ordering.* Molecular Crystals and Liquid Crystals, 1984. **104**: p. 179 - 185.
7. White, R.H., *Biosynthesis of lipoic acid - extent of incorporation of deuterated hydroxyoctanoic and thiooctanoic acids into lipoic acid.* Journal of the American Chemical Society, 1980. **102**(21): p. 6605-6607.
8. Terasawa, T. and T. Okada, *Reaction of Mixed Carboxylic Anhydrides with Grignard-Reagents - Application to Preparation of Keto Esters - Scope and Limitations.* Tetrahedron, 1977. **33**(6): p. 595-598.
9. Coleman, P.J., K.M. Brashear, B.C. Askew, J.H. Hutchinson, C.A. McVean, L.T. Duong, B.P. Feuston, C. Fernandez-Metzler, M.A. Gentile, G.D. Hartman, D.B. Kimmel, C.T. Leu, L. Lipfert, K. Merkle, B. Pennypacker, T. Prueksaritanont, G.A. Rodan, G.A. Wesolowski, S.B. Rodan, and M.E. Duggan, *Nonpeptide $\alpha_v\beta_3$ Antagonists. Part 11: Discovery and Preclinical Evaluation of Potent $\alpha_v\beta_3$ Antagonists for the Prevention and Treatment of Osteoporosis.* Journal of Medicinal Chemistry, 2004. **47**(20): p. 4829-4837.

10. Chhabra, S.R., B. Hothi, D.J. Evans, P.D. White, B.W. Bycroft, and W.C. Chan, *An appraisal of new variants of Dde amine protecting group for solid phase peptide synthesis.* Tetrahedron Letters, 1998. **39**(12): p. 1603-1606.
11. Atherton, E., Sheppard, R. C., *Solid phase peptide synthesis a practicle approach*. 1989: IRL Press at Oxford University Press.
12. Wang, S.S., *p-alkoxybenzyl alcohol resin and p-alkoxybenzyloxycarbonylhydrazide resin for solid phase synthesis of protected peptide fragments.* Journal of the American Chemical Society 1973. **95**(4): p. 1328-33.
13. Diaz-Mochon, J.J., L. Bialy, and M. Bradley, *Full orthogonality between Dde and Fmoc: the direct synthesis of PNA--peptide conjugates.* Organic Letters 2004. **6**(7): p. 1127-9.
14. Coste, J., D. Le-Nguyen, and B. Castro, *PyBOP:A New Peptide Coupling Reagent Devoid of Toxic By-Product.* Tetrahedron Lett., 1990. **31**(2): p. 205-208.
15. Douglas, P., M. Kriek, P. Bryant, and P.L. Roach, *Lipoyl synthase inserts sulfur atoms into an octanoyl substrate in a stepwise manner.* Angewandte Chemie International Edition 2006. **45**(31): p. 5197-9.